Human Vascular Microphysiological Systems for Drug Screening

by

Cristina Elena Fernandez

Department of Biomedical Engineering
Duke University

Date:_____

Approved:

_____
George A. Truskey, Supervisor

_____
William M. Reichert

_____
Brenton D. Hoffman

_____
Thomas J. Povsic

_____
William E. Kraus

Dissertation submitted in partial fulfillment of
the requirements for the degree of Doctor
of Philosophy in the Department of
Biomedical Engineering in the Graduate School
of Duke University

2016

ABSTRACT

Human Vascular Microphysiological Systems for Drug Screening

by

Cristina Elena Fernandez

Department of Biomedical Engineering
Duke University

Date:_____

Approved:

_____
George A. Truskey, Supervisor

_____
William M. Reichert

_____
Brenton D. Hoffman

_____
Thomas J. Povsic

_____
William E. Kraus

An abstract of a dissertation submitted in partial fulfillment of the requirements for the degree of Doctor of Philosophy in the Department of Biomedical Engineering in the Graduate School of Duke University

2016

Abstract

Endothelial dysfunction is the predominant pathophysiological state prior to the onset of atherosclerosis. Currently, treatments for endothelial dysfunction are evaluated *in vitro* using two-dimensional (2D) cell culture assays or *in vivo* animal models. Microphysiological systems are small-scale three-dimensional (3D) tissue models that recapitulate the native tissue structure and function. An ideal microphysiological system is comprised of human cells embedded within a 3D matrix introduced to physiological fluid perfusion. Immune challenge in the form of cytokines or immune cells further recapitulates the native microenvironment.

A vascular microphysiological system was developed from a small-diameter tissue engineered blood vessel (TEBV) in a perfusion culture circuit. TEBVs were created from collagen gels embedded with human neonatal dermal fibroblasts and plastically compressed to yield collagen constructs with high fiber densities. TEBVs are rapidly producible and can be directly introduced into perfusion culture immediately after fabrication. Endothelium-independent vasoconstriction in response to phenylephrine and endothelium-dependent vasodilation in response to acetylcholine were used to analyze the health and function of the endothelium non-destructively over time.

Endothelial dysfunction was induced through introduction of the pro-inflammatory cytokine tumor necrosis factor – α (TNF-α). Late-outgrowth endothelial

progenitor cells derived from the peripheral blood of coronary artery disease patients (CAD EPCs) were evaluated as a potential endothelial source for autologous implantation in both a two-dimensional (2D) direct co-culture model as well as a 3D model as an endothelial source for a tissue engineered blood vessel. CAD EPCs demonstrated similar adhesive properties to a confluent, quiescent layer of smooth muscle compared to human aortic endothelial cells. Within the TEBV system, CAD EPCs demonstrated the capacity to elicit endothelium-dependent vasodilation. CAD EPCs were compared to adult EPCs from young, healthy volunteers. Both CAD EPCs and healthy volunteer EPCs demonstrated similar endothelium-dependent vasoactivity in response to acetylcholine; however, in response to TNF-α, CAD EPCs demonstrated a reduced response to phenylephrine at high doses.

The treatment of TEBVs with statins was explored to model the drug response within the system. TEBVs were treated with lovastatin, atorvastatin, and rosuvastatin for three days prior to exposure to TNF-α. In all three cases, statins prevented TNF-α induced vasoconstriction in response to acetylcholine within the TEBVs, compared to TEBVs not treated with statins. Overall, this work characterizes and validates a novel vascular microphysiological system that can be tested *in situ* in order to determine the effects of various patient populations and drugs on endothelial health and function under healthy and inflammatory conditions.

Dedication

This is dedicated to my grandmother, Lilia Díaz de Pozo.

Contents

Abstract iv

List of Tables xiii

List of Figures xiv

Acknowledgements xvi

1. Introduction 1

1.1 Research Overview 1

1.2 Motivation and Significance 4

1.3 Hypothesis and Specific Aims 4

1.4 Structure and Composition of Native Vasculature 7

1.4.1 Endothelial Cells 8

1.4.2 Vascular Smooth Muscle Cells 9

1.4.3 Vascular Extracellular Matrix 10

1.4.4 Interactions between Vascular SMCs and Endothelium 12

1.5 Cell Sources for Vascular Tissue Engineering 13

1.6 Tissue Engineered Blood Vessels 16

1.6.1 TEBVs Made from Biodegradable, Synthetic Polymers 18

1.6.2 TEBVs made from Decellularized Vessels 20

1.6.3 TEBVs Made from Natural Scaffolds 22

1.7 Atherosclerosis and Endothelial Dysfunction 26

1.8 Microphysiological Systems 28

1.9 In vitro Models of Endothelial Dysfunction 30

1.10 Overview of the Dissertation 32

2. Late Outgrowth Endothelial Progenitors from Patients with Coronary Artery Disease: Endothelialization of Confluent Stromal Cell Layers 35

2.1 Introduction 35

2.2 Materials and Methods 38

2.2.1 Cell Isolation and Culture 38

2.2.2 Cell Media 39

2.2.3 CAD EPC/HAEC Co-Culture with SMCs 40

2.2.4 CAD EPC/HAEC Confluency Measurements 40

2.2.5 Parallel Plate Flow Chamber 41

2.2.6 Strength of Adhesion Study 42

2.2.7 Cell Alignment under Flow 42

2.2.8 Nitric Oxide Quantification 44

2.2.9 Integrin Blocking Assays 44

2.2.10 Statistical Analysis 45

2.3 Results 45

2.3.1 CAD EPC Confluence over SMC in Co-Culture 45

2.3.2 Percent Retention 48

2.3.3 Cell Alignment under Flow and in Static Conditions 49

2.3.4 Integrin-Blocking Studies 53

2.4 Discussion 54

2.5 Conclusion 60

2.6 Chapter-Specific Acknowledgements 60

3. Development and Optimization of a Human Tissue Engineered Vascular Microphysiological System for *in vitro* Drug Screening 62

3.1 Introduction 62

3.2 Methods 68

3.2.1 Cell Isolation and Culture 68

3.2.2 Flow Cytometry 69

3.2.3 TEBV Fabrication, Endothelialization, and Perfusion 70

3.2.4 Burst Pressure Analysis and Mechanical Testing of TEBVs 71

3.2.5 Determination of TEBV Inner Diameter 73

3.2.6 Analysis of TEBV Vasoactivity 74

3.2.7 RNA Isolation and Reverse Transcriptase-Polymerase Chain Reaction Analysis 75

3.2.8 Immunofluorescent Staining of TEBVs 76

3.2.9 Quantification of Nitric Oxide Produced by TEBVs 77

3.2.10 Statistical Analysis 77

3.3 Results 77

3.3.1 Generation of Small-Diameter, Endothelialized TEBVs 77

3.3.2 Mechanical Strength and Stability of TEBVs 80

3.3.3 Contractile and Extracellular Matrix Protein Expression 83

3.3.4 Vasoactivity 86

3.3.5 Responses to Caffeine and Theophylline 90

3.4 Discussion 92

3.5 Chapter-Specific Acknowledgements 95

4. Effect of Inflammation and Statins on a Human Vascular Microphysiological System Model 97

4.1 Introduction 97

4.2 Methods 101

4.2.1 Cell Isolation and Culture 101

4.2.2 Flow Cytometry 103

4.2.3 TEBV Fabrication, Endothelialization, and Perfusion Culture 103

4.2.4 Analysis of TEBV Vasoactivity 105

4.2.5 Activation of TEBVs with TNF-α 105

4.2.6 Treatment of TEBVs with Statins 106

4.2.7 Quantification of Nitric Oxide Produced by TEBVs 107

4.2.8 RNA Isolation and Reverse Transcriptase-Polymerase Chain Reaction Analysis 107

4.2.9 Immunofluorescent Staining of TEBVs 108

4.2.10 β-galactosidase assay for Cell Senescence in 2D 109

4.2.11 NF-kB P65 Nuclear Translocation and SIRT1 Expression 109

4.2.12. U937 Monocyte Adhesion to 2D EPC Cultures 111

4.2.13 Statistical Analysis 112

4.3 Results 113

4.3.1 Comparison of CAD EPCs to Healthy Volunteer EPCs 113

4.3.2 Response of TEBVs to TNF-α 114

4.3.3 TEBV Response to Statins 120

4.3.4 Effect of TNF-α and Statins on EPC Senescence in 2D 126

4.3.5 Effects of Statins and TNF-α on U937 Monocyte Adhesion to Endothelium in 2D 128

4.3.6 Effect of Statins and TNF-α on SIRT1 Expression and P65 Nuclear Translocation 131

4.4 Discussion 134

4.5 Chapter-Specific Acknowledgements 137

5. Dissertation Summary and Future Work 139

5.1 Dissertation Summary 139

5.2 Strengths and Weaknesses of Work 146

5.3 Work Recommended to Complete Studies 153

5.4 Future Directions for TEBV Project 155

5.5 Implications toward Cardiovascular Tissue Engineering 158

Appendix A: Licensing Information for Previously Published Work 159

Appendix B: Protocol for Constructing Collagen I Vascular Constructs 173

Appendix C: TEBV Media Compositions 177

Appendix D: TEBV Vasoactivity Assay 179

Appendix E: Primers for qRT-PCR 181

Appendix F: Antibodies for Flow Cytometry 182

Appendix G: Antibodies for Immunofluorescence 183

Appendix H: Protocol for Cell Separation and RNA Isolation from Endothelialized TEBVs 184

References 189

Biography 217

List of Tables

Table 1: Endothelialization of Vascular Grafts 24

Table 2: Characteristic Properties of CAD EPCs vs. CB EPCs 56

Table 3: TEBV Vasoactivity 66

Table 4: TEBV Collagen Fiber Density 78

Table 5: Human Vasoactivity Responses 93

Table 6: Sample TEBV Calculations 174

Table 7: Primers for qRT-PCR 181

Table 8: Antibodies for Flow Cytometry 182

Table 9: Primary Antibodies for Immunofluorescence 183

List of Figures

Figure 1: Co-culture of CAD EPCs or HAECs with SMCs for one week. 47

Figure 2: Cell Retention after Supraphysiological Shear Stress. 48

Figure 3: Fluorescence micrographs of CAD EPCs and HAECs after 48 hours of static culture or exposure to physiological shear stress. 50

Figure 4: Orientation and Elongation of CAD EPCs and HAECs on SMCs. 51

Figure 5: Cell Area of both CAD EPCs and HAECs in Co-Culture did not decrease with Flow. 52

Figure 6: Nitrite Release of CAD EPCs under Flow Conditions. 52

Figure 7: Integrin blocking indicates functional CAD EPC Binding Mechanisms. 54

Figure 8: TEBV Fabrication and Culture 72

Figure 9: TEBV Fabrication 79

Figure 10: TEBV Mechanical Strength and Stability 81

Figure 11: TEBV Mechanical Testing 82

Figure 12: Expression of α-SMA in hNDF TEBVs after 24 Hours of Culture 84

Figure 13: Contractile Protein Expression of Endothelialized TEBVs Made with hNDFs or hMSCs 84

Figure 14: Contractile and Extracellular Matrix Protein Expression 85

Figure 15: TEBV Endothelialization and Nitric Oxide Production 87

Figure 16: TEBV Endothelial Response and Vasoactivity 88

Figure 17: TEBV Response to Caffeine and Theophylline 91

Figure 18: Baseline Adhesion Molecule Expression of EPCs 114

Figure 19: Vasoactive Response of CAD EPC TEBVs to 200 U/mL TNF-α 117

Figure 20: Adhesion Molecule Expression in TEBVs after 200 U/mL TNF-α 118

Figure 21: Recovery of TEBVs to Acute Exposure to 500 U/mL TNF-α 119

Figure 22: TEBV Vasoactivity Response to Statins and 200 U/mL TNF-α 122

Figure 23: Nitric Oxide Production of Statin-Treated TEBVs exposed to 200 U/mL TNF-α. 123

Figure 24: Effect of Rosuvastatin Treatment on TEBV Exposure to 500 U/mL TNF-α ... 125

Figure 25: Effect of Statins toward Mediating TNF-α-Induced Senescence 127

Figure 26: Effects of Rosuvastatin and TNF-α on U937 Monocyte Adhesion to EPCs ... 130

Figure 27: Effect of Statins and 200 U/mL TNF-α on EPC SIRT1 Expression..... 132

Figure 28: Effect of Statins and TNF-α on P65 Nuclear Translocation 133

Acknowledgements

I would first and foremost like to express my sincere gratitude to my adviser, Dr. George Truskey. I am extremely grateful for his support and advising. I am honored to have had the opportunity to work in his lab, where I have learned many valuable skills and truly developed as a scientist. I would also like to thank Dr. Monty Reichert for his support, encouragement, and advising throughout my time at Duke. I am especially grateful to both of them for inviting me to join the microphysiological systems project.

I am very grateful for the support from members of my thesis committee, including Dr. Brenton Hoffman, for his vast knowledge of atherosclerosis and mechanotransduction and Dr. Thomas J. Povsic for providing keen insight into the field of cardiovascular surgery and endothelial progenitor cells. I would also like to thank Dr. William Kraus, Dr. Hardean Achneck, and Dr. Kam Leong for serving on my thesis committee.

I would like to recognize all of those with whom I have collaborated on the microphysiological systems project, particularly Dr. Kam Leong and members of the Leong lab, including Feng Zhao, Youngmee Jung, Hayeun Ji, Hon Fai Chen, and Zaozao Chen. I would also like to thank Leigh Atchison and Ellen Weburg for being wonderful team members on the tissue engineered blood vessel project. The Truskey lab has been a wonderful place to work and learn, and this would not be possible without the kind and collaborative environment fostered by all of its members.

I would like to acknowledge the efforts of the amazing undergraduate students and master's students with whom I have worked, including Izundu Obi-onuoha, Samantha Perez, Hillary Bedell, Kayla Henderson, and Allison Braithwaite. Their work ethic and drive was incredible to watch, and I am honored to have had the opportunity to watch them grow as scientists. I would like to thank Ringo Yen for designing and optimizing the chamber design for our tissue engineered blood vessels.

Graduate school is long and takes many turns, and I would not have survived had it not been for the support of my closest friends, near and far. Thank you for being pillars of support throughout my time in graduate school, and making the years spent in Durham, North Carolina such a wonderful experience.

Most importantly, I would like to thank my parents for their endless love and support, their relentless encouragement of my education, and the sacrifices they made so that I could live the life that I enjoy. I would not be who I am without you.

1. Introduction

1.1 Research Overview

Over 80% of proposed pharmaceutical drug candidates that enter clinical trials fail due to concerns with human efficacy and toxicity[1]. Most of these drug candidates fail during clinical development in Phases II and III, the most expensive phases of the drug development pipeline[2]. The financial and societal impacts of these high attrition rates are staggering, considering that the total pre-approval cost estimate of a new pharmaceutical drug compound was estimated to be $802 million dollars in 2000[3]. A critical need exists for an alternative to the standard pre-clinical testing model.

Currently, *in vitro* cell based assays are used to evaluate the toxicity and efficacy of a compound. Successful compounds are evaluated further with animal models and mathematical models that estimate drug distribution kinetics and effects on target organs and the body[4]. Animal studies can provide substantial insight into drug effects and interactions; however, animal responses to drugs may exhibit differences in toxic doses and drug metabolism[5]. Recently, studies indicated that mouse disease models demonstrate poor correlations with human inflammatory diseases, further illustrating the need for human tissue models that recapitulate healthy and diseased physiological conditions[6].

Microphysiological systems (MPS) are perfused small-scale models of one or more human tissues or organs[7] comprised of human primary cells or induced

pluripotent stem cells (iPSCs) with the ultimate potential of becoming models to study disease or tools for precision medicine. Three-dimensional (3D) human tissue models are an important development toward accurately modeling disease and predicting drug responses on an organ scale. Many pre-clinical studies are conducted on two-dimensional (2D) plastic or glass substrates; however, *in vivo*, tissues are comprised of complex extracellular matrices embedded with mixed populations of cells and perfused with fluids.

3D tissue models have the potential to allow us to evaluate human biological interactions and diseases by taking advantage of natural spatiotemporal cues, physiological fluid perfusion, a variety of cell types, and the complex extracellular matrix that are present in tissues but are absent from 2D culture plates[8]. A human tissue-engineered blood vessel (TEBV) capable of responding to vasoactive stimuli would pose a promising model for the evaluation and screening of pharmaceutical drug candidates for toxicity and efficacy within the circulatory system.

Cardiovascular disease (CVD) is the leading cause of death in the United States. In 2010, 83.6 million Americans were estimated to live with CVD, leading to direct and indirect costs of $315.4 billion[9]. Atherosclerosis is the underlying pathological process behind CVD that causes the narrowing of the vasculature with plaques and an overgrowth of vascular smooth muscle cells (SMCs), predisposing the patient to cardiac incidents, such as heart attack or stroke. Atherosclerosis is an inflammatory disease that

begins with activation of the vascular endothelium, leading to endothelial dysfunction. Understanding the mechanisms behind endothelial dysfunction could lead to the development of more targeted and effective therapies, potentially reducing the demand for such invasive treatments.

Advanced atherosclerosis may require interventional treatments such as percutaneous coronary intervention (PCI) or coronary artery bypass (CABG). In 2010, 492,000 PCI and 158,008 CABG treatments were performed in the United States[9]. Autologous grafts from sources such as the internal mammary artery or the saphenous vein are the ideal replacements for diseased vessels[10]; however, patients with coronary artery disease often have atherosclerotic lesions in other regions of the body. Up to 30 percent of patients requiring lower limb bypass are lacking a suitable autologous vein[11], indicating a need for both implantable tissue engineered blood vessels as well as more effective treatments for atherosclerosis.

In this work, we have focused on understanding the behavior of human late-outgrowth, peripheral blood-derived endothelial progenitor cells from coronary artery disease patients (CAD EPCs). We have examined their behavior in 2D culture as well as in 3D culture using a vascular microphysiological system under both healthy and inflammatory conditions that mimic the inflammatory environment experienced by dysfunctional endothelium. Finally, we have evaluated their response to statins,

commonly prescribed medications for this patient population, within our vascular microphysiological system.

1.2 Motivation and Significance

Understanding the behavior of endothelium derived from different patient populations is critical toward development of more targeted therapies for atherosclerosis. To date, endothelialized tissue engineered blood vessels have not demonstrated the function *in vitro* that is required to assess the vasoactive responses of drugs. Techniques for the *ex vivo* analysis of endothelial function have been previously established using animal models; however, we sought to develop a system that was capable of robustly analyzing the functionality of TEBVs non-destructively using the same assays that can be used to assess endothelial function in human patients. A rapidly producible, physiologically accurate human TEBV with a confluent, functional endothelium could fulfill a pressing need as both a medical device and a vascular model for *in vitro* drug testing.

1.3 Hypothesis and Specific Aims

The central goal of this dissertation was to create a vascular microphysiological system in which to study the responses of healthy and dysfunctional endothelium. We designed an endothelialized tissue engineered blood vessel capable of vasoactive

responses. We used clinically relevant assays to assess the endothelial health and contractility of the TEBV non-destructively over time. Previous work from our group indicates that late outgrowth endothelial progenitor cells from coronary artery disease patients (CAD EPCs) can be highly proliferative, and can exhibit behavior similar to that of healthy endothelium, such as network formation and production of flow-dependent genes eNOS and KLF2. Our central hypothesis is that CAD EPCs can exhibit vasoactive behavior within a tissue-engineered blood vessel. We address this hypothesis through three specific aims.

Specific Aim 1: Characterization of CAD EPC Adhesion over SMCs in a Direct 2D Co-Culture Model. This aim explores the adhesive properties of CAD EPCs over a confluent, quiescent layer of human aortic smooth muscle cells (SMCs) compared to that of human aortic endothelial cells (HAECs). Characterizing the adhesive properties of CAD EPCs is critical toward validating them as a potential endothelial source for *in vitro* MPS studies within a TEBV and also for potential autologous implantation applications. We assessed their strength of adhesion over SMCs using a parallel plate flow chamber and supraphysiological levels of steady, laminar shear stress. We also evaluated their potential to align with flow when directly co-cultured over SMCs through exposure to 48 hours of steady, laminar shear stress in a parallel plate flow chamber. Lastly, we compared their integrin binding mechanisms to that of HAECs by using antibodies to block integrins and plating the EPCs over a confluent, quiescent layer of SMCs.

Specific Aim 2: Development and Characterization of a Human Vascular Microphysiological System for *in vitro* Drug Screening. In this aim, we developed an arteriolar scale tissue engineered blood vessel by embedding human neonatal dermal fibroblasts (hNDFs) within a collagen gel that was plastically compressed to increase the fiber density. We evaluated the mechanical stability and burst pressure of the TEBVs, and noted that addition of endothelium increased the burst pressure. We evaluated the extracellular matrix and contractile protein expression of the hNDFs within the TEBVs. We also adapted a clinically relevant technique to assess the vasoactivity of the TEBVs using both endothelium-independent and endothelium-dependent compounds *in situ*, allowing us to monitor the health of the TEBV in real time over the course of several weeks. Lastly, we assessed the response of the TEBVs to phosphodiesterase inhibitors caffeine and theophylline, demonstrating the capacity of our vasoactive TEBV model to respond to various drug stimuli.

Specific Aim 3: Assessment of TEBV response to TNF-α and Statins. In this aim, we evaluated the response of CAD EPCs to the pro-atherosclerotic cytokine tumor necrosis factor – α (TNF-α). We evaluated the expression of the adhesion molecules VCAM-1, ICAM-1, and E-selectin within the TEBV, and characterized the change in endothelial-specific vasoactivity elicited by acute exposure to 200 U/mL TNF-α. We also evaluated the response of the TEBV to three statins: lovastatin, atorvastatin, and rosuvastatin, in order to assess the pleiotropic effects of statins on the TEBV and assess

the effects of statin treatment on the vasoactivity and nitric oxide production of the TEBVs before and after exposure to TNF-α. Finally, we evaluated the behavior of CAD EPCs and EPCs from young, healthy volunteers within the TEBV model, assessing their response and recovery from a high dose of TNF-α after treatment with rosuvastatin.

1.4 Structure and Composition of Native Vasculature

Understanding the structure of the vasculature is critical for creating a tissue engineered blood vessel that properly recapitulates the native microenvironment. Large vertebrate arteries are comprised of three layers: a tunica intima, a tunica media, and a tunica adventitia[12]. The tunica intima is comprised of endothelial cells and the basement membrane on the basal side of the endothelium. The tunica media contains smooth muscle cells and elastin arranged in lamellae, in addition to collagen fibers, fibrillin microfibrils, and a proteoglycan-rich ECM. Finally, the tunica adventitia is the outermost layer of the vessel wall that is comprised of an external elastic lamina and fibroblasts. Larger vessels also have nerves and smaller vessels and capillaries in the tunica adventitia.

The field of TEBVs mostly focuses on the development of an intact tunica intima and tunica media, since the primary focus of TEBVs is to replace vessels in small diameter (< 6mm) applications. Since microphysiological systems primarily focus on isolating a functional unit of a particular organ or tissue, our central goal was to design a

vascular microphysiological system that could effectively recapitulate the structure and function of an arteriole. Arterioles consist of one or two layers of smooth muscle and an endothelial layer. As part of the resistance vasculature, arterioles are crucial toward hemodynamic regulation, controlling blood pressure, and distributing blood throughout tissues[13].

1.4.1 Endothelial Cells

Endothelial cells comprise the innermost layer of the vasculature, and play a key role in the maintenance of an anti-thrombogenic interface between the blood and the vasculature[14]. Endothelial cells produce nitric oxide, which prevents platelet aggregation, and secrete procoagulating factors such as von willebrand factor. Furthermore, endothelial cells produce basement membrane proteins such as fibronectin, laminin, and various collagens, as well as growth factors that assist in the influence of the underlying stromal cells through paracrine signaling.

Endothelial cells attach to a 50-100 nm thick basement membrane that provides structural support and allows for cellular signaling[15]. The basement membrane is pervasive throughout all endothelium or epithelium in the body, and has a classic structure comprised of different combinations of laminin, nidogen, perlecan, and collagen IV[16,17]. Laminin and collagen IV are arranged in single layer sheets parallel to the surface and play roles in endothelial cell attachment through integrin binding. Vascular basement membrane in particular contains von Willebrand factor produced by

endothelial cells and megakaryocytes, which plays a role in hemostasis and thrombosis[18]. Endothelial cell adhesion to the basement membranes is critical for their proliferation and migration, as well as for blood vessel morphogenesis, survival, and stabilization[19].

1.4.2 Vascular Smooth Muscle Cells

In addition to endothelial cells and the basement membrane, vascular stabilization requires the aid of mural cells, which may be pericytes or smooth muscle cells in small and large vessels, respectively[20]. A gradient of cells exists along capillary beds ranging from pericytes found next to capillaries to smooth muscle cells surrounding larger vessels and terminal arterioles and venules. Pericytes are proposed to be multipotent mesenchymal SMC precursors due to the intermediate levels of muscle actin detected in pericytes between that found in vascular SMCs and ECs. Pericytes may further differentiate into SMCs to allow capillaries to meet increased blood flow demands. Other functions of pericytes include phagocytosis and regulation of blood flow and capillary growth[21].

Smooth muscle cells serve to provide support against the pulsatile forces of blood flow in the vasculature. SMCs in quiescent vessels exist in the contractile state, marked by low proliferation, while SMCs in injured or remodeling vasculature are present in the synthetic state, marked by high production of ECM proteins such as fibronectin and collagen[22,23]. *In vivo*, SMCs in the contractile state are immersed in the

ECM and are surrounded by a basement membrane comprised of laminin and collagen IV. Vascular SMCs are bound to the ECM through integrins, syndecans, and a dystrophin-glycoprotein complex (DGPC) specific to muscle cells that serves to link actin filaments to the ECM. The DGPC contains a cell surface receptor called α-dystroglycan that connects the DGPC to laminin and perlecan produced by SMCs, and plays a role in laminin assembly on cell surfaces. Laminin has been implicated in maintaining SMCs in their contractile phenotype, since adhesion receptors to laminin, $\alpha_1\beta_1$, $\alpha_7\beta_1$, and α-dystroglycan have been found to be expressed only on SMCs in the contractile phenotype[24].

1.4.3 Vascular Extracellular Matrix

Although significant strides have been made in understanding many of the different components of the vascular ECM, much remains to be investigated regarding how all of the different components work in concert together. The manner in which endothelial cells and smooth muscle cells communicate and translate forces has yet to be fully understood. The effects of endothelial cells on the extracellular matrix proteins produced by smooth muscle cells has been investigated[25], although much more work needs to be performed in this area.

Collagen is a primary component of the basement membrane and ECM of blood vessels. Collagen IV is the primary collagen expressed in basement membranes, while collagen I is primarily expressed in smooth muscle cell ECM[26]. The intimal endothelial

layer and the medial SMC layer of vessels are separated by the internal elastic lamina, which is comprised of cross-linked elastin and fibrillin microfibrils and glycoproteins[27]. Elastin provides elasticity to the vessel wall and provides several regulatory functions in the vascular extracellular matrix. Elastin comprises 30-40% of the dry weight of the thoracic aorta and approximately 50% of the abdominal aorta[28]. SMC production of tropoelastin, the precursor of elastin, is greatly influenced by mechanical forces acting on SMCs. Vascular SMCs embedded in 3D collagen gels that were exposed to long-term cyclic distention increased production of elastin[29].

Elastin production has generally been limited in TEBVs. Elastin modulates blood vessel mechanics at low strains and modulates vessel elasticity and resilience[30], which is crucial toward enabling TEBVs to withstand native pressure fluctuations[31]. Elastin is critical toward actin stress fiber organization and signaling[32]. Arterial SMC proliferation is regulated by interactions between elastin receptors and soluble degradation products of elastin within the vascular wall[33], and SMC proliferation is uncontrolled in its absence[34]. Compared to 2D surfaces, SMC proliferation is reduced on 3D collagen or fibrin gels[35]. The quiescent, contractile phenotype of SMCs is promoted in a collagenous microenvironment, which can limit the synthesis of elastin precursors and assembly of elastin structures in the ECM[36].

Laminin is a critical component of the endothelial basement membrane as well as the medial ECM[37]. Laminin structure is comprised of α, β, and γ subunits that may be

rearranged in various configurations. Cells attach to laminin through various adhesion mechanisms including integrins, syndecans, and dystroglycan[38]. Laminin-8 and laminin-10 are expressed in the endothelial basement membrane, and other laminin isoforms may also be expressed.

1.4.4 Interactions between Vascular SMCs and Endothelium

Co-cultures between vascular SMCs and ECs have strived to elucidate the mechanisms of communication between these two cell types. Direct co-culture between ECs and confluent, quiescent human aortic SMCs have shown increased expression of calponin, a marker for increased differentiation to the contractile phenotype[39]. Furthermore, ECs co-cultured over SMCs have indicated greater presence of anti-thrombogenic genes under flow, including Krüppel-like Factor-2 (KLF-2), endothelial nitric oxide synthase (eNOS), and thrombomodulin[40,41].

Vascular SMCs co-cultured with ECs were found to enhance the assembly of focal adhesions in ECs by decreasing the microtuble to tubulin ratio of ECs, which lowered the stability of the microtubule cytoskeleton polymerization state. Furthermore, both ERK and paxillin exhibited increased phosphorylation in ECs co-cultured with vascular SMCs for 12 hours, which was an effect specific to vascular SMCs[42]. Communication of ECs with SMCs may be performed either through a direct mechanotransduction pathway or through signaling from growth factors in the microenvironment. Cytokines such as PDGF-BB and TGF-β1 produced by ECs due to

shear stress may have impacts on the SMCs below them[43]. Furthermore, endothelial cell plasminogen activator inhibitor-1 (PAI-1) may modulate flow-induced SMC migration, preventing intimal thickening in a healthy artery[44].

Gap junctions, comprised of connexin (Cx) proteins, mediate intercellular communication through small molecule transport[45]. Cx37, Cx40, Cx43, and Cx45 are abundantly expressed within the vasculature[46]. Under atherosclerotic conditions, Cx43 and Cx40 are upregulated in synthetic SMCs[47,48], while Cx37 and Cx40 are downregulated in endothelium[49].

1.5 Cell Sources for Vascular Tissue Engineering

Vascular SMCs are typically isolated from explanted arteries using a collagenase digestion. SMCs within healthy, mature vasculature express contractile proteins smooth muscle α-actin (α-SMA), calponin, SM-22α, caldesmon, smooth muscle myosin heavy chain, and smoothelin[22]. However, SMCs typically have limited proliferation capacity and are therefore not usually a viable source of autologous cells for a tissue engineered blood vessel. Alternative sources of smooth muscle cells for tissue engineering applications include human neonatal dermal fibroblasts[50] or mesenchymal stem cells. Mesenchymal stem cells are commonly derived from human bone marrow or adipose tissue, and may exert immunoprotective effects, making them a potential allogeneic source of cells for tissue engineering applications[51].

Autologous ECs are most commonly obtained from patients through invasive methods such as trypsin or collagenase digestion from a patient's excised jugular, radial, or saphenous vein, or by obtaining microvascular ECs from liposuctioned adipose tissue[52]. Since adult vascular cells such as SMCs and ECs have limited expansion capabilities of about 70 cell cycles, obtaining the necessary amount of cells to cover a TEVG is difficult, and will increase production time, costs, and reduce shelf life of the grafts. Despite the recent push for an "off-the-shelf" TEBV comprised of biodegradable synthetic polymer scaffolds that will be repopulated with cells *in situ*, preconditioned vascular grafts seeded with autologous cells from the patient have the greatest potential toward creating a vasoresponsive TEBV. Adult stem and induced pluripotent stem cells have great potential for use in TEBVs[53]. Induced pluripotent stem cells (iPSCs) may be reprogrammed into ECs[54]. Fibroblasts have also been directly reprogrammed into ECs capable of reendothelializing decellularized vessels[55]. Bone marrow-derived mesenchymal stem cells (MSC) may be differentiated into both endothelium and smooth muscle cells, allowing MSCs from one patient to be used in TEBVs as both the endothelium and the medial cell source[56].

Since their initial discovery in 1997[57], peripheral blood-derived endothelial progenitor cells (EPCs), have been extensively explored as an endothelium source for TEBVs. EPCs home to sites of injury and repairing endothelial damage[58] and promoting the formation of new blood vessels[59]. EPCs may be expanded *ex vivo* from umbilical cord

blood[41] and adult peripheral blood[60] and used to endothelialize vascular constructs[61,62]. EPCs were seeded on tubular fibrin scaffolds and remained adherent after short-term exposure to shear stress[63]. Late EPCs expressing characteristics of mature ECs may be isolated from the peripheral blood of CAD patients and used to improve the patency of small-caliber synthetic vascular grafts[64,65].

It is possible that ECs could play a significant role already in the remodeling of TEBVs *in vivo* – therefore, their homing properties to these sites should be studied extensively. EPCs deposit and remodel ECM to a greater extent than ECs. EPCs seeded in the elongated conformation representative of *in vivo* conditions deposited more laminin, fibronectin, and collagen IV after 24 and 48 hours than ECs[66]. Much remains to be studied regarding the true role of EPCs, and their identity as progenitor cells is still under question.

Primary human vascular cells may be readily differentiated toward a mature phenotype; however, their accessibility, proliferative capacity, and potential for aging and senescence limit their capacity for larger scale production applications. Induced pluripotent stem cells (iPSCs) have emerged as a viable alternative to primary cells within tissue engineered constructs. Adult stem and induced pluripotent stem cells have great potential for use in TEBVs[53], and provide the opportunity to evaluate constructs with all cell sources derived the same donor. Several techniques have emerged to reprogram iPSCs into ECs[54]. Fibroblasts have also been directly reprogrammed into ECs

capable of reendothelializing decellularized vessels[55]. Bone marrow-derived mesenchymal stem cells (MSC) may be differentiated into both endothelium and smooth muscle cells, allowing MSCs from one patient to be used in TEBVs as both the endothelium and the medial cell source[56]. Recently, our group and collaborators developed a TEBV from endothelial progenitor cells directly reprogrammed into functional smooth muscle cells.[67] While iPS cells hold great promise, a chief limitation is that they often do not express the phenotype of differentiated cells. Efforts are needed to ensure that iPS cells exhibit a similar phenotype to those in the native adult vessel wall. Some recent results with endothelial cells derived from iPS cells provide one strategy to promote differentiation of endothelial cells with highly specialized barrier function[68]. Recently, a technique was described to create iPSC-derived mature smooth muscle cells and endothelial cells within 6 days[69]. Adaptation of such protocols could lead to rapid production of TEBVs made from a single donor.

1.6 Tissue Engineered Blood Vessels

An ideal TEBV for MPS applications would be comprised of human cells in a biological or biodegradable synthetic matrix, have a small inner diameter to reduce fluid volumes, exhibit enough mechanical strength to withstand physiological stresses, and be produced rapidly to facilitate efficient drug screening. The medial wall cells should exhibit a smooth muscle phenotype, be quiescent and be able to contract and relax in

response to agonists or inhibitors. Most importantly, the TEBV must be endothelialized to enable physiologically relevant dilation and constriction in response to stimuli.

TEBVs comprised of human cells and natural matrix components would be an ideal replacement for integration with the native vasculature. However, endothelialization of TEBVs comprised of natural matrix components has been attempted with mixed results[70-74], and limited characterization of endothelial functionality[63,74]. TEBVs have been made from several natural matrix components, including fibroblast sheets[75], fibrin[29,50], and decellularized vessels[72], and while many indicate favorable results, they often require long culture times ranging from several weeks to several months in order to approach the mechanical properties of the native vasculature. Endothelialization of TEBVs comprised of natural matrix components has been attempted with mixed results[70-73] and limited characterization of endothelial functionality[63,74].

The adhesion of ECs to vascular grafts depends largely upon three factors: 1) the composition of the medial scaffold, 2) the presence and/or type of medial cells, and 3) mechanical preconditioning. The scaffold used for the TEBV media directly impacts the initial mechanical properties of the graft. Compliance mismatch is a primary mode of failure for small-diameter synthetic grafts, and finding the ideal medial scaffold material is not trivial. Early work in the field attempted to use collagen gels as the medial source for TEBVs[76]; however, the mechanical properties of these scaffolds were substantially

lower than a native artery. As a result, various other scaffold materials have been explored, including biodegradable polymers, decellularized arteries, and natural materials.

1.6.1 TEBVs Made from Biodegradable, Synthetic Polymers

Biodegradable scaffolds comprised of synthetic polymers such as poly(glycolic acid) (PGA), poly (ε-caprolactone), (PCL), poly(L-lactic acid) (PLLA) or combinations of these have been a popular option to develop a biological TEBV with high initial mechanical properties more closely resembling that of a native artery. Biodegradable, synthetic polymers were initially considered to serve as a temporary scaffold while the seeded cells matured and secreted their own ECM protein scaffold through remodeling. Early studies with biodegradable polymers attempted seeding the grafts with endothelium with varying degrees of success. Although studies of TEBVs seeded with ECs have indicated a confluent EC layer after in vivo implantation, it is unclear whether the ECs lining the lumen repopulated the graft during implantation or were part of the original source. For example, autologous ovine ECs were seeded onto woven PGA mesh grafts that were implanted as pulmonary artery interposition grafts. An EC layer was indicated after 11 weeks with Factor VIII staining; however the confluence and origin of the EC layer was not described[77]. Some evidence of endothelium has been indicated on PGA/PLLA grafts after 6 weeks of implantation in mice[78].

However, despite the moderate success of TEBVs made from biodegradable polymers in clinical studies[79], little is known about the mechanisms regulating the formation of neovascular tissue and remodeling of these TEBVs[80]. Recent advances in noninvasive monitoring techniques have allowed for the study of the mechanisms of neovessel development after implantation of biodegradable TEBVs. Hjortnaes et. al. used intravital fluorescence microscopy and histology to indicate that seeded GFP-labeled human MSCs were replaced by host murine cells after 35 days of implantation of a PGA-PLLA graft seeded with human MSCs and EPCs[81]. Serial MRI was used to evaluate the fate of seeded macrophages in venous grafts in a venous TEBV implanted in SCID/BG mice, indicating a total loss of signal and implying a loss of the implanted cells on to PGA mesh grafts[82].

Over time, endogenous cells eventually replace stem cells originally seeded into TEBVs made from biodegradable synthetic polymers after in vivo implantation, indicating a potential to take advantage of the inflammation and regeneration processes of endogenous cells to repopulate the lumen of TEBVs[83,84]. TEBVs were recently made with monocyte chemoattractant protein-1 (MCP-1)-releasing alginate beads intended to attract monocytes to the graft site and repopulate the graft via a remodeling-dependent pathway[85]. Recently, an electrospun graft with immobilized stromal cell derived factor-1α was created with the effort to recruit autologous EPCs and SMPCs to the graft[86].

Efforts to induce EPC homing toward biodegradable polymeric vascular grafts have recently been reviewed extensively[87,88].

1.6.2 TEBVs made from Decellularized Vessels

Decellularized vessels, either from allogeneic or xenogenic sources, have also been a widely attempted approach for TEBVs. In this approach, the extracellular matrix proteins left behind after a detergent wash comprise the scaffold for autologous cells, yielding a largely nonimmunogenic construct[89-91]. Partial endothelialization has been achieved using decellularized porcine aortas seeded with human ECs[73]. However, a medial layer of cells is often required for better endothelialization and function. Porcine aortas have been seeded with human myofibroblasts and peripheral vascular ECs, yielding a functional EC layer capable of NO production[92]. Decellularized canine arteries have been used as a scaffold for ECs and SMCs differentiated in vitro from bone marrow mononuclear cells. After 8 weeks of implantation in a canine model, grafts were able to remain patent and regenerate a vascular endothelium, media, and adventitia[93].

While grafts are often preconditioned to allow for development of greater mechanical strength with time, the maintenance of a confluent endothelial layer is often an afterthought and improperly characterized. The Niklason group fabricated experimental vascular constructs comprised of SMCs seeded on woven PGA scaffolds conditioned with pulsatile radial stress for 8 weeks. A suspension of ECs was injected

into the lumen of the grafts and allowed to adhere for 90 minutes, and grafts were conditioned for 3 more days before being implanted into pigs[94]. Grafts have also been constructed from poly(carbonate-urea)urethane scaffolds seeded with human vascular SMCs and ECs from cord blood vessels. Preconditioning of the SMCs with pulsatile stresses indicated a much greater retention of ECs on the lumen of the grafts in vitro[95]. Furthermore, dynamic co-culturing of SMCs and HUVECs led to greater integration and proliferation of SMCs into a decellularized arterial media, and greater confluence of endothelium[96].

A functional endothelial layer is important toward the maturation of a vascular graft. Decellularized arteries from sheep seeded with autologous ECs have yielded ECMs more closely resembling that of native tissue post-implantation as compared to bare decellularized vascular constructs[97]. This indicates that signaling from the implanted ECs has an effect on the ECM onto which they are adhered. While some groups have focused on the use of decellularized grafts due to their anti-thrombogenicity and off-the-shelf attractive qualities, bare decellularized grafts do not yield a vasoresponsive graft – which is important toward the complete inclusion of the graft into the vascular system[98]. Decellularized porcine arteries dual seeded with vascular SMCs and ECs exhibited greater wall maturation and greater contractile responses to phenylephrine and serotonin[99].

1.6.3 TEBVs Made from Natural Scaffolds

Medial scaffolds made from natural polymers such as collagen or fibrin have also been explored as substrates for TEBVs. Bilayered fibrin and SMC scaffolds were shown to require the presence of SMCs for contractility[100]. Blood outgrowth EPCs grown on remodeled fibrin scaffolds were found to adhere to the surface and deposit collagen IV and laminin[63]. Due to the highly collageneous environment in native vessels, collagen substrates have been explored as scaffolds for TEBVs. However, cell-mediated contraction of the collagen tends to occur, and the collagen scaffolds are typically not strong enough to meet the mechanical demands of the vasculature[76].

Recently, a new approach for the production of TEBVs that employs dense collagen gels has been published[101]. This approach embeds human airway SMCs into a collagen gel matrix that has been plastically compressed to increase the mechanical strength of the gel. These vessels have been shown to exhibit burst pressures around 1000 mm Hg after 1 week in perfusion culture. Dense collagen gels containing fibroblasts have been formed into tubular structures capable of remodeling over 7 days culture[102,103].

Endothelialization of vascular grafts may be accomplished *in vitro* through the seeding of ECs into the graft lumen, or *in situ* through migration of ECs from the neighboring native vessels at the anastomosis site or repopulation of the graft lumen by circulating EPCs from the peripheral blood[104]. The endothelial coverage on TEBVs has

not been as well characterized as it has been on synthetic vascular grafts[105-109], and much of the data reported has been mostly qualitative. Table 1 summarizes the current literature regarding the endothelialization of TEBVs. While many groups have reported confluent coverage initially *in vitro*, the endothelium does not remain confluent over long periods of *in vitro* conditions. Furthermore, while other groups have reported a confluent endothelium upon explantation after *in vivo* conditions, it is difficult to ascertain the origin of the ECs attached to the lumen of the graft.

Table 1: Endothelialization of Vascular Grafts

Medial Source	EC Source	EC Coverage Characterization	Resulting EC Coverage	Ref.
SMCs and fibroblasts in a collagen mold with a Dacron support	Bovine aortic ECs	H&E	Qualitative assessment – 92% coverage stated	[76]
Woven PGA scaffolds with SMCs	Bovine aortic ECs	SEM	Qualitative assessment: partial endothelialization	[94]
Decellularized porcine aorta	Human ECs	SEM, H&E, Factor VIII or CD31 staining	Qualitative assessment: partial endothelialization	[73]
PGA grafts seeded with ovine vascular myofibroblasts	Ovine ECs	H&E, Factor VIII staining	Qualitative assessment: representative image	[110]
Decellularized porcine iliac vessels	Ovine EPCs	Fluorescence microscopy	80% after 10 days, 10% after 130 days	[111]
Collagen fiber mesh with polyurethane film	Canine EPCs	SEM images, H&E, Factor VIII staining	Qualitative assessment – representative image	[62]
Decellularized rat arteries	Rat ECs	SEM, H&E, vWF staining	Qualitative assessment: representative image	[112]
Human dermal fibroblast sheets from CVD patients	Saphenous vein ECs	TEM, vWF staining	Qualitative assessment – representative image	[113]
Remodeled fibrin-based scaffolds by rat aortic SMCs	Rat aortic ECs	ECs were labeled with DiI-Ac-LDL	>98% surface coverage after 2 days, >75% after 21 days.	[114]
Bi-layered collagen I membrane with SMCs	Rat ECs	H&E Staining	Qualitative assessment – representative image	[115]
Cryopreserved arteries treated with polyelectrolytes	HUVECs	SEM, H&E, vWF and PECAM staining	Qualitative assessment – representative image	[116]

Medial Source	EC Source	EC Coverage Characterization	Resulting EC Coverage	Ref.
Tubular fibrin scaffold	EPCs	SEM, vWF staining	Qualitative assessment - representative image	[117]
Decellularized canine ureters with myofibroblasts	Canine ECs	Factor VIII staining	Qualitative assessment – representative image	[118]
Canine granulation tissue	Canine aortic ECs	SEM, H&E, TEM	Qualitative assessment- representative image	[70]
RGDS-containing PEGDA hydrogels	Bovine aortic ECs	Ac-LDL uptake	Qualitative assessment – representative image	[119]
Decellularized ovine arteries with SMCs derived from MSCs	ECs derived from MSCs	SEM, H&E, fluorescence	Qualitative assessment – representative image	[56]
PGA-PLLA matrix with 3:1 human MSCs and EPCs	Cord blood EPCs	GFP labeling of MSCs and EPCs, H&E, CD31	Qualitative assessment – representative image	[81]
ECM from dermal fibroblasts seeded in fibrin gels	Human Blood Outgrowth ECs (EPCs)	Cell coverage after 20 min various shear stress,	94.4% coverage after 20 min 25 dyn/cm^2 shear stress	[63]
PGA matrix seeded with SMCs and decellularized	Autologous human ECs	Light microscopy	Qualitative assessment: 0 to 60% coverage	[72]
PGA matrix seeded with SMCs and decellularized	Porcine EPCs or ECs	GFP-labeling of EPCs/ECs	64 ±9% coverage	[91]
Decellularized porcine carotid artery with human SMCs	Human vascular ECs	SEM, CD31 staining	Qualitative assessment – representative image	[98]
Decellularized porcine arteries with sheep SMCs	HUVECs	GFP-labeling of HUVECs	Qualitative assessment – representative image	[96]

1.7 Atherosclerosis and Endothelial Dysfunction

Atherosclerosis has both inflammatory and mechanical origins[120-122] and is promoted by high levels of blood cholesterol transported by low-density lipoprotein (LDL). Excess LDL may be trapped in the vascular intima and oxidized (oxLDL), activating the endothelium and initiating an inflammatory response[123]. Activated endothelial cells express Vascular Cell Adhesion Molecule-1 (VCAM-1), Intracellular Adhesion Molecule-1 (ICAM-1), and E-selectin on their luminal surface and secrete chemokines to attract monocytes and T-lymphocytes to the lesion site[124]. The resulting inflammatory environment facilitates the development of a lipid-rich plaque and SMC over-proliferation, leading to an atherosclerotic lesion[125].

The adaptive immune response plays a substantial role in the progression of atherosclerosis. Pro-inflammatory cytokines differentiate naïve CD4+ T-cells into various proatherogenic and atheroprotective T-helper subtypes that produce IFN-ϒ and TNF-α or IL-10 and TGF-β, respectively[126]. TNF-α plays a substantial role in activation of endothelial cells and vascular wall cells during inflammation[127]. IL-4 synthesized by T-cells may play an anti-atherosclerotic role by inhibiting SMC growth and promoting production of matrix metalloproteinases[128], and by reducing histamine production in the arterial wall, downregulating production of LOX-1 genes that promote phagocytosis of oxidized lipids by monocytes and T-cells in the vascular intima[129].

Vascular elasticity decreases with age and in atherosclerosis[130,131] due to endothelial dysfunction, increased collagen I production, broken elastin fibers, and an over-proliferation of vascular SMCs[132-134]. Contractile SMCs in the medial wall of healthy arteries express α-smooth muscle actin (α-SMA), calponin, and smooth muscle myosin heavy chain[22]. Vascular SMCs under atherosclerotic inflammatory conditions de-differentiate toward a synthetic phenotype that produces extracellular matrix (ECM) proteins such as collagen I and fibronectin[125,135] due in part to cytokines released from activated macrophages such as interleukin-8 (IL-8)[136], IL-18[137], and tumor necrosis factor-α (TNF-α)[138]. Arterial stiffening increases endothelial permeability to LDL and monocytes[139].

The vascular endothelium lines the inner surface of all blood vessels, making contact with blood and regulating thrombosis, permeability and vascular tone. The endothelium modulates vasodilation through release of nitric oxide and prostacyclin in response to changes in flow or stimuli with vasoactive compounds such as acetylcholine[140]. Vasodilation of the coronary or brachial arteries after an infusion of acetylcholine can be used to assess endothelial dysfunction and predict future cardiac events[141]. The vasoconstrictor endothelin-1 is produced during inflammation or in low shear stress environments and its receptors are upregulated during disease[142]. Hypertension, diabetes mellitus[143] hypercholesterolemia[144], and complications from

chronic smoking[145] induce endothelial activation and dysfunction, leading to reduced vasodilation in response to changes in flow and ultimately atherosclerosis[120].

Damage to the endothelium is caused by reactive oxygen species (ROS). Low and moderate levels of ROS promote inflammation by activating the transcription factor NF-κB, which regulates a number of pro-inflammatory genes. Further, ROS decrease the activity of nitric oxide synthase and react with nitric oxide to form peroxynitrite, resulting in reduced NO concentration and impaired vasodilation. Reduced NO bioavailability triggers endothelial activation and promotes the production of pro-inflammatory cytokines such as tumor necrosis factor – α (TNF-α) and interleukin-6 (IL-6). Activated endothelium express cell surface adhesion molecules such as VCAM-1, ICAM-1, and E-selectin on their surface, promoting adhesion of leukocytes to the vascular wall[146].

1.8 Microphysiological Systems

In 2012, the Microphysiological Systems Program was created by the National Center for Advancing Translational Sciences (NCATS), funded by the National Institutes of Health (NIH) and the NIH Common fund, in addition to efforts by the Defense Advanced Research Projects Agency (DARPA) began an initiative to create microphysiological systems, or organs on chips, with the ultimate goal being to create physiologically relevant human tissues as an alternative to monolayer cell cultures or

animal studies. Ultimately, the goal was to study drug and environmental toxicology on human organs to reduce the loss of viable drug candidates in the drug development pipeline. Two-dimensional cell monolayer cultures fail to recapitulate the complex interactions between cells and their matrix, other cells, and the tissue and organ microenvironment[8].

Studying cells in 3D environments is an important step toward understanding their behavior *in vivo*, as cell behavior can vary from 2D to 3D matrices. Studies of smooth muscle cells in 3D collagen type I gels have indicated a reduction in cell proliferation relative to 2D cultures and a down-regulation of the expression of smooth muscle α-actinin (SMA)[147]. Furthermore, the effects of growth factors and other signaling proteins may be affected in 3D matrices. For example, TGF-β and PDGF effects on smooth muscle actin expression are less marked in 3D collagen gels, while SMCs tend to increase collagen synthesis and reduce FAK phosphorylation in 3D vs. 2D collagen gels[148]. However, just as with 2D substrates, the substrate chemistry can have substantial effects on the cell reaction. Introduction of TGF-β and insulin in 3D fibrin gels increases the mechanical properties of the gel due to increased collagen production by SMCs[149]. Much of the work that has been conducted in 2D models must be adapted to 3D models to obtain a clearer understanding of the effects *in vivo.* Shear effects on cell co-cultures have been investigated in 3D matrices with an endothelial cell monolayer and embedded vascular SMCs[150].

Microphysiological systems have been created for a variety of organ systems, both individually and interconnected. Most systems are based on the simplest functional organ unit that replicates tissue-specific architecture and a subset of tissue functions to allow predictive *in vitro* studies of normal physiology and disease[151]. Disease modeling is critical toward understanding the mechanisms and evolution of human diseases. Microphysiological systems provide the benefit of understanding the progression of diseases within the context of an accurately recapitulated 3D tissue microenvironment. Furthermore, for the first time, phenotypic changes on the cellular level can be coupled with measureable changes in tissue function. While previously this was only feasible with *ex vivo* animal models, we can now use tissues derived from human cells to measure changes in function in real time.

1.9 In vitro Models of Endothelial Dysfunction

Activation of an endothelial monolayer with tumor necrosis factor-α (TNF-α) is a common model used to study endothelial response to inflammation[139,152]. Other studies have evaluated the effect of SMC presence on endothelial activation in indirect[153] and direct[154] co-culture models. Indirect co-culture with a synthetic SMC layer leads to greater endothelial activation, while direct co-culture with a quiescent, contractile SMC layer attenuates the activation response to TNF-α. Recently, a microfluidic chip system with endothelium grown in microchannels activated with TNF-α was used to simulate

endothelial microvasculature with increased permeability[155]. Endothelial monolayers have also been treated with a combination of TNF-α and freshly isolated triglyceride-rich lipoproteins isolated from the blood plasma of normal volunteers and hypertriglyceridemic patients after a high-fat meal to evaluate the effect of triglyceride-rich lipoproteins on the expression of VCAM-1 in endothelium[156]. These studies focus on the impact of inflammatory molecules toward increasing endothelial dysfunction. These studies have created invaluable tools for the isolation of variables in the atherosclerotic pathway. However, despite the inclusion of immune cells and inflammatory molecules, two-dimensional cell culture models on hard plastic substrates do not properly recreate the environment of the native vasculature. Recently, the first three-dimensional tissue-engineered artery model for atherosclerotic conditions was introduced[157], consisting of a TEBV with endothelium activated with either TNF-α or LDL. The adhesion and extravasation of circulating monocytes was evaluated.

Using endothelialized human TEBVs enables the potential cause of inflammation and injury of the vessel wall to be assessed with human cells under physiological conditions. Furthermore, *in vitro* models provide the capacity to isolate and manipulate variables within the tissue microenvironment to evaluate specific tissue responses. For example, leukocytes can be added in the presence of pro-inflammatory cytokines such as tumor necrosis factor – α to examine the effect of a drug candidate toward mediating the inflammatory response. By directly comparing TEBVs made with either animal cells or

human cells, it may be possible to determine the differential response to drugs that produce DIVI in animals but not humans. Finally, iPS cells could be differentiated into smooth muscle cells and endothelium, and used to produce TEBVs with cells from the same individual to examine the effect of genetic variations upon drug responses. Such TEBVs could be used to examine therapeutic solutions for specific patient populations.

1.10 Overview of the Dissertation

In **Chapter 2**, we discuss Specific Aim 1, which assessed the potential for CAD EPCs to behave similarly to mature endothelial cells over a confluent, quiescent smooth muscle cell (SMC) layer. We evaluated the potential for CAD EPCs to form networks and confluent monolayers over a confluent, quiescent SMC layer in a direct 2D co-culture model previously developed in our lab. We also evaluated the potential for CAD EPCs to align with flow over SMCs and compared the effects of blocking integrins toward their adhesion to a confluent SMC layer. This work demonstrated that CAD EPCs exhibit similar adhesion properties to HAECs and are suitable for use in a tissue engineered blood vessel model or in other autologous implantation applications.

In **Chapter 3**, we discuss Specific Aim 2, in which we developed a human vascular microphysiological model for drug screening. We created a small-diameter tissue engineered blood vessel by embedding human neonatal dermal fibroblasts (hNDFs) within a collagen gel that was plastically compressed to increase the fiber

density. We evaluated the mechanical stability and burst pressure of the TEBVs, and noted that addition of endothelium increased the burst pressure. We evaluated the extracellular matrix and contractile protein expression of the hNDFs within the TEBVs. We also adapted a clinically relevant technique to assess the vasoactivity of the TEBVs using both endothelium-independent and endothelium-dependent compounds *in situ*, allowing us to monitor the health of the TEBV in real time over the course of several weeks. Lastly, we assessed the response of the TEBVs to phosphodiesterase inhibitors caffeine and theophylline, demonstrating the capacity of our vasoactive TEBV model to respond to various drug stimuli.

In **Chapter 4**, we discuss Specific Aim 3, in which we evaluated the response of CAD EPCs to the pro-atherosclerotic cytokine tumor necrosis factor – α (TNF-α). We evaluated the expression of the adhesion molecules VCAM-1, ICAM-1, and E-selectin within the TEBV. We also characterized the change in endothelial-specific vasoactivity elicited by acute exposure to 200 U/mL TNF-α. Lastly, we evaluated the response of the TEBV to three statins: lovastatin, atorvastatin, and rosuvastatin, in order to assess the pleiotropic effects of statins on the TEBV. We assess the changes in vasoactivity and nitric oxide production of the TEBVs. We evaluate the behavior of CAD EPCs as well as EPCs from young, healthy volunteers within the TEBV model, assessing their response and recovery from a high dose of TNF-α after treatment with rosuvastatin.

In **Chapter 5**, we provide a summary of the main findings of this work, and discuss the specific implications this work has toward the field of cardiovascular medicine, tissue engineering, and *in vitro* disease modeling. Lastly, we discuss several avenues for future work within this tissue model.

2. Late Outgrowth Endothelial Progenitors from Patients with Coronary Artery Disease: Endothelialization of Confluent Stromal Cell Layers

Text and figures presented in this chapter have been previously published in the following form: Fernandez CE, Obi-onuoha IC, Wallace CS, Satterwhite LL, Truskey GA, Reichert WM. Late Outgrowth Endothelial Progenitors from Patients with Coronary Artery Disease: Endothelialization of Confluent Stromal Cell Layers**.** *Acta Biomaterialia* 10 (2), 893-900 (2014)[158]. License information can be found in Appendix A.

2.1 Introduction

Growing an intact layer of autologous endothelium in the lumen of small diameter blood vessel substitutes has been a long-sought goal in cardiovascular medicine[87,159,160]. The adhesion and proliferation of endothelial cells (ECs) onto the lumen of synthetic vascular grafts has been well characterized[105-109]; however, forming a layer of intact endothelium on the luminal surface of tissue engineered blood vessels (TEBVs) has been met with varying degrees of success inconsistent results have been reported[72,73,111,113,116].

Autologous ECs are most commonly obtained from patients through invasive methods such as trypsin or collagenase digestion from a patient's excised jugular, radial, or saphenous vein, or by obtaining microvascular ECs from liposuctioned adipose

tissue[52]. In contrast, cultured endothelial progenitor cells (EPCs) obtained from patient peripheral blood offer a noninvasive source of autologous ECs.

EPCs were first reported by Asahara *et al.*[57]. Depending on the method of culture, EPCs may be defined as colony forming unit ECs (CFU-ECs) or blood outgrowth endothelial cells (BOECs)[60]. CFU-ECs appear earlier in the *ex vivo* expansion process, and differentiate into monocytic cells that can exhibit phagocytosis, and can function as antigen presenting cells[161]. BOECs appear at least two weeks later during *ex vivo* expansion[162] and appear phenotypically as endothelial cells that exhibit robust proliferation capacity. Because of their early and late appearance during ex vivo expansion, CFU-ECs and BOECs, respectively, are more simply referred to as "early outgrowth" and "late outgrowth" EPCs[163].

Our group has characterized the phenotypic properties of late outgrowth EPCs derived from the peripheral blood of patients with significant coronary artery disease (CAD)[64]. These "CAD EPCs" were shown to have similar proliferative capacity and surface antigen expression to late outgrowth EPCs derived from healthy patients. Further, they function similar to EPCs derived from healthy individuals and human aortic endothelial cells. We have also shown that CAD EPCs may be successfully grafted onto the lumen of small diameter ePFTE vascular grafts, and that the CAD EPC treated grafts dramatically improved the short and long term patency compared to bare grafts in a rodent femoral artery model[164].

Late outgrowth EPCs have been studied as a cell source for TEBV endothelialization because of their ease of isolation from peripheral blood. The majority of work on the attachment and growth of late outgrowth EPCs on the stromal cells that make up the TEBV media has involved cord blood derived EPCs (CB EPCs)[41,165,166]. These studies mainly out of the Truskey group have shown that CB EPCs have the capacity to be cultured to confluence over human aortic smooth muscle cells (SMCs)[41]. Late outgrowth EPCs from healthy volunteers have also been seeded over medial surfaces made of dermal fibroblasts entrapped within tubular fibrin gels[63].

Individuals with CAD are the primary candidates for receiving an endothelialized small-diameter TEBV, and therefore the target source of autologous cells. While much of the work on EPCs involves cells isolated from healthy individuals, understanding the behavior of peripheral blood EPCs isolated from CAD patients is critical toward the implementation of autologous endothelium for TEBVs. In the current study, we examined if CAD EPCs also have suitable capacity to be cultured to confluence using the same direct co-culture system employed for CB EPCs and HAECs[39-41]. CAD EPCs were evaluated for their potential to create and maintain a confluent endothelium, and their ability to align and produce nitric oxide after exposure to long-term laminar shear stress. The strength of cell adhesion was evaluated by assessing cell retention after exposure to a burst of high shear stress. Additionally, the adhesive

properties of CAD EPCs over confluent, quiescent SMCs were evaluated by blocking with various integrin antibodies. Parallel studies were also performed using HAECs.

2.2 Materials and Methods

2.2.1 Cell Isolation and Culture

The Duke University Institutional Review Board approved a protocol for collection of human blood from consenting patients undergoing left heart catheterization at Duke University Medical Center. All patients were males over the age of 55 with advanced CAD documented by angiography. CAD EPCs were isolated and grown as previously stated [64,167] Approximately 50 mL of blood was diluted 1:1 with Hanks balanced salt solution (HBSS; Gibco). Equal volumes of blood-HBSS mixture was slowly layered over an equal volume of Histopaque (Sigma) and centrifuged at 740 g for 30 minutes. Afterward, the platelet-rich plasma layer was aspirated, and the buffy coat cells collected and washed with complete EC media. Mononuclear cells were plated onto 6-well TCPS plates (BD Biosciences) pre-coated with 50 μg mL^{-1} rat tail collagen type I (BD Biosciences) in 0.02 N acetic acid. For the first 7 days after isolation, media was changed daily to remove non-adherent cells. Colonies of CAD EPCs appeared two weeks post-isolation. Colonies were passaged onto TCPS T-25 flasks (BD Biosciences) and allowed to grow to confluence. CAD EPCs were proliferative and exhibited healthy morphology through P11.

Human Aortic Endothelial Cells (HAECs) were purchased from Lonza (Walkersville, MD). Cells were passaged every 4 days. Both CAD EPCs and HAECs were maintained in EC media described below. Smooth muscle cells were purchased from Lonza and maintained in SMC growth media. A low trypsin concentration was used as previously indicated to increase EC adhesion to substrates[168]. All cells were passaged with 0.025% trypsin/EDTA (Lonza) and trypsin neutralizing solution (Lonza). SMCs were plated on T-75 flasks (BD Biosciences) that had been coated with 10 $\mu g\ mL^{-1}$ human serum fibronectin (Millipore) for one hour. Media was changed every other day. CAD EPCs, HAECs, and SMCs were used from passage 6 to 10. CAD EPCs from four different donors were used.

2.2.2 Cell Media

CAD EPCs and HAECs were maintained in EC media comprised of Endothelial Basal Medium-2 (EBM-2) with EGM-2 Single Quots kit (Lonza) supplemented with 10% heat-inactivated fetal bovine serum (HI-FBS) (Gibco) and 1% Pen/Strep (Lonza). SMCs were maintained in Smooth Muscle Basal Medium (SmBM) supplemented with SmGM-2 Single-Quots kit (Lonza). The quiescent phenotype of SMCs was induced using a serum-free media made of DMEM/F-12 (Lonza) with 1x Insulin-Transferrin-Selenium supplement and 1% Pen/Strep. Co-cultures were maintained after 24 hours of EC seeding in co-culture media made from EBM-2 supplemented with 3.3% HI-FBS and 1% Pen/Strep. Flow studies were conducted with flow media made from low glucose

DMEM supplemented with 3.3% HI-FBS, 1x Insulin-Transferrin-Selenium supplement, and 1% Pen/Strep.

2.2.3 CAD EPC/HAEC Co-Culture with SMCs

CAD EPCs and HAECs were directly cultured over SMCs as previously described[40]. Briefly, SMCs were seeded at a density of at least 70,000 cells/cm^2 and allowed to become confluent. Quiescent phenotype was induced after 24 hours in culture by changing media to serum-free quiescent media. Cells were maintained in quiescent media for 1-2 days, and then ECs were seeded at various densities in EC media. For co-cultures lasting longer than 24 hours, media was changed to co-culture media after 24 hours and changed every other day. Cells were maintained in an incubator at 37 °C and 5% carbon dioxide/ 95% air.

2.2.4 CAD EPC/HAEC Confluency Measurements

CAD EPCs were evaluated for their potential to maintain a confluent endothelium over a confluent, quiescent SMC layer compared to HAECs. HAECs and CAD EPCs were stained with 2 μM Cell Tracker Green (CMFDA) and seeded over confluent, quiescent SMCs at 30,000, 50,000, 70,000, 90,000, and 110,000 cells/cm^2. Co-cultures were imaged at day 1, 3, 5, and 7 with fluorescence microscopy. ECs were stained with Ac-LDL-DiI at day 5 after the CMFDA had metabolized. Five random images per sample were taken using fluorescence microscopy at 10X magnification (Nikon TE2000U, Tokyo, Japan) and digital camera (DS-Qi1Mc, Nikon) at day 1, 3, 5 and

7. On day 7 cells were washed with DPBS and fixed in methanol for 10 minutes at -20 °C. Cells were rinsed with DPBS and incubated with 10% goat serum (Gibco) for 30 minutes at room temperature to block non-specific binding. ECs were incubated with mouse anti-human primary antibody (Platelet-EC adhesion molecule, 1:200, BD Pharminogen) in 10% goat serum for 1 hour at room temperature. Cells were rinsed several times with DPBS and incubated with a goat anti-mouse Alexa Fluor 488 secondary antibody (1:500, Invitrogen) in 10% goat serum for 1 hour at room temperature. Samples were rinsed with DPBS and maintained in VectaShield (Vector Labs) containing DAPI. Each experiment was performed three times. Confluence of the cultures was analyzed using Image J software (version 10.2, National Institutes of Health, Bethesda, MD) and normalized to 100% confluence over SMCs.

2.2.5 Parallel Plate Flow Chamber

A previously described parallel-plate flow chamber connected to a circular flow loop was used for both the long-term flow studies as well as the short-term cell adhesion studies[39]. A steady, laminar fluid flow provided the desired wall shear stress (τ_w, defined in Equation 1).

$$\tau_w = \frac{6\mu Q}{wh^2} \quad (1),$$

where Q is the volumetric flow rate, μ is the fluid viscosity (0.86 Cp), w is the channel width (1.9 cm) and h is the local channel height (212 μm).

2.2.6 Strength of Adhesion Study

The strength of adhesion of CAD EPCs and HAECs over confluent, quiescent SMCs were compared in the parallel plate flow chamber. Slide flasks (Nunc) were seeded with SMCs as described above. CAD EPCs or HAECs were stained with Calcein-AM and seeded subconfluently over confluent, quiescent SMC surfaces at a density of 20,000 cells/cm^2 to easily visualize individual adhered cells and the co-culture was sealed into the flow chamber. Cells were allowed to adhere for either 15 minutes or 24 hours and then exposed to a steady laminar shear stress of 100 dynes/cm^2 for 10 minutes. This supraphysiological level of shear stress was used to demonstrate the strength of adhesion of the ECs. Ten random images per sample were taken on a fluorescence microscope at 4x. Adhered cells before and after exposure to shear stress were counted with ImageJ software. The percentage of cells retained was determined by dividing the average number of remaining cells post-flow by the average number of cells initially adhered.

2.2.7 Cell Alignment under Flow

The alignment of CAD EPCs and HAECs over confluent, quiescent SMCs was measured in the parallel plate flow chamber. SMCs were seeded on slide flasks and allowed to become confluent and quiescent as described above. CAD EPCs or HAECs were seeded over confluent, quiescent SMCs at 110,000 cells/cm^2 in EC media. After 24 hours, the media was changed to co-culture media. Co-cultures were maintained

another 24 hours, sealed into the flow chamber, then exposed to a physiological level of steady laminar shear stress of 15 dynes/cm^2 for 48 hours. A static control was maintained in flow media for 48 hours.

Samples were fixed in methanol for 10 minutes at -20 °C. Confluence and alignment of ECs was evaluated by examining the presence of platelet-EC adhesion molecule (PECAM) within the cell junctions. Cells were rinsed with DPBS and incubated with 10% goat serum (Gibco) for 30 minutes at room temperature to block non-specific binding. ECs were incubated with mouse anti-human primary antibody (PECAM, 1:200, BD Pharminogen) in 10% goat serum for 1 hour at room temperature. Cells were rinsed several times with DPBS and incubated with a goat anti-mouse Alexa Fluor 488 secondary antibody (1:500, Invitrogen) in 10% goat serum for 1 hour at room temperature. Samples were rinsed with DPBS and maintained in VectaShield (Vector Labs) containing DAPI and covered with a cover glass. Each sample was imaged using a Zeiss LSM 510 inverted confocal microscope at 20X. Four random images per sample were taken and fifteen random cells per field-of-view were analyzed for cell roundness and cell orientation angle with ImageJ as previously described[41]. Cell roundness was calculated using the following equation:

$$Roundness = \frac{4A}{\pi L^2} \quad (2),$$

where A = the cell area measured, and L = maximum chord length. A cell roundness of 1 refers to a circle, and a cell roundness of 0 refers to a straight line, where roundness

values closer to 0 indicate more elongated cells. The cell orientation angle was computed in reference to 0° being the flow direction, where an angle of 0° indicated complete alignment and an angle of 45° indicates no alignment.

2.2.8 Nitric Oxide Quantification

Production of nitric oxide (NO) by CAD EPCs seeded over confluent, quiescent SMCs was evaluated through direct measurement of nitrite (NO_2^-), a stable byproduct of NO oxidation in the presence of oxygen. At the 48-hour time point 100-μL media samples were collected from the CAD EPC cell alignment studies for both cells exposed to flow and static controls. Media samples were frozen down to -80 °C immediately following collection. Samples were later brought to room temperature and an Ionics/Sievers Nitric Oxide Analyzer (NOA 280, Sievers Instruments, Boulder, CO) was used to measure the nitrite concentration using chemiluminescence as previously described[169]. Nitrite concentrations released per million CAD EPCs seeded were evaluated as a representation of nitric oxide production under flow as previously described[170]. Three samples per condition were analyzed.

2.2.9 Integrin Blocking Assays

The integrin binding of CAD EPCs and HAECs was evaluated by blocking with anti-integrin antibodies as previously demonstrated[171]. CAD EPCs or HAECs were stained with Cell Tracker Green CMFDA, trypsinized, and resuspended in DPBS (Gibco). ECs were then incubated with 10 μg/mL mouse-anti-$\alpha_5\beta_1$, 20 μg/mL mouse-

anti-$\alpha_v\beta_3$ antibodies (Abcam), alone or in combination, for 30 minutes at 37 ºC with gentle rotation. Controls were ECs incubated with DPBS.

Cells were seeded onto confluent, quiescent SMCs in 48-well TCPS culture plates (BD Biosciences) at a density of 20,000 cells/cm^2 and allowed to adhere in a humidified incubator at 37 °C for 15 minutes, then rinsed with DPBS and fixed with 3.7% paraformaldehyde at room temperature for 10 minutes. Cells were imaged on a fluorescent microscope at 10X. Ten images per well were captured and analyzed for the number of cells adhered using ImageJ.

2.2.10 Statistical Analysis

Results are expressed as mean ± SEM. Statistical analyses were performed using MATLAB (MathWorks, version R2012a). A two-way analysis of variance (ANOVA) followed by Tukey-Kramer post-hoc tests or student's t-test with a Bonferroni correction was used to determine the significance between groups. All measurements were performed in triplicate.

2.3 Results

2.3.1 CAD EPC Confluence over SMC in Co-Culture

CAD EPCs or HAECs were seeded over confluent, quiescent SMCs and evaluated at 1 (24h) and 7 days for the formation and maintenance of a confluent endothelium (Figure 1). Networks characteristic of EC vessel formation were most

prevalent at low seeding densities for CAD EPCs and HAECs, both of which transitioned to confluence with increased seeding density. The average percent cell coverage of both CAD EPCs and HAECs on SMCs increases steadily with seeding density. Two-way ANOVA tests showed these trends to be significantly different between CAD EPCs and HAECs for both 1 day and 7 days ($p<0.05$). On average CAD EPCs also exhibited greater percent coverage over SMCs for all but one seeding density at both 1 and 7 days; however, this difference within a given seeding density was only statistically significant at 110,000 cells/cm^2 for both 1 day and 7 days ($p < 0.05$, student's t-test with Bonferroni correction), with the largest difference occurring at 7 days ($87.65 \pm 1.67\%$ confluence CAD EPCs v. $63.03 \pm 0.89\%$ confluence for HAECs).

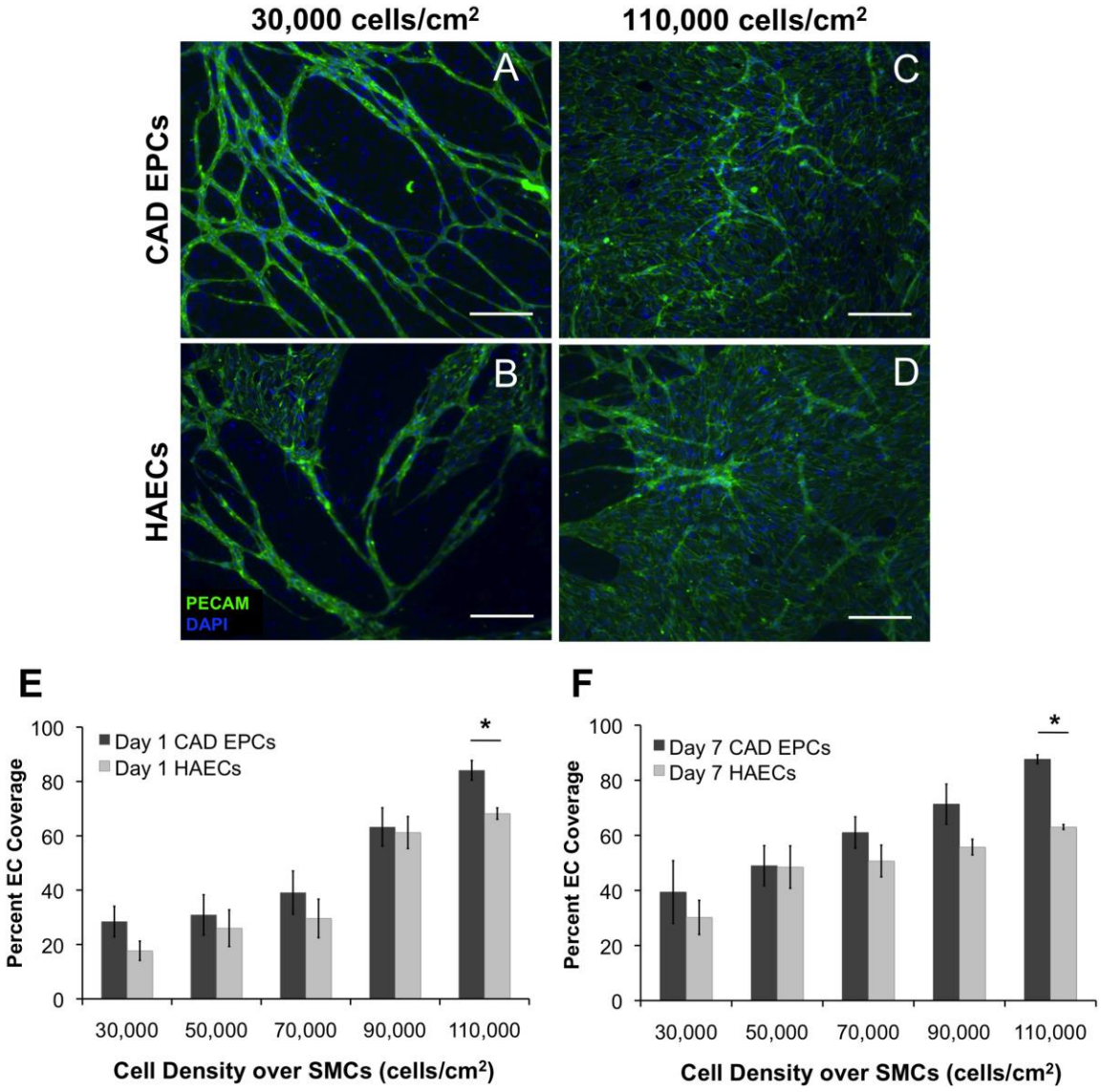

Figure 1: Co-culture of CAD EPCs or HAECs with SMCs for one week.

A-J: representative images of co-cultures after 7 days. ECs are stained with PECAM antibody. EC and SMC nuclei are stained with DAPI. Scale bars represent 100 μm. Bottom: percent EC coverage after one day (K) and seven days (L), normalized against 100% coverage. A two-way ANOVA indicated significant effects due to both cell density and cell type ($p < 0.05$, n=3).

2.3.2 Percent Retention

CAD EPCs and HAECs seeded subconfluently over SMCs were allowed to adhere for 15 minutes or 24 hours and then exposed to 100 dynes/cm^2 shear stress for 10 minutes. Seventy to 80% of both CAD EPCs and HAECs remained attached after 15 minutes and greater than 90% remained attached after 24 hours (Figure 2). The difference in percent retention between 15 min and 24 hours was significant for both CAD EPCs and HAECs ($p < 0.05$).

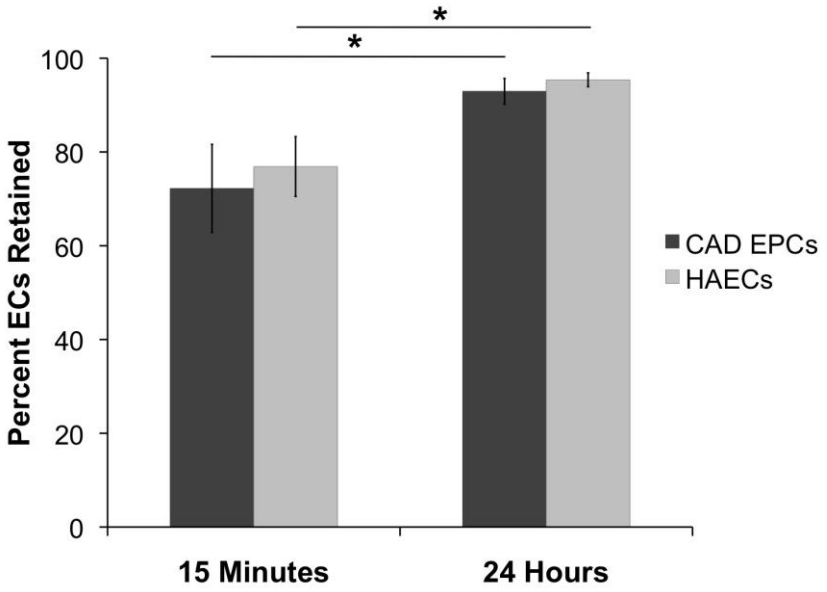

Figure 2: Cell Retention after Supraphysiological Shear Stress.

CAD EPCs or HAECs cultured over SMCs for either 15 minutes or 24 hours were exposed to 10 minutes of 100 dynes/cm^2 steady, laminar shear stress. Both CAD EPCs and HAECs experienced greater adhesion to SMCs after 24 hours (*$p < 0.05$, $n = 3$).

2.3.3 Cell Alignment under Flow and in Static Conditions

The alignment (cell orientation angle) and elongation (cell roundness) of CAD EPCs and HAECs over confluent, quiescent SMCs were measured after 48h exposure to 15 dynes/cm^2 shear stress and under static conditions (Figures 3 and 4). CAD EPCs exposed to flow exhibited significantly greater alignment and elongation compared to HAECs exposed to flow and to CAD EPC cultured under static controls ($p < 0.05$). HAECs showed significantly greater alignment ($p < 0.05$) but not cell elongation compared to HAEC static controls. There were no significant differences in average cell area between CAD EPCs and HAECs measured following exposure to flow or under static conditions (Figure 5). CAD EPCs from three different donors exhibited significantly greater production of nitrite under flow than under static conditions ($p < 0.05$) (Figure 6).

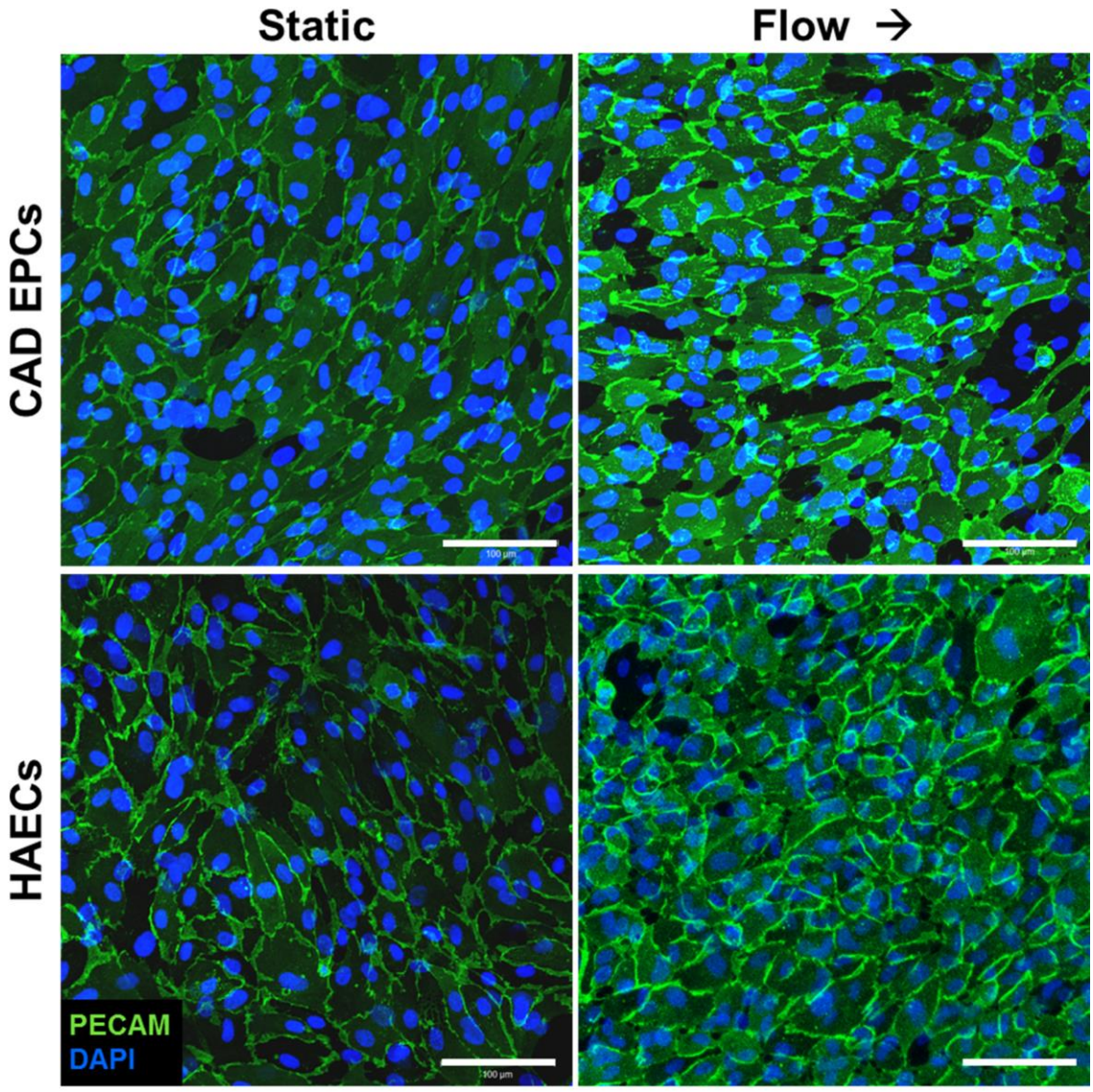

Figure 3: Fluorescence micrographs of CAD EPCs and HAECs after 48 hours of static culture or exposure to physiological shear stress.

CAD EPCs or HAECs were seeded over confluent, quiescent SMCs. Cell junctions are indicated with a PECAM antibody. Arrow indicates direction of flow. Scale bars represent 100 μm.

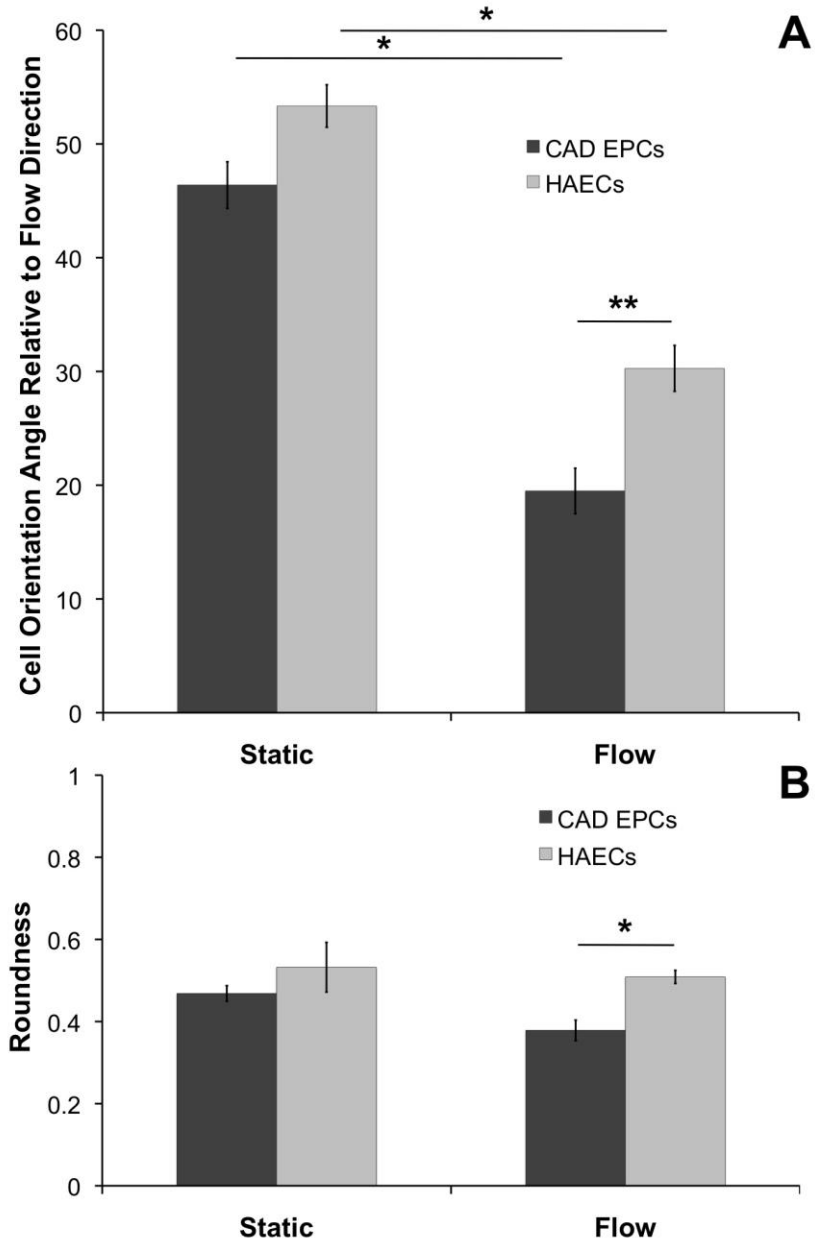

Figure 4: Orientation and Elongation of CAD EPCs and HAECs on SMCs.

CAD EPCs experience greater alignment toward the direction of flow (p < 0.05) and greater elongation (*p < 0.05) than HAECs (n =3). 0 refers to perfect alignment with the direction of flow, and 0 refers to a perfect line, while 1 refers to a perfect circle. Results reported as mean ± SEM, n = 3.**

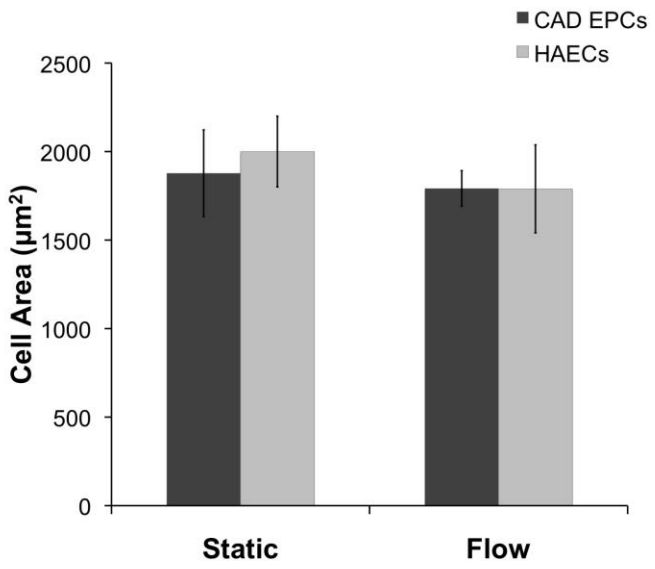

Figure 5: Cell Area of both CAD EPCs and HAECs in Co-Culture did not decrease with Flow.

Data reported as mean ± SEM (n = 3).

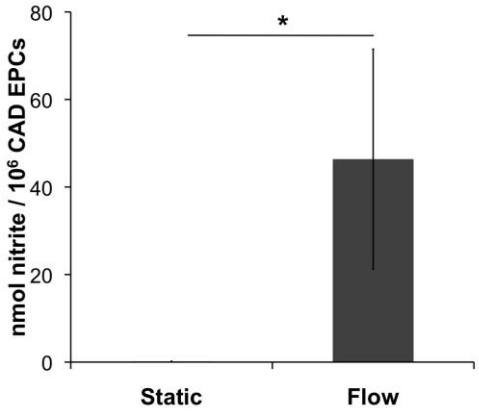

Figure 6: Nitrite Release of CAD EPCs under Flow Conditions.

The amount of nitrite released was calculated taking into account the volume of media in the static and flow samples and the number of CAD EPCs seeded per sample. Data reported as mean ± standard deviation (*p < 0.05, n = 3).

2.3.4 Integrin-Blocking Studies

CAD EPCs and HAECs incubated with various anti-integrin antibody solutions exhibited a similar binding profile over confluent, quiescent SMCs (Figure 7). All antibody solutions had significant blocking effects compared to controls ($p < 0.05$). For all antibody solutions, the blocking behavior of HAECs and CAD EPCs was not significantly different. Blocking with anti-$\alpha_5\beta_1$ significantly decreased adhesion compared to blocking with anti-$\alpha_v\beta_3$ for both CAD EPCs and HAECs ($p < 0.05$). The combination of both antibodies significantly decreased adhesion compared to anti- $\alpha_5\beta_1$ alone for both CAD EPCs and SMCs ($p < 0.05$).

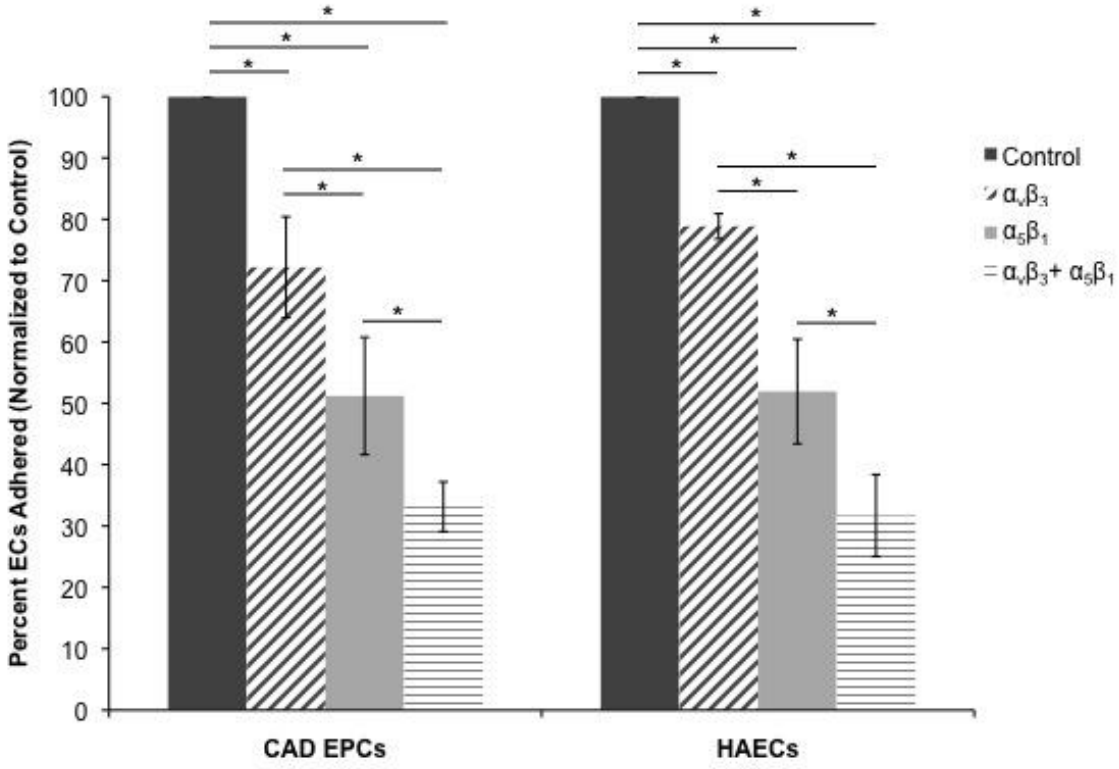

Figure 7: Integrin blocking indicates functional CAD EPC Binding Mechanisms.

A reduction in the number of cells bound to a confluent, quiescent SMC layer after blocking the functional integrins for fibronectin indicates the functional presence of these integrin subsets on the surface of the CAD EPCs. (*p < 0.05, n = 3).

2.4 Discussion

In previous studies we demonstrated that a homogeneous population of late outgrowth CAD EPCs can be isolated from patient peripheral blood and cultured to display mature and fully differentiated EC characteristics[64]. CAD EPCs are highly proliferative and exhibit the characteristics of healthy ECs. CAD EPCs are positive for EC markers CD31 and CD105 and negative for CD133 and hematopoietic markers CD45

and CD14. We also showed that a layer of CAD EPCs dramatically improved the patency of small diameter ePTFE vascular grafts in a rat femoral artery model[164].

One of the primary concerns voiced about the use of adult late outgrowth EPCs as an endothelial source is their rare occurrence in peripheral blood[60]. CB-EPCs have been favored by some because they are relatively abundant and highly proliferative, likely due to increased telomerase activity[162]. However, we have previously shown that CAD EPCs are also highly proliferative and comparable to late outgrowth EPCs from young, healthy patients[64]. All successfully isolated CAD EPC cultures expanded to greater than 10^7 cells over 3-6 passages, while late outgrowth EPCs from healthy donors exhibited limited proliferation in about half of the successfully isolated colonies. This was consistent with the observation that peripheral blood EPC counts are increased in patients with angiographically documented CAD[172].

The current study employed a direct co-culture model to examine whether late outgrowth CAD EPCs were also suitable candidates for endothelializing small-diameter TEBVs. This direct co-culture model has been used previously with HAECs[40,173] and CB-EPCs[41,165]. To our knowledge this study is the first examination of the interaction between adult peripheral blood EPCs and SMCs in general, and between CAD EPCs and SMCs in particular. These studies are a necessary first step towards employing CAD EPCs as an autologous source for TEBV endothelialization.

Previously, the direct co-culture model employed in the current study was used to characterize the attachment and growth of CB EPCs to layers of quiescent SMCs[41,165]. Our studies followed the co-culture protocol described in these studies. Table 2 directly compares results from our recent publication on CAD EPCs and the current study with recently reported data on CB EPCs mostly from the Truskey group. All CAD EPC and CB EPC studies used HAECs as control cells. This comparison indicates that CAD EPCs preformed similarly to CB EPCs.

Table 2: Characteristic Properties of CAD EPCs vs. CB EPCs

	CAD EPCs	**CB EPCs**
Proliferation potential	High[163]	High[162]
Capillary-like network formation in Matrigel	Yes[64]	Yes[170,174]
Average cell area over SMCs after 4 days (μm^2)	1878 ± 244	1700 ± 100[165]
Percent retention on SMCs after high shear stress	> 90%	> 90%[41]
Alignment with flow over fibronectin-coated Teflon-AF	Yes[64]	Yes[41]
Alignment with flow over confluent, quiescent SMC layer	Yes	Yes[41,165]

CAD EPCs maintained stable attachment and growth on confluent layers of SMCs over 1 and 7 days (Figure 1). The extent of cell coverage increased with seeding density for CAD EPCs and HAECs, with CAD EPCs exhibiting significantly greater coverage over SMCs than did HAECs at 1 day and at 7 days when complete data sets were taken into consideration ($p < 0.05$). For any given cell seeding density, however, there were no significant differences in CAD EPCs or HAECs on average, except for

SMCs seeded with 110,000 cells CAD EPCs HAECs for 1 or 7 days ($p < 0.05$). Because a seeding density of 110,000 cells/cm^2 CAD EPCs resulted in ~90% coverage on SMCs at both 1 and 7 days, all subsequent co-cultures used this seeding density.

Greater capillary-like network formation was noted after 7 days in co-cultures with HAECs and CAD EPCs seeded at 30,000 cells/cm^2. Others have noted greater network formation with blood derived EPCs on PLLA scaffolds or Matrigel in the presence of perivascular cells such as SMCs[175,176] or MSCs[177]. Our observations reinforce the observation that ECs seeded at low densities result in greater network formation[166], and that EC-SMC interactions are critical for vascular development[178-180]. Furthermore, late outgrowth EPCs from either adult peripheral blood or umbilical cord blood form networks more readily than ECs derived from arterial or venous endothelium[177], indicating that less differentiated or less mature endothelial cells are more favorable for tissue engineering applications.

Both CAD EPCs and HAECs exhibited greater than 90% retention when cultured over SMCs for 24 hours and exposed to a short burst of supraphysiological shear stress of 100 dynes/cm^2 (Figure 2). CB EPCs also exhibited greater than 90% retention over confluent, quiescent SMCs upon exposures to bursts of supraphysiological shear stress[41]. This indicates that EPCs seeded onto SMCs remain strongly adhered after initial attachment.

Alignment in the direction of flow is a key characteristic of endothelium. We have previously showed that CB EPCs and CAD EPCs aligned in the direction of flow when seeded over fibronectin-coated Teflon-AF, which was used to mimic the surface properties of an ePTFE synthetic vascular graft surface[64,181]. However, ECs are known to exhibit different adhesion characteristics over substrates of a softer modulus, such as those that would be experienced in TEBVs[182]. Furthermore, biological substrates such as a monolayer of other cells have been shown to behave differently than passive substrates of similar modulus such as polyacrylamide gels[165]. Therefore, it was important to evaluate the behavior of CAD EPCs over a monolayer of SMCs in order to evaluate their potential as an endothelial source for TEBVs.

Both CAD EPCs and HAECs exposed to physiological shear stress for 48 hours aligned in the direction of flow, with CAD EPCs exhibiting greater elongation and alignment than did HAECs. Neither CAD EPCs nor HAECs exhibited a change in area before or after exposure to long-term shear stress when cultured over SMCs. This was consistent with results reported for CB EPCs cultured over SMCs[165]. We have shown previously that CAD EPCs exhibit greater mRNA expression of Krüppel-like factor 2 (KLF-2) under flow than under static conditions when seeded over fibronectin-coated Teflon-AF[64]. The increased alignment with flow exhibited by CAD EPCs may be due in part to the expression of KLF-2.

We have previously confirmed that CAD EPCs seeded on fibronectin-coated Teflon-AF released significantly greater NO after 24 hours of flow at physiological shear stress than under static conditions[64]. In the current study, nitrite production was directly measured as a representation of NO production due to the short half-life of NO in aqueous solutions. After 48 hours of flow at physiological shear stresses, CAD EPCs produced an average of 46 nmol nitrite per million cells seeded (Figure 6). A recently published study of nitrite production of CB EPCs seeded on fibronectin-coated glass showed that CB EPCs produced approximately 20 nmol nitrite per million ECs seeded after 48 hours[170].

CAD EPC adhesion over confluent, quiescent SMCs was significantly blocked by antibody solutions against $\alpha_5\beta_1$ and $\alpha_v\beta_3$ integrins alone, and by combinations of antibodies against $\alpha_5\beta_1$ and $\alpha_v\beta_3$ integrins ($p < 0.05$). This behavior is similar to that exhibited by HAECs. CB EPCs and HAECs have also exhibited binding to fibronectin-coated surfaces that was dependent only on the $\alpha_v\beta_3$ and $\alpha_5\beta_1$ integrins [39,41]. These results further demonstrate that EPCs isolated from CAD patients exhibit healthy EC behavior.

Finally, CB EPCs may be attractive due to their potential for allogeneic transplantation[183,184], however it is important to note that CB EPCs are not immune-competent. Late-outgrowth EPCs from rat peripheral blood elicited substantially less alloimmune reaction than rat aortic ECs[185], However, a comparison of CB EPCs and

HUVECs from the same patient found that CB EPCs expressed the same pattern of class I and II MHC molecules as HUVECs, indicating that they would likely be rejected in the case of an allogeneic implant without matching MHC types[186]. For this reason alone, use of CAD EPCs as an autologous endothelial source may be preferred to avoid potential immune rejection.

2.5 Conclusion

CAD EPCs exhibit confluence over SMCs for 7 days and maintained a confluent layer more effectively compared to HAECs, attached to SMCs within 15 minutes and remain strongly adhered, and exhibited greater alignment with flow compared to HAECs. These results were essentially equivalent to that observed for CB EPCs adhesion on SMCs. CAD EPCs exhibited binding dependence on the $\alpha_5\beta_1$ integrin on confluent, quiescent SMCs as did CB EPCs. These results demonstrate that peripheral blood EPCs isolated from CAD patients may be a viable source of autologous endothelium for use in TEBVs.

2.6 Chapter-Specific Acknowledgements

The authors would like to thank Matthew Novak from Duke University for his help with statistical analysis of the data. This work was supported by National Institutes of Health (NIH) Grant R01HL-44972 (W.M.R.), a NIH biotechnology training

grant T32 GM-8555 fellowship (C.E.F.), and NIH Grant UH2TR000505 and the NIH Common Fund for the Microphysiological Systems Initiative (G.A.T.).

3. Development and Optimization of a Human Tissue Engineered Vascular Microphysiological System for *in vitro* Drug Screening

Text and figures presented in this chapter have been previously published in the following form: Fernandez CE, Yen RW, Perez SM, Bedell HW, Povsic TJ, Reichert WM, Truskey GA. Human Vascular Microphysiological System for in vitro Drug Screening. *Scientific Reports* 6:21579 (2016)[187].

3.1 Introduction

Currently, over 80% of proposed pharmaceutical drug candidates that enter clinical trials fail due to concerns with human efficacy and toxicity[1]. While pre-clinical animal studies provide great value, animal responses to drugs may exhibit differences in toxic doses and drug metabolism[5]. Microphysiological systems (MPS) are perfused small-scale models of one or more human tissues or organs[7] comprised of human primary cells or induced pluripotent stem cells (iPSCs) with the ultimate potential of becoming models to study disease or tools for precision medicine. In order to accurately model disease and predict drug responses on an organ scale, three-dimensional (3D) human tissue models are critical. Many pre-clinical studies are conducted on two-dimensional (2D) plastic or glass substrates; however, *in vivo*, tissues are comprised of complex extracellular matrices embedded with mixed populations of cells and perfused with fluids.

In addition to facilitating more accurate disease models through interaction with immunological stimuli, human MPS may serve as a bridge in the drug development pipeline between 2D cell culture studies and *in vivo* animal studies. Assessment of toxicity within the vasculature is of particular importance, since drug-induced vascular injury (DIVI), which typically manifests in preclinical animal studies through inflammation and changes in vascular tone, precludes many drug candidates from continuing along the pipeline despite uncertain characterization of human DIVI response[188]. In humans, cancer chemotherapeutics cause vascular damage affecting flow-mediated vasodilation[189,190]. Three-dimensional (3D) tissue models have the potential to allow us to evaluate human biological interactions and diseases by taking advantage of natural spatiotemporal cues, physiological fluid perfusion, a variety of cell types, and the complex extracellular matrix that are present in tissues but are absent from 2D culture plates[8]. A human tissue-engineered blood vessel (TEBV) capable of responding to vasoreactive stimuli would pose a promising model for the evaluation and screening of pharmaceutical drug candidates for toxicity and efficacy within the circulatory system.

An ideal TEBV for MPS applications would be comprised of human cells in a biological or biodegradable synthetic matrix, have a small inner diameter to reduce fluid volumes, exhibit enough mechanical strength to withstand physiological stresses, and be produced rapidly to facilitate efficient drug screening. The medial wall cells should

exhibit a smooth muscle phenotype, be quiescent and be able to contract and relax in response to agonists or inhibitors. Most importantly, the TEBV must be endothelialized to enable physiologically relevant dilation and constriction in response to stimuli.

TEBVs have been constructed using three general approaches: natural or biodegradable synthetic matrices populated *in vitro* with cells, self-assembled cell sheets, or *in vivo* repopulation of decellularized natural or synthetic vessel matrices[191,192]. Despite their biomimetic properties, the sizes and long culture times for fabrication of TEBVs by many of the current creates challenges in applying these procedures to *in vitro* drug testing[75]. While TEBVs constructed from natural matrix components such as collagen[76,193] and fibrin[29,50] have traditionally exhibited poor mechanical strength, plastic compression of collagen gels embedded with smooth muscle cells increases the collagen fiber density and yields rapidly-producible tubular structures with high mechanical strength[101].

A functional TEBV requires a confluent endothelial layer. The endothelium plays a major role in regulating leukocyte and platelet adhesion, permeability, vascular tone, as well as modulating vasodilation through release of nitric oxide in response to changes in flow or stimuli with vasoreactive compounds such as acetylcholine[194]. Endothelial coverage of TEBVs prior to implantation in animal models has been assessed with characteristic endothelial markers such as von Willebrand factor (vWF)[72,94]. Under static *in vitro* conditions, endothelium seeded on TEBVs made from cultured SMC and fibroblast sheets demonstrated nearly confluent coverage, expressed vWF and inhibited

platelet adhesion[75]. After exposure to physiological shear stresses for 24-48 hours, endothelial progenitor cells (EPCs) remain adherent to fibrin scaffolds embedded with either human neonatal dermal fibroblasts (hNDFs) or smooth muscle cells (SMCs), deposit collagen IV and laminin, and upregulate cell adhesion molecules VCAM-1 and ICAM-1 upon exposure to pro-inflammatory cytokines such as tumor necrosis factor-α (TNF-α)[63,74].

Non-destructive evaluation of TEBV maturation and vasoactivity is beneficial toward effective monitoring of responses to drugs or stimuli. Table 3 summarizes previous vasoactivity assessments performed on TEBVs. Although TEBVs have been assessed for endothelium-independent vasoconstriction or vasodilation using a variety of agents, TEBVs comprised of human cells have yet to be evaluated for endothelium-dependent vasoactivity under physiological fluid perfusion conditions. One important clinical assessment of cardiovascular health, which predicts future cardiac events, involves infusion of acetylcholine to induce vasodilation of the coronary or brachial arteries[195-197]. Acetylcholine is a muscarinic cholinergic agonist that stimulates release of nitric oxide, prostacyclin, and endothelium-derived hyperpolarizing factor in vessels with healthy, intact endothelium. Conversely, acetylcholine activates the muscarinic receptors on the smooth muscle cells in vessels with dysfunctional or damaged endothelium, leading to vasoconstriction[195,198]

Table 3: TEBV Vasoactivity

Tissue Type	ECs?	Vasoactive Agent added to Medium	Assessment Method	Ref.
TEBV comprised of human umbilical vein derived SMCs	No	Multiple doses: Endothelin-1 Endothelin-2	Destructive; Isometric force measurements of TEBV rings.	[199]
Rat aortic SMCs in collagen gel mold	No	Multiple doses: Endothelin-1 Bradykinin Phenylephrine BHT-920 ATP disodium salt 5-hydroxytryptamine	Destructive; Isometric force measurements of TEBV rings.	[200]
Bovine SMCs cultured on biodegradable PGA scaffold	Yes; bovine ECs	Multiple doses: Serotonin Endothelin-1 Prostaglandin	Destructive; Isometric force measurements of TEBV rings.	[94]
Silastic tubing embedded within the peritoneal cavity of rats	Yes; non-thrombotic mesothelial cells lining intima	Single doses: KCl Acetylcholine Phenylephrine	Destructive; Isometric force measurements of TEBV rings.	[201]
Nanopatterned human bone-marrow derived MSCs grown on a scaffold-free matrix	Yes; human cord-blood derived EPCs	Single dose; Phenylephrine	Non-destructive; changes in TEBV diameter analyzed under perfusion as a result of exposure to vasoactive agents	[202]
Human NDFs or bone-marrow derived MSCs embedded in a dense collagen gel matrix	Yes; adult peripheral blood EPCs	Multiple doses: Phenylephrine Acetylcholine Caffeine Theophylline	Non-destructive; changes in TEBV diameter analyzed under perfusion as a result of exposure to vasoactive agents under varying doses.	Current study

In this study, dense collagen gels[101,203] embedded with human neonatal dermal fibroblasts (hNDFs) or human bone marrow-derived mesenchymal stem cells (hMSCs) were used to construct TEBVs that can be perfused under physiological conditions in a few hours. We compared hNDFs to hMSCs as a medial cell source to determine the cell source that would provide the greatest mechanical properties and contractility within 1-2 weeks. TEBV lumens were endothelialized with endothelial progenitor cells derived from patients with coronary artery disease (CAD EPCs)[158,204]. We used CAD EPCs because they express markers of healthy endothelium and function similar to human aortic ECs[27], and provide the potential for future studies of a population pre-disposed to atherosclerosis. Perfused and endothelialized TEBVs exhibited high mechanical strength and contractility after one week and maintained these properties for five weeks *in vitro*. Phenylephrine and acetylcholine were used to non-destructively measure endothelium-independent vasoconstriction and endothelium-dependent vasodilation, respectively. We have used the non-specific phosphodiesterase inhibitors caffeine and theophylline to evaluate drug-induced vasodilation. We further evaluated endothelial function by measuring nitric oxide production.

3.2 Methods

3.2.1 Cell Isolation and Culture

All isolations of endothelial progenitor cells from blood were performed in accordance with the protocol approved by the Duke University Institutional Review Board for the collection of peripheral blood from consenting patients undergoing left heart catheterization at Duke University Medical Center. Informed consent was obtained from all donors prior to blood withdrawal. CAD EPCs from four donors over the age of 55 with advanced CAD were isolated and grown as previously stated [204]. CAD EPCs were maintained in EC medium comprised of Endothelial Basal Medium (EBM-2) with an EGM-2 Single Quots Kit (Lonza) supplemented with 10% heat-inactivated fetal bovine serum (HI-FBS, Gibco) and 1% Pen/Strep (Lonza). CAD EPCs were passaged at 80% confluence using 0.025% trypsin/EDTA (Lonza) and neutralized with 1:1 ratio of EC medium. Cells in passages 6-9 were used for all experiments.

Human neonatal dermal fibroblasts were purchased from Clonetics and maintained in hNDF medium comprised of Dulbecco's Modified Eagle's Medium (DMEM) with 4.5 g/L glucose (Gibco) supplemented with 10% HI-FBS, 1% Pen/Strep, 1x Non-essential amino acids (NEAA, Gibco), 1x Sodium Pyruvate (Gibco), 1x Glutamax (Gibco) and 0.1% β-mercaptoethanol (Gibco). hNDFs were passaged at 80% confluence using 0.05% trypsin/EDTA (Lonza) and neutralized with a 1:1 ratio of hNDF media. Passages 8-12 were used for all experiments. Human bone marrow-derived MSCs used

in this study were generously provided by Darwin J. Prockop of Texas A&M Institute for Regenerative Medicine.

TEBVs under static and flow conditions were maintained in culture medium comprised of DMEM with 1.1 g/L glucose, L-glutamine, and 110 mg/L sodium pyruvate (Gibco) supplemented with 3.3% HI-FBS, 1x NEAA, 1% Pen-Strep, and 0.1% β-mercaptoethanol. After 1 week in culture, 2 mg/mL ε-aminocaproic acid was added to the TEBV medium to minimize TEBV constriction under long-term culture conditions.

3.2.2 Flow Cytometry

CAD EPCs were characterized using flow cytometry. Cells were positive for endothelial cell markers CD31 and CD144, and negative for CD45, CD115, and CD14. Mouse IgG1 and untreated cells were used as controls. Antibodies (Biolegend) were conjugated with either FITC or phycoerythrin. Detailed antibody information can be found in Supplementary Table S4. CAD EPCs were passaged using 0.025% trypsin/EDTA at 80% confluence. Approximately 500,000 CAD EPCs were resuspended in 100 µL 1% bovine serum albumin buffered with Dulbecco's PBS with calcium and magnesium. Cells were incubated at room temperature for 30 minutes with 5 µL of preconjugated antibody before washing with 1% BSA solution. Cells were collected after centrifugation at 400x g for 7 minutes and fixed using 10% neutral buffered formalin before storage at 4°C until analysis. Flow cytometry analysis was performed by collecting 9,000 events per sample.

3.2.3 TEBV Fabrication, Endothelialization, and Perfusion

TEBVs were fabricated from collagen gels and plastically compressed to increase the collagen fiber density[103,203]. Rat-tail collagen I (BD Biosciences) was diluted to 2.05 mg/mL using 0.6% acetic acid (Sigma). A serum-free 10x Dulbecco's Modified Eagle's Medium (DMEM) was added at a 1:10 ratio to the collagen (Sigma). The pH was raised to 8.5 using 5M sodium hydroxide (Sigma). A suspension of hNDFs was added at an initial cell density of $5x10^5$ cells/mL. Gel solutions were immediately transferred to a 3-cc syringe with a closed two-way luer-lock stopcock (Cole-Parmer) attached. An 810-μm diameter steel mandrel was inserted in the center to create the TEBV lumen and held in place with Parafilm (Kimberly Clark) at the top of the syringe. Solutions were allowed to gel for 30 minutes at room temperature. Immediately afterward, gel solutions were suspended on 10 KimWipes under a 0.8 μm membrane filter (Whatman). After removal of the water, TEBVs were immediately placed in TEBV media until mounting in a chamber.

TEBVs were mounted in custom-made vascular perfusion chambers that could accommodate 1-2 TEBVs on grips (0.760 mm outer diameter) (Fig. 1). TEBVs were sutured in place using 4-0 black silk sutures. Endothelialization was performed by injecting 500,000 CAD EPCs through the lumen of each TEBV, and the chamber was sealed and rotated at 10 rotations per hour (rph) on a custom-made rotation platform for 30 minutes at 37 ºC to allow for cell adhesion. A peristaltic pump (Masterflex) with a

minicartridge pump head with 8 rollers (Ismatec) was used to create pulseless flow through the TEBVs. Flow circuits accommodating 1 or 2 TEBVs were created using a reservoir and a combination of silicone and PharMed BPT tubing (Cole-Parmer). Circuits contained 35 mL of flow media as described above per TEBV. Media was changed every 2-3 days. TEBVs were maintained at a flow rate of 2 mL/min throughout all experiments.

3.2.4 Burst Pressure Analysis and Mechanical Testing of TEBVs

TEBVs were maintained in perfusion chambers with one end sealed, and the other end attached to a differential pressure gauge (Keller). TEBVs were filled passively with PBS until failure[50].

Circumferential tensile strength was analyzed using a micro-strain analyzer (TA Instruments) with modified grips as shown in Fig. S1. TEBVs were cut in 5 mm sections and mounted through grips with diameters of 300 μm. Cyclic pre-conditioning was performed by stretching the lumen to a strain of 20% for 6 cycles[149]. An optimized strain rate of 0.08 mm/s was used to stretch rings until failure.

Grip diameters were taken into account in calculating the strain (ε), where D = grip diameter. Stress (σ) was calculated by assuming conservation of volume.

$$\varepsilon = \frac{L_i - L_s}{L_s};\ L_s = 2D + L_0$$

$$\sigma = \frac{F}{A}\left(1 + \frac{\Delta L}{L_0}\right)$$

Ultimate tensile stress was defined as the maximum stress before failure. The Young's modulus (E) was calculated by dividing stress by strain.

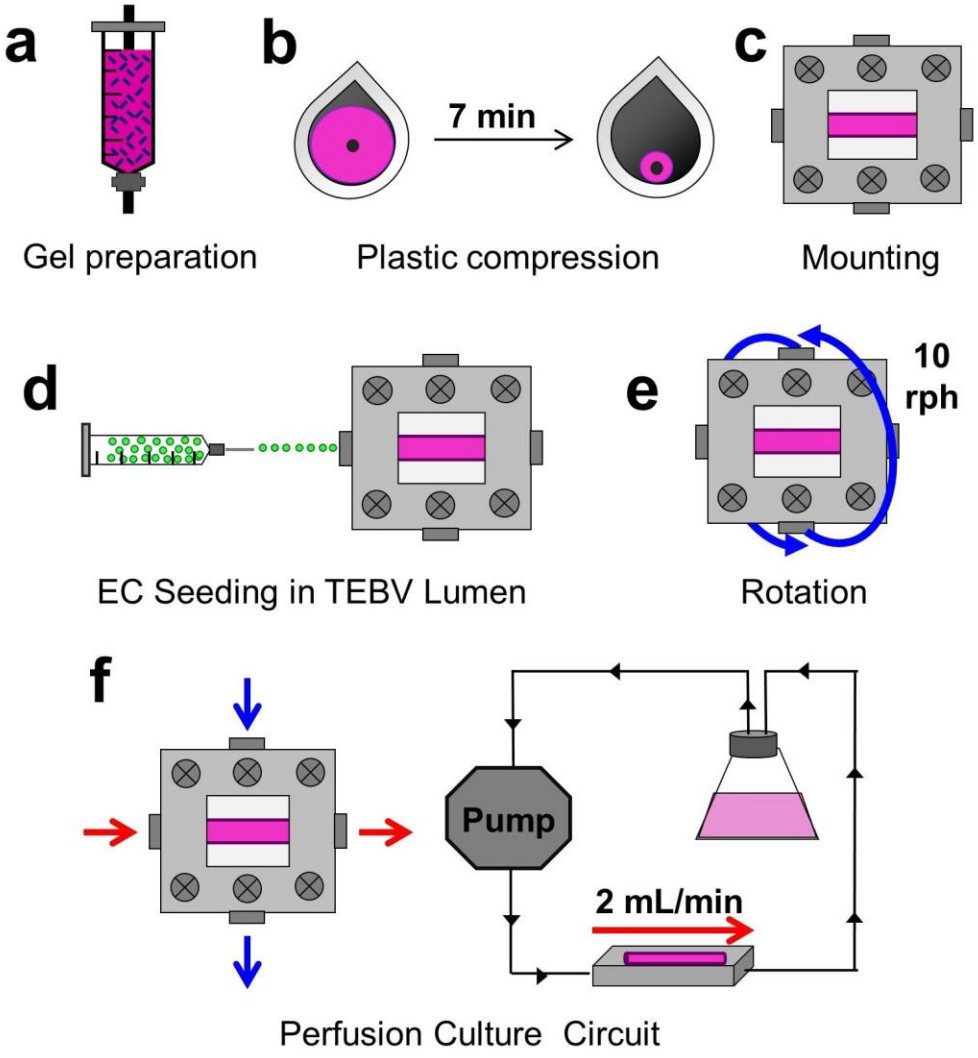

Figure 8: TEBV Fabrication and Culture

A suspension of hNDFs in collagen is poured into the mold containing an 810-μm diameter mandrel and allowed to gel for 30 minutes (A). Collagen fiber density increases through plastic compression and removal of water (B). Compressed TEBVs are immediately mounted in custom chambers (C). CAD EPCs are seeded into the lumen of the TEBV (D) and the chamber is rotated at 10 rph for 30 minutes (E). After endothelialization, TEBVs are mounted into the perfusion circuit and cultured for at least 1 week at a flow rate of 2 mL/min (F).

3.2.5 Determination of TEBV Inner Diameter

The intraluminal pressure drop across the TEBV was found using strain gauge pressure transducers (Model SPR 524, Millar, Houston, TX) flanking the inlet and outlet of the TEBV. Pressure drop was recorded using a custom Labview program as the TEBV was perfused at flow rates ranging from 2 – 3.5 mL/min. Inlet pressures ranged from 9.5-20 mm Hg. Intraluminal pressure drops ranged from 0.5 – 5 mm Hg over a 5-week perfusion period. Poiseulle's law was used to calculate the inner radius (R), where η = 0.083 g/cm-sec as determined by a viscometer, and L = 1 cm.

$$R = \left[\frac{8\eta LQ}{(\pi \Delta P)}\right]^{1/4}$$

The accuracy of the pressure measurements was corroborated by evaluating various sizes of rigid tubing of known inner diameter in place of the TEBV. Inner diameters of 517±31 μm and 729±53 μm were obtained for tubing of inner diameters of 535 μm and 735 μm, respectively, as measured optically. TEBV outer diameter was evaluated using a stereomicroscope (Amscope) combined with a video camera and imaging software. TEBV wall thickness was evaluated by subtracting the calculated inner diameter from the measured outer diameter.

To assess whether any vessel changes occurred during these measurements, we computed the strain from the Law of Laplace assuming the vessel behaved like an elastic material for small deformations. Based on the Young's modulus computed from the

ultimate tensile, the strains ranged between 0.007-0.012, suggesting that the radius change induced by expansion of the vessel wall was between 2.8% and 4.9%.

3.2.6 Analysis of TEBV Vasoactivity

TEBVs were placed under a stereoscope connected to a video camera (Amscope). Video recordings of the vessel outer diameter were analyzed using Image J. Endothelium-independent vasoconstriction response was evaluated by adding 1 μM phenylephrine (Sigma) to the flow circuit. After 5 minutes, 1 μM acetylcholine (Sigma) was added to the flow circuit to assess the endothelium-dependent vasodilation response[196]. For long-term studies, drug-induced vasoactivity was assessed weekly. A silicone syringe port (Ibidi) was added to the flow circuit and drugs were added to the system via a syringe connected to a sterile 27-gauge needle. Dose-response curves for phenylephrine and acetylcholine were evaluated in TEBVs cultured with and without endothelium for 1 week and with endothelium for 5 weeks. Dose response studies were performed by increasing drug concentration in the flow circuit every 5 minutes. Phenylephrine and acetylcholine dose responses were evaluated using concentrations ranging from 10^{-9} to 10^{-4} M. Caffeine and theophylline (Sigma) dose responses were evaluated using concentrations ranging from 10^{-9} to 10^{-2} M. To evaluate the effect of eNOS inhibition on TEBV vasodilation, L-N^G-Nitroarginine methyl ester (L-NAME, Sigma) was added to the flow circuit to obtain a final concentration of 3.2 uM and TEBVs were incubated for 10 minutes at 37 C prior to performing an acetylcholine dose-

response curve[205]. Changes in outer diameter are expressed as percent change from the baseline outer diameter.

3.2.7 RNA Isolation and Reverse Transcriptase-Polymerase Chain Reaction Analysis

NCBI reference sequences for the mRNA of each gene were obtained from PubMed, and primer sequences (Appendix) were generated using the online design program Primer-Blast. Primer pairs that demonstrated uniform and single-product melt curves upon reaction with hNDF reference RNA were selected. Primer efficiencies were calculated using standard curves with reference RNA. Primer efficiencies between 90-115% were deemed acceptable.

Cells were extracted from the TEBV matrix by submerging TEBVs in 1 mg/mL collagenase solution in PBS at 37 ºC for 30 minutes. TEBVs were spun down at 300 x g for 5 minutes to pellet cells. EPCs and hNDFs were separated using 25 μL CD31 Dynabeads (Life Technologies). Total RNA from hNDFs was isolated using an Aurum Total RNA Mini Kit (BioRad). RNA purity and concentration was assessed using a NanoDrop Spectrophotometer. Reverse transcription of RNA into cDNA was performed using 250 ng of hNDF RNA using the iScript cDNA Synthesis Kit (BioRad). RT-PCR was performed using the iQ SYBR Green Supermix (Bio-Rad) and the CFX Connect Real-Time PCR Detection System (Bio-Rad). Fold change from reference RNA was calculated as previously described [206]. Calponin fold change was normalized to a TEBV cultured for 24 hours under static conditions.

3.2.8 Immunofluorescent Staining of TEBVs

TEBVs were fixed in 10% formalin for 30 minutes, rinsed three times with DPBS, then cut *en face*. For imaging of contractile proteins and vWF, cells were permeabilized with 0.1% Triton-X in PBS for 5 minutes, and then rinsed three times with DPBS. Blocking was performed with 10% goat serum (Gibco) in DPBS for at least 8 hours at room temperature. Primary antibody staining was performed at 1:100 in 10% goat serum overnight. The following primary antibodies were used: rabbit anti-αSMA, rabbit anti-calponin, rabbit anti-vWF, rabbit anti-laminin, rabbit anti-collagen IV, mouse anti-fibronectin. All primary antibodies were purchased from Abcam. Detailed antibody information can be found in the Appendix. After staining overnight with primary antibody, samples were rinsed 3 times with DPBS and stained for 1 hour at room temperature with 1:500 goat anti-rabbit Alexa Fluor 594 or goat anti-mouse Alexa Fluor 488 (Life Technologies). Samples were rinsed 3 times and stained with 1 μL/mL Hoechst 33342 dye in DPBS for 5 minutes at room temperature, then rinsed 3 times with DPBS. Samples were mounted onto slides using FluorSave reagent (Calbiochem) and covered with a cover slip. Z-stack images of TEBVs were obtained on a Zeiss 510 inverted confocal microscope at 20X magnification. Images were analyzed using a Zeiss LSM image browser and Image J (NIH).

3.2.9 Quantification of Nitric Oxide Produced by TEBVs

After 1 week and 5 weeks of culture under perfusion, 5 mL media samples were removed from the flow circuit and maintained at -20ºC. After thawing, proteins were removed using 10,000 MWCO spin columns (Corning) microcentrifuged at 10,000 rpm for 5 minutes. Total nitrite and nitrate in each sample was assessed using a Greiss reagent assay kit (Pierce). Absorbance at 540 nm was measured using a μQuant microplate reader (Bio-Tek). Samples were normalized to pure media controls.

3.2.10 Statistical Analysis

Statistical analyses were performed using JMP 11 (SAS Institute). All data were analyzed by one-way or two-way analysis of variance (ANOVA) with post hoc Tukey's test to compare means. A one-way repeated measures ANOVA was performed for all time and dose-dependent assays. All data are represented as means ± SEM. P values < 0.05 were considered significant. Power calculations were performed to ensure sample sizes yielded a power greater than 0.8.

3.3 Results

3.3.1 Generation of Small-Diameter, Endothelialized TEBVs

TEBVs with dense collagen gel matrices were constructed by first embedding human neonatal dermal fibroblasts (hNDFs) or mesenchymal stem cells (hMSCs) in rat-tail collagen I matrices[101,203]. The hNDF-collagen I mixture was poured into a 3-cc syringe

(BD Biosciences) containing a concentric stainless steel mandrel 810 μm in diameter and allowed to gel for 30 minutes (Fig. 8). Afterward, TEBVs were plastically compressed by suspension on absorbent tissue paper, which reduced water volume and increased collagen fiber density (Table 4).

Table 4: TEBV Collagen Fiber Density

Initial CFD (%)	Water Loss (%)	Final CFD (%)	Fold Increase in Collagen Density
0.23 ± 0.01	96.2 ± 0.8	6.2 ± 1.2	26.1 ± 5.9

After compression, TEBVs were immediately placed in warmed media and mounted onto custom-made perfusion bioreactor chambers. To create an endothelial layer, 500,000 CAD EPCs were injected into the TEBV lumen (Fig. 8a), mounted on a custom rotation platform, and rotated at 10 rph for 30 minutes at 37 ºC (Fig. 8e). Endothelialized TEBVs were immediately perfused at 2 mL/min to produce an initial laminar shear stress of 6.8 dynes/cm^2. Time-averaged arterial wall shear stress ranges from 5-12 dynes/cm^2 in healthy adult humans[207]. TEBVs were perfused for 1-5 weeks to evaluate maturation and vasoactivity over time (Fig. 8f). Plastic compression substantially reduced TEBV outer diameter (Fig. 9a-b). A live-dead assay performed on TEBVs 24 hours after compression indicates cell survival after compression (Fig. 9c). TEBVs cultured for one week demonstrated a uniform distribution of medial cells throughout the vessel wall (Fig. 9d).

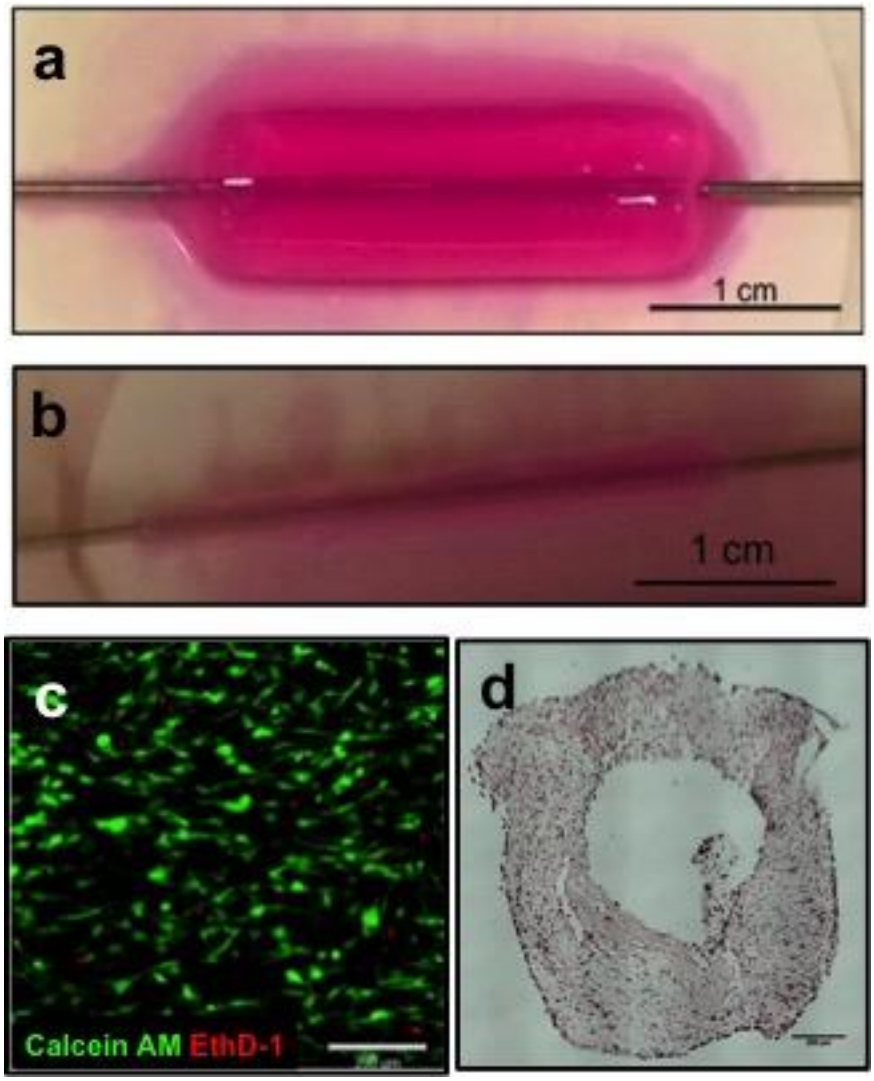

Figure 9: TEBV Fabrication

TEBVs before (A) and after compression (B). Live-dead assay performed 24 hours after compression (C). H&E cross-section of TEBV after 1 week of perfusion culture (D). Scale bars indicate 200 μm unless otherwise noted.

3.3.2 Mechanical Strength and Stability of TEBVs

Burst pressure was measured by pressurizing TEBVs with PBS until failure[208], and circumferential strength of TEBV slices was measured using a tensile testing apparatus with modified grips as previously described[101,149]. TEBVs comprised of collagen only maintained in PBS for 24 hours initially exhibited high tensile strength and burst pressure (Fig. 10a, Fig. 11). Burst pressures decreased slightly after introduction of hNDFs into the scaffold for 24 hours, and dropped substantially after 1 week under static conditions. Mechanical properties increased with mechanical stimulation. After one week, hNDF TEBVs matured under perfusion demonstrated significantly higher burst pressures compared to those under static conditions ($p < 0.005$). Endothelialized TEBVs matured for one week under physiological perfusion demonstrated the greatest burst pressures. After 1 week, perfused, endothelialized TEBVs exhibited greater tensile stress and Young's modulus (Fig. 11).

TEBV wall thickness was assessed by measuring inner and outer diameters at one-week intervals over a 5-week perfusion period as described in Materials and Methods. Both the inner and outer diameter declined between the first and second week of perfusion, and stabilized by the third week (Fig. 10b). The pressure drop across the lumen of the TEBVs ranged from 0.5 mmHg – 5 mmHg at flow rates of 1.5 - 4 mL/min.

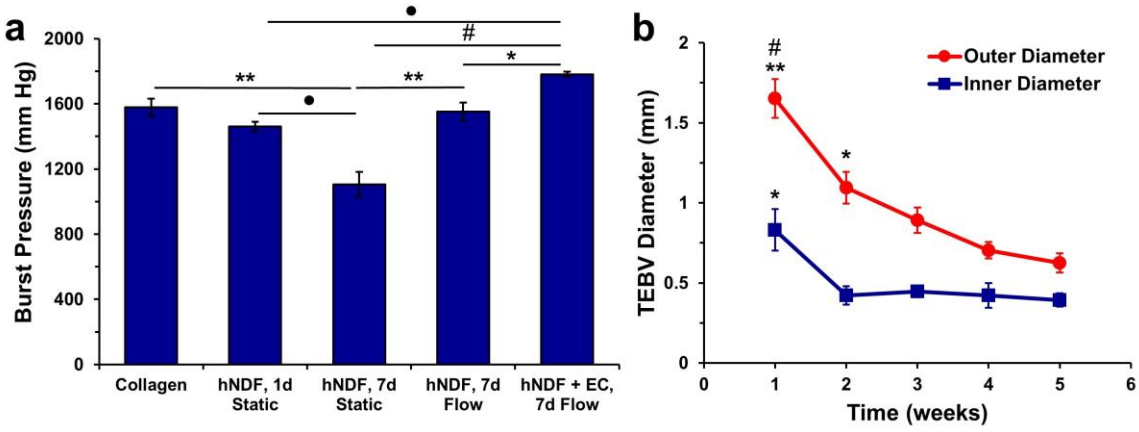

Figure 10: TEBV Mechanical Strength and Stability

TEBVs comprised of collagen only maintained under static conditions for 24 hours demonstrated burst pressures of 1577.6 ± 54.5 mm Hg. TEBVs embedded with hNDFs and maintained under static conditions for 24 hours after preparation exhibited burst pressures of 1460.1 ± 28.8 mm Hg, but 1 week of culture under static conditions led to burst pressures of 1104.5 ± 77.1 mm Hg. Exposure to flow increased the mechanical properties of the TEBVs after 7 days, leading to burst pressures of 1552.6 ± 54.9 mm Hg. Endothelialized TEBVs perfused for 7 days yielded burst pressures of 1777.6 ± 15.8 mm Hg Values are reported as mean ± SEM, n = 3, 4 TEBVs. (*: $p < 0.05$, ●: $p < 0.01$, **: $p < 0.005$, #: $p < 0.0001$) (A). A one-way ANOVA and the post-hoc Tukey test indicated that the inner diameter stabilized after the second week in culture (*$P < 0.05$ with respect to weeks 2-5). The outer diameter stabilizes after the third week in culture (* $P < 0.05$ with respect to week 5; **$P < 0.005$ with respect to weeks 2 and 3; # $P < 0.0001$ with respect to weeks 4 and 5.) Values are mean ± SEM. Four independent experiments were conducted. (B).

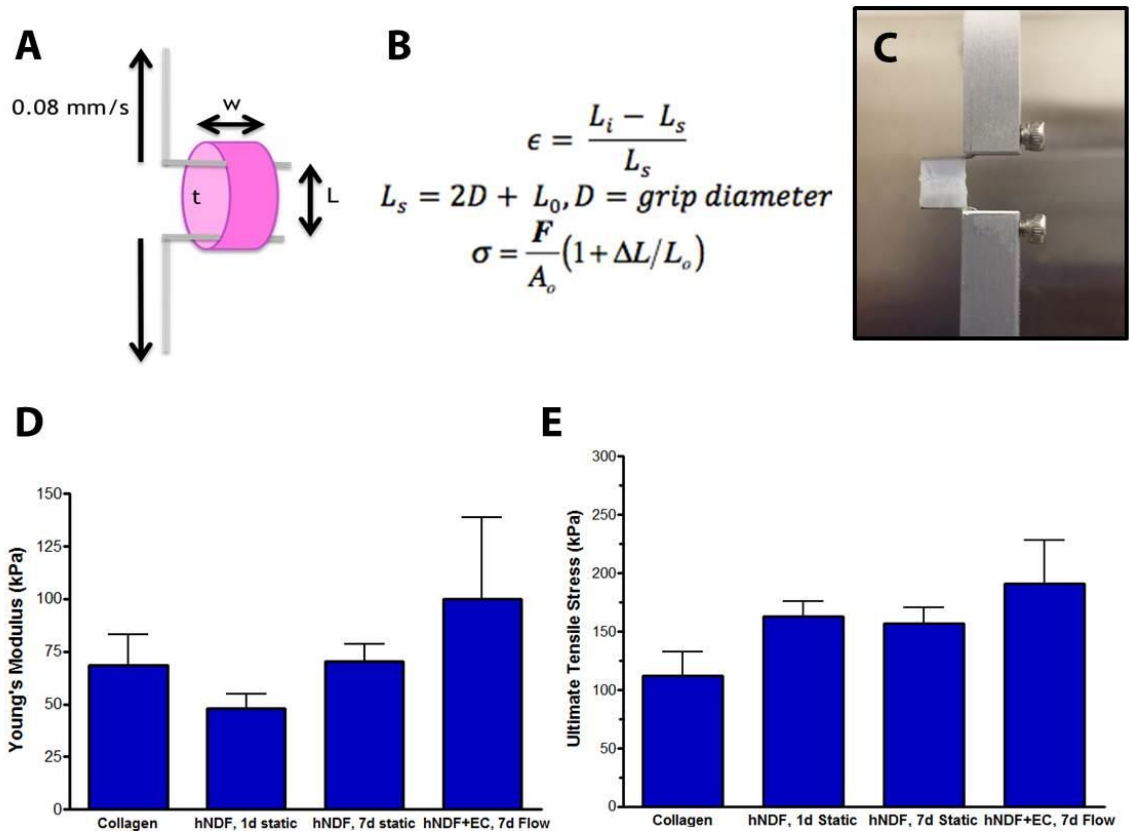

Figure 11: TEBV Mechanical Testing

TEBVs were cut into rings approximately 5 mm in width (w) and mounted on modified grips (A). Stress and strain were calculated by taking the diameter change into account as the TEBV was pulled in tension (B). TEBVs stretched significantly throughout the mechanical test (C). Mechanical stimulation had a demonstrated impact on TEBV Young's modulus (D), and ultimate tensile stress (E). Data shown as mean ± SEM, n = 3-7 TEBVs.

3.3.3 Contractile and Extracellular Matrix Protein Expression

At fabrication, hNDFs in TEBVs expressed low levels of α-SMA (Figure 12). Mechanical stimulation increased the expression of mRNA specific to the contractile proteins α-smooth muscle actin (α-SMA) and calponin in hNDFs (Fig. 14a). After 1 week of perfusion, hNDFs expressed α-SMA and calponin (Fig. 14d, e), indicating differentiation toward a myofibroblast phenotype[22]. Endothelialized TEBVs composed of hMSCs also expressed α-SMA and calponin after 1 week; however, to a lesser extent than hNDFs (Fig. 14h, i). TEBVs perfused for up to 5 weeks at a laminar flow rate of 2 mL/minute maintained production of α-SMA and calponin throughout this period (Fig. 13). Fibronectin expression was evaluated as a marker of TEBV remodeling[209]. Endothelialized hNDF TEBVs demonstrated greater fibronectin expression compared to endothelialized hMSC TEBVs (Fig. 14b, c). TEBVs made with hNDFs and hMSCs expressed endothelial basement membrane proteins collagen IV (Fig. 14f, g), and laminin (Fig. 14j, k) after 1 week. Thus, after 1 week of perfusion, TEBVs composed of hNDFs are more phenotypically mature compared to hMSCs.

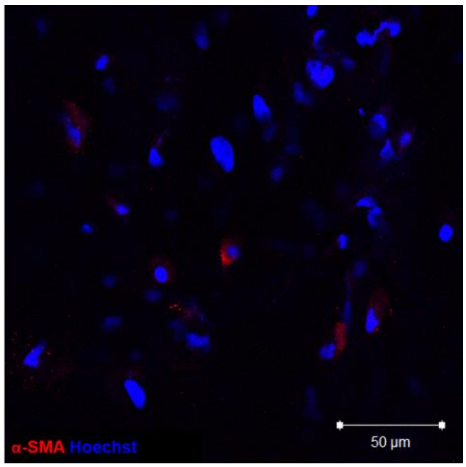

Figure 12: Expression of α-SMA in hNDF TEBVs after 24 Hours of Culture

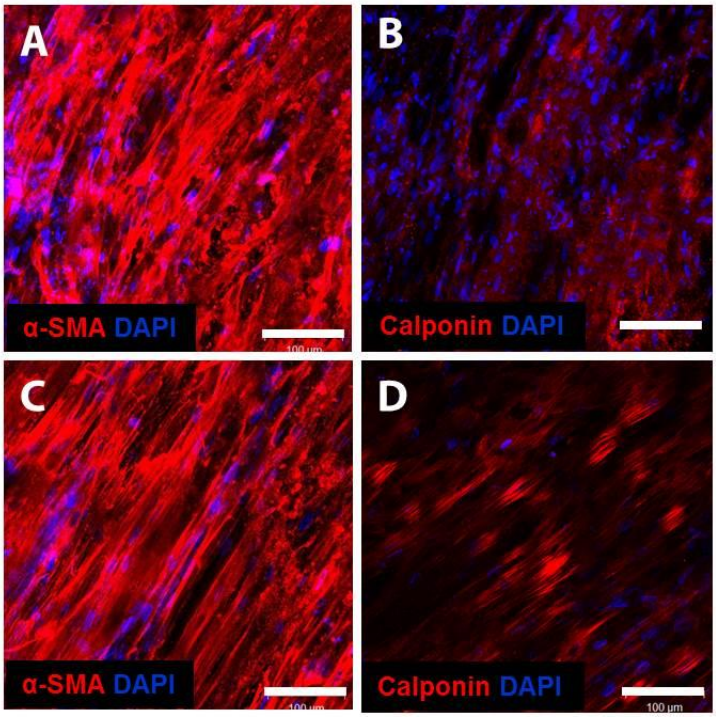

Figure 13: Contractile Protein Expression of Endothelialized TEBVs Made with hNDFs or hMSCs

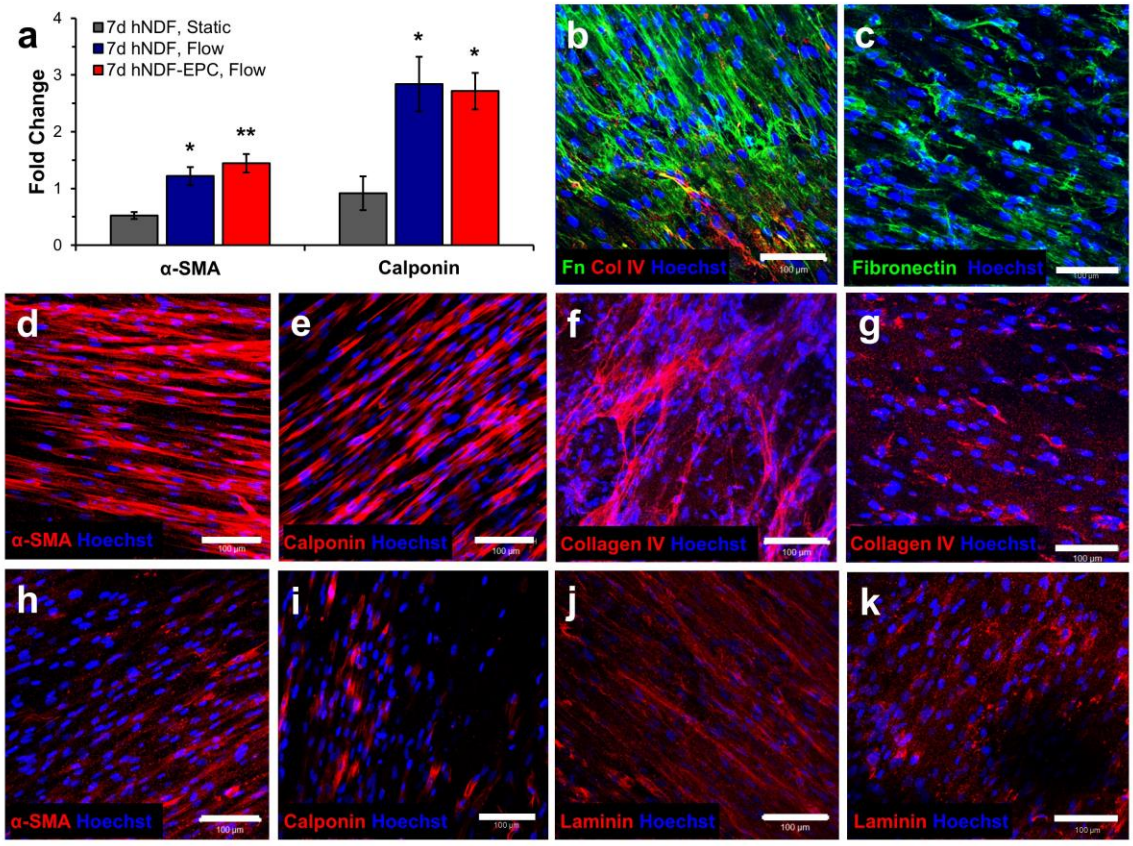

Figure 14: Contractile and Extracellular Matrix Protein Expression

Perfusion for 1 week increased mRNA expression of α-SMA and calponin compared to TEBVs under static conditions. One-way ANOVAs with post-hoc Tukey's tests were performed on the results of four independent experiments performed with hNDF-only TEBVs and hNDF TEBVs under flow and three independent experiments performed with endothelialized TEBVs matured for 1 week under physiological perfusion. (*$p < 0.05$, **$p < 0.005$; mean ± SEM). Calponin results were normalized to reference RNA derived from a TEBV matured under static conditions for 24 hours (A). Endothelialized TEBVs composed of hNDFs demonstrated greater expression of contractile proteins α-SMA and calponin after 1 week in perfusion culture (B and C), compared to endothelialized TEBVs composed of hMSCs (D and E). After 1 week of perfusion culture, endothelialized TEBVs composed of hNDFs produced more basement membrane proteins fibronectin (F), collagen IV (H), and laminin (J) than endothelialized TEBVs composed of hMSCs (G, I, K), respectively. All scale bars represent 100 μm.

3.3.4 Vasoactivity

Endothelial presence was verified by staining the lumen of the TEBVs for von Willebrand factor (vWF), which is expressed in the Weibel-Palade bodies of healthy endothelium. Endothelialized TEBVs cultured for 1 week and 5 weeks both expressed vWF (Fig. 15a, b, respectively). Isotype matched controls indicated no background staining of endothelium. Nitric oxide in the culture medium was evaluated by assessing total nitrite and nitrate, the stable byproducts of nitric oxide metabolism (Fig. 15c). NO production of endothelialized TEBVs after 1 week in culture was similar to values after 5 weeks. TEBVs without endothelium cultured for one week produced significantly less NO in the culture media than that produced in the presence of endothelium ($p<0.05$).

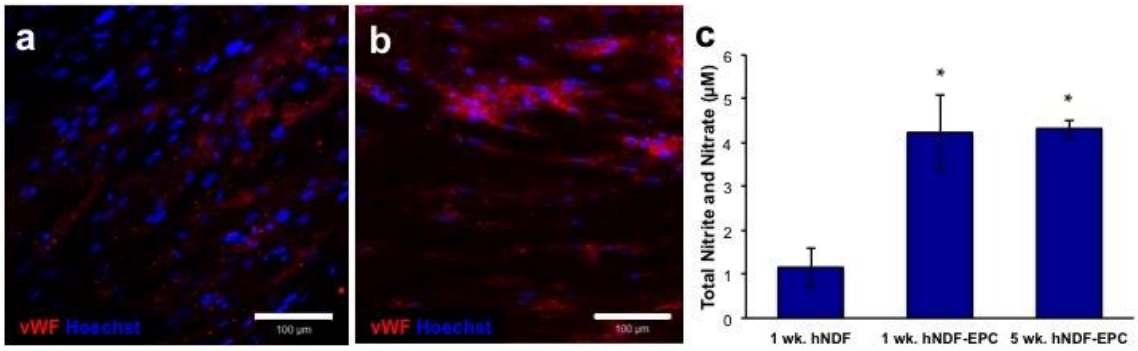

Figure 15: TEBV Endothelialization and Nitric Oxide Production

TEBVs maintain endothelial coverage and NO production over long-term perfusion culture and exhibit vasoactivity in response to drug stimuli. Endothelialized TEBVs expressed vWF after 1 week (A) and 5 weeks (B). Endothelialized TEBVs produce nitric oxide after 1 week in culture and sustain production for 5 weeks in culture. Endothelialized TEBVs elicit significantly greater production of NO compared to TEBVs matured for one week without endothelium (Nitrates and nitrites were sampled from media perfused through TEBV for 48 hours and values represent mean ± SEM. The NO output from six hNDF-only TEBVs was collected in three independent experiments and averaged to produce one value per experiment (N =3). The NO output from four independently cultured TEBVs was evaluated at 1 and 5 weeks (N = 4). Four separate CAD EPC donors were evaluated and pooled. A one-way ANOVA with a post-hoc Tukey's test indicates a significant effect of treatment on NO production (* $P < 0.05$), with respect to TEBVs without endothelium cultured for 1 week under perfusion (C).

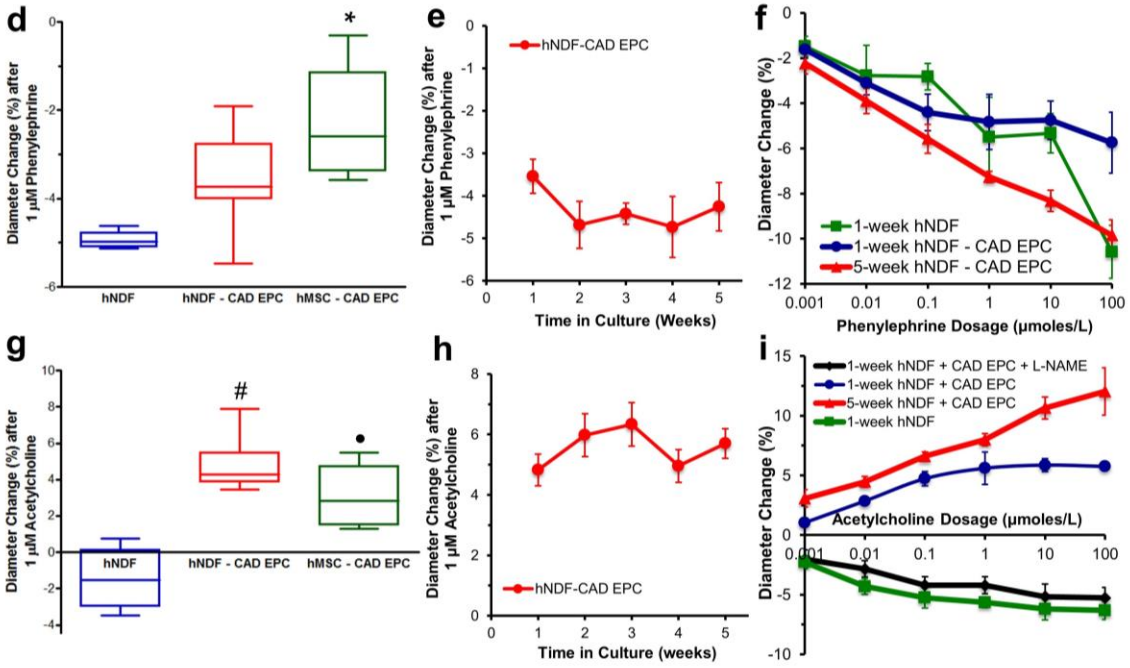

Figure 16: TEBV Endothelial Response and Vasoactivity

Endothelialized TEBVs elicit greater vasoconstriction to 1 µM phenylephrine after one week compared to endothelialized TEBVs with hNDFs and hMSCs (* $P < 0.05$ with respect to hNDF) (D). Endothelialized TEBVs composed of hNDFs maintain a consistent vasoconstriction response to 1 µM phenylephrine over the course of 5 weeks of perfusion (E). A one-way repeated measures ANOVA indicated a significant effect of treatment with respect to a phenylephrine dose response curve ($P < 0.05$). (F). Endothelialized TEBVs composed of hNDFs or hMSCs elicited a vasodilation response to acetylcholine, compared to TEBVs without endothelium which constricted (● $P < 0.01$ and # $P < 0.0001$ compared to non-endothelialized hNDFs) (G). Endothelialized hNDF TEBVs maintained a consistent vasodilation response to acetylcholine over the course of 5 weeks in culture (H). Endothelialized hNDF TEBVs perfused for 5 weeks elicited greater vasodilation in response to increasing doses of acetylcholine in comparison to endothelialized TEBVs perfused for 1 week. TEBVs cultured for 1 week without endothelium elicit increasing vasoconstriction in response to increasing doses of acetylcholine until 1 µM. TEBVs pre-treated with L-NAME exhibit constriction in response to increasing doses of acetylcholine. Four hNDF-only TEBVs, four endothelialized TEBVs cultured for 1 week, and three endothelialized TEBVs cultured for 5 weeks were analyzed. A one-way repeated measures ANOVA confirmed a significant effect of treatment on the acetylcholine dose response ($P < 0.0001$). (I).

After 1 week of perfusion, hNDF TEBVs with and without endothelium constricted after perfusion with 1 μM phenylephrine. Endothelialized hMSC TEBVs perfused for 1 week elicited a smaller contractile response to phenylephrine (Fig. 16d) than TEBVs made with hNDFs. Endothelialized hNDF TEBVs cultured at 2 mL/min for five weeks maintained a steady constriction response to 1 μM phenylephrine (Fig. 16e). TEBVs exhibited a dose response to phenylephrine after 7 days in culture. The magnitude of the response to phenylephrine increased after five weeks in culture, likely due to greater contractile behavior of the medial cells (Fig. 16f).

Acetylcholine elicits endothelium-dependent vasodilation through nitric oxide release in arteries with healthy endothelium. Exposure to 1 μM acetylcholine elicited dilation in endothelialized TEBVs made from either hNDFs or hMSCs cultured for 1 week, and constriction in TEBVs made using hNDFs but without endothelium (Fig. 16g). Endothelialized hNDF TEBVs perfused at 2 mL/min for five weeks maintained a steady vasodilation response to 1μM acetylcholine, indicating sustained endothelial health over time (Fig. 16h). An acetylcholine dose response curve indicates that endothelialized hNDF TEBVs cultured for 1 week plateau in their response at doses above 1 μM acetylcholine. However, endothelialized TEBVs cultured for 5 weeks exhibited increasing vasodilation for acetylcholine doses as high as 100 μM (Fig. 16i). In contrast, TEBVs cultured for one week without endothelium demonstrate a dose-dependent vasoconstriction in response to acetylcholine with a plateau response after 1 μM.

Endothelialized TEBVs pre-treated with the nitric oxide synthase inhibitor L-N^G-Nitroarginine methyl ester (L-NAME) for 10 minutes demonstrated vasoconstriction in response to acetylcholine suggesting that vasodilation was due to release of nitric oxide (Fig. 16i).

3.3.5 Responses to Caffeine and Theophylline

Caffeine and theophylline are vasodilators that cause drug-induced vascular injury (DIVI) in several species[210]. Caffeine stimulates NO production in endothelium and inhibits myosin light chain kinase activity on SMCs. Caffeine produces vasodilation of human mammary arteries in the presence of functional and dysfunctional endothelium[211]. TEBVs cultured for one week with and without endothelium exhibited a dose-dependent vasodilation response to caffeine concentrations ranging from 10^{-9} to 10^{-2} M (Fig. 17a) that elicited similar trends to human mammary arteries with functional and dysfunctional endothelium[211]. Theophylline is a less active metabolite of caffeine[211]. Following short-term exposure to theophylline concentrations ranging from 10^{-9} to 10^{-4} M, endothelialized TEBVs cultured for one week exhibited a smaller dose-dependent vasodilation as similar does of caffeine (Fig. 17b). TEBV response to drugs known to cause drug-induced vascular injury provides a promising avenue for studying the effects of this phenomenon *in vitro*.

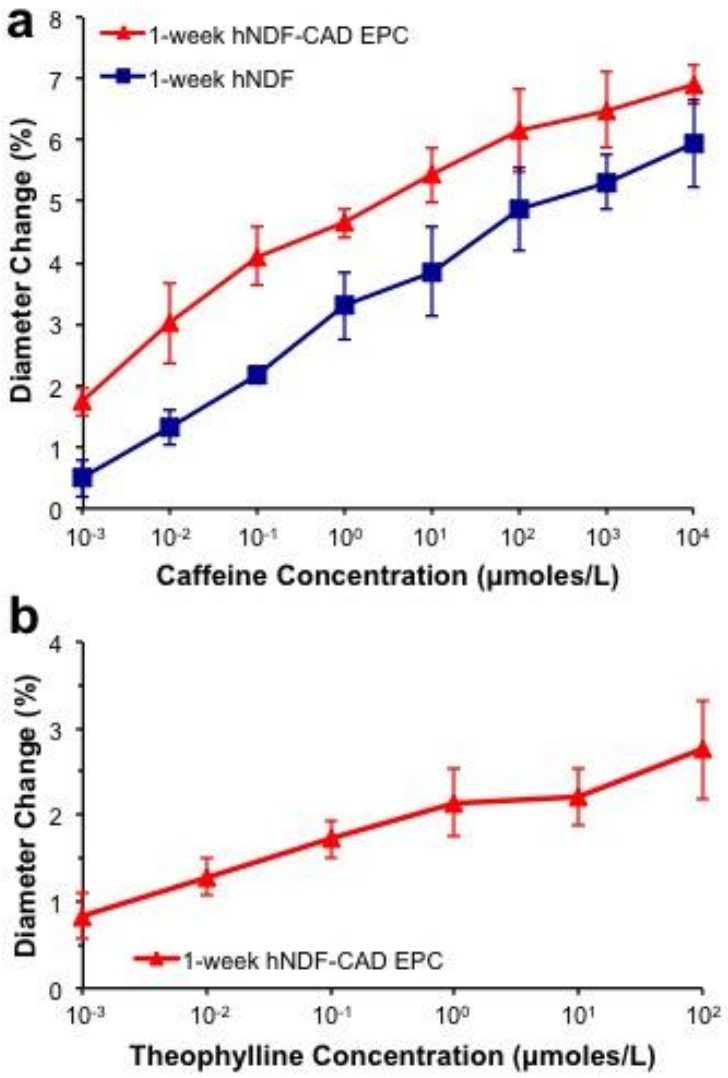

Figure 17: TEBV Response to Caffeine and Theophylline

TEBVs perfused for one week elicit dose-dependent vasodilation in response to caffeine (A) and theophylline (B). A two-way repeated measures ANOVA demonstrates a significant effect of dose and the presence of the endothelium in response to caffeine (#: $P < 0.05$). Data reported as mean ± SEM, n = 3 TEBVs (A). TEBVs exhibit dose-dependent vasodilation in response to theophylline. A one-way repeated measures ANOVA demonstrates a significant effect of dose ($P < 0.05$). Data reported as mean ± SEM, n = 6 TEBVs tested in three independent experiments (B).

3.4 Discussion

The human TEBVs developed in this study had several novel features. They could be prepared with inner diameters of 500-800 μm and perfused in less than three hours. In contrast, other approaches to prepare TEBV require 6-8 weeks in vitro culture before the mechanical strength is sufficient to enable perfusion[50,212]. After 1 week of perfusion, medial hNDFs or hMSCs expressed contractile proteins α-smooth muscle actin and calponin, indicating a switch to a contractile phenotype[22]. TEBVs also produced the extracellular matrix proteins laminin, collagen IV, and fibronectin and exhibited burst pressures similar to human saphenous veins (1599±877 mm Hg)[208]. Quantifiable and physiologically relevant reactions to vasoactive stimuli occurred after only 1 week. TEBVs released nitric oxide, elicited endothelium-independent vasoconstriction to phenylephrine and endothelium-dependent vasodilation in response to acetylcholine, and maintained these responses during 5 weeks of *in vitro* perfusion culture.

Non-destructive monitoring of maturation and function is critical for an effective microphysiological system for drug screening. In this study, vasoactivity was quantified *in situ* to evaluate the TEBV maturation and endothelial health. Prior work, as referenced in Table 3, has evaluated endothelium-independent vasoconstriction of TEBVs in response to serotonin, endothelin-1, and prostaglandin[94,199]. The vasoconstriction of TEBVs produced with collagen gels embedded with rat smooth muscle cells has been

evaluated destructively through changes in tension upon exposure to endothelin-1, bradykinin, phenylephrine, and sodium nitroprusside[200]. Recently, we evaluated endothelium-independent vasoconstriction in a TEBV after six weeks of fabrication using the cell sheet method[202]. In the current study, monitoring vasoconstriction and vasodilation non-destructively allowed us to evaluate the function of both endothelial cells and medial cells within the TEBVs over time. Most importantly, the TEBVs in this study produced physiological responses to drug stimuli (Table 5), suggesting functional maturation after only 1 week of perfusion at physiological flow rates. Lastly, the raw vasoactive responses of our TEBVs are within the physiological range for human native arteries, since human radial arteries dilate between 3-10%[213].

Table 5: Human Vasoactivity Responses

Drug	Target	EC_{50}	Reference
Phenylephrine	Human saphenous vein	10^{-5} M	[214]
Acetylcholine	Human brachial artery	0.537×10^{-6} M	[215]
Theophylline	Human dorsal hand vein	84 μg/min	[216]
Caffeine	Human mammary artery	10^{-6} M	[211]

We used CAD EPCs to evaluate the responses of a population pre-disposed to endothelial activation. Late-outgrowth EPCs are harvested from adult peripheral blood or umbilical cord blood with a minimally invasive vein puncture and cultured *ex vivo* to yield characteristics of mature endothelium[162], allowing for the characterization of TEBVs constructed from cells from various donor populations. CAD EPCs behave

similarly to endothelium from healthy patients when seeded over synthetic substrates *in vitro*[204] and in direct co-culture with human aortic smooth muscle cells *in vitro*[158].

Evaluating drug-induced vasodilation in a human model would be a significant development in the progress toward finding human biomarkers for DIVI. DIVI typically manifests in animal studies through changes in vascular tone, leading to endothelial dysfunction and inflammation[217]. Endothelial dysfunction has been detected in patients who have undergone treatment with cytotoxic drugs for chemotherapy[218]. Caffeine and theophylline are nonspecific phosphodiesterase inhibitors that elicit vasodilation. A previous study noted that human mammary arteries with healthy endothelium demonstrated greater vasodilation in response to caffeine compared to those with dysfunctional endothelium[211]. Our study noted a statistically significant increase in vasodilation in endothelialized TEBVs compared to non-endothelialized TEBVs. TEBVs also elicited a short-term dose-dependent response to theophylline, suggesting that a DIVI response may be measured in this system.

A limitation of our study was that TEBVs were matured under laminar flow using a peristaltic pump, during which only flow rate was controlled. Cyclic mechanical stress through pulsatile flow increases extracellular matrix production and mechanical strength of TEBVs[29,50]; however, laminar flow is sufficient to evaluate the effects of drug stimuli on the endothelium. Pressures in our system were lower than those encountered in the arterial systems and raising the pressure may facilitate differentiation.

Ideally, adult SMCs would be used as the cell source for the vessel wall; however, adult SMCs exhibit limited population doublings *in vitro* before undergoing senescence[219]. We performed this study with hNDFs as a proof of concept due to their attainability, contractile properties, and proliferative capacity. We also examined hMSCs, which have been used to create functional TEBVs[220], and may be differentiated to express characteristic SMC markers. We are currently evaluating the response of our model with SMCs derived from induced pluripotent stem (iPS) cells, which would enable us to examine patient specific functional changes. Overall, this study indicates that rapidly producible dense collagen gel TEBVs have the potential to serve as *in vitro* models for drug testing under healthy and induced inflammatory conditions.

3.5 Chapter-Specific Acknowledgements

Sincere thanks go to Ringo Yen for his contributions toward designing and optimizing the culture chambers for the TEBVs, as well as for optimizing and performing pressure transducer assays. Samantha Perez performed mechanical testing assays with the TEBVs. The authors would like to thank S.J. Owen from the Duke Biomedical Engineering Machine Shop for his help constructing the custom rotation device and tensile testing device, as well as the Duke Physics Machine Shop for their assistance manufacturing the custom TEBV chambers. Funding: This work was supported by NIH grants UH2TR000505, 4UH3TR000505, and the NIH Common Fund

for the Microphysiological Systems Initiative (to G.A.T.), NIH grants R01HL044972 and R21EB017868 (to W.M.R.), and American Heart Association Pre-doctoral Fellowship 14PRE20500062 (to C.E.F.). We acknowledge the support of NIH grant P 40 RR017447 to Darwin Prockop "Preparation and Distribution of Adult Stem Cells" for providing the adult human MSC.

4. Effect of Inflammation and Statins on a Human Vascular Microphysiological System Model

Portions of the text and figures presented in this chapter have been previously published in the following form: Fernandez CE, Yen RW, Perez SM, Bedell HW, Povsic TJ, Reichert WM, Truskey GA. Human Vascular Microphysiological System for in vitro Drug Screening. *Scientific Reports* 6:21579 (2016)[187].

4.1 Introduction

Microphysiological systems (MPS) are perfused small-scale models of one or more human tissues or organs[7] comprised of human primary cells or induced pluripotent stem cells (iPSCs) with the ultimate potential of becoming models to study disease or tools for precision medicine. A human tissue-engineered blood vessel (TEBV) capable of responding to vasoactive stimuli would pose a promising model for the evaluation and screening of pharmaceutical drugs that impact vascular tone and function. In Specific Aim 2, we developed a rapidly producible, arteriolar scale TEBV capable of endothelium-dependent and independent vasoactivity[187].

An ideal TEBV for MPS applications would be comprised of human cells in a biological or biodegradable synthetic matrix, have a small inner diameter to reduce fluid volumes, exhibit enough mechanical strength to withstand physiological stresses, and be produced rapidly to facilitate efficient drug screening. The medial wall cells should

exhibit a smooth muscle phenotype, be quiescent and be able to contract and relax in response to agonists or inhibitors. Most importantly, the TEBV must be endothelialized to enable physiologically relevant dilation and constriction in response to stimuli.

An effective microphysiological system must be capable of measuring tissue responses under both healthy and diseased conditions. Changes in vascular tone are a critical measurement of vascular health; therefore, non-destructive evaluation of TEBV maturation and vasoactivity is beneficial toward effective monitoring of responses to drugs or stimuli. One important clinical assessment of cardiovascular health, which predicts future cardiac events, involves infusion of acetylcholine to induce vasodilation of the coronary or brachial arteries[195-197]. Acetylcholine is a muscarinic cholinergic agonist that stimulates release of nitric oxide, prostacyclin, and endothelium-derived hyperpolarizing factor in vessels with healthy, intact endothelium. Conversely, acetylcholine activates the muscarinic receptors on the smooth muscle cells in vessels with dysfunctional or damaged endothelium, leading to vasoconstriction[195,198].

Endothelial activation and dysfunction affects patients with hypercholesterolemia[144], diabetes mellitus[143], and complications from chronic smoking[145], leading to atherosclerosis[120]. Atherosclerosis has both inflammatory and mechanical origins[120-122] and is promoted by high levels of blood cholesterol transported by low-density lipoprotein (LDL). Excess LDL may be trapped in the vascular intima and oxidized (oxLDL), activating the endothelium and initiating an inflammatory

response[123]. Activated endothelial cells express Vascular Cell Adhesion Molecule-1 (VCAM-1), Intracellular Adhesion Molecule-1 (ICAM-1), and E-selectin on their luminal surface and secrete chemokines to attract monocytes and T-lymphocytes to the lesion site[124]. The resulting inflammatory environment facilitates the development of a lipid-rich plaque and SMC over-proliferation, leading to an atherosclerotic lesion[125].

Activated or dysfunctional endothelium exhibit reduced vasodilation in response to acetylcholine[195]; therefore, the assay we developed in Specific Aim 2 to assess the maturation and health of our TEBV is ideal for assessing the behavior of our vascular microphysiological system under inflammatory conditions. Acute endothelial activation was induced in response to the pro-inflammatory cytokine TNF-α to validate the inflammatory response of our TEBV system. TNF-α promotes expression of cell-surface adhesion molecules such as VCAM-1, ICAM-1, and E-selectin, which facilitate leukocyte adhesion to the vascular wall[221].

Statins, or 3-hydroxy-3-methylglutaryl coenzyme A (HMG-CoA) reductase inhibitors, reduce LDL levels in hypercholesterolemic patients. In 2003-2004, over 24 million Americans were on statin therapy[222]. In addition to lowering blood cholesterol, statins reduce endothelial dysfunction[223], stabilize plaques[224] inhibit leukocyte adhesion[225], suppress vascular SMC proliferation[226], and increase circulating EPC levels[227]. The mechanisms by which statins elicit these pleiotropic effects on the vasculature are incompletely understood. Krüppel like factor 2 (KLF2) is an endothelial

transcription factor that induces the expression of the vasodilation and anti-thrombotic proteins eNOS and thrombomodulin[228]. Increased KLF2 expression downregulates the expression of adhesion molecules such as VCAM-1 and E-selectin[229]. In endothelium, KLF2 expression inhibits oxidative stress-mediated cell injury. KLF2 expression is induced by shear stress and has been demonstrated to be upregulated in response to statins[230,231].

In this aim, we have assessed the inflammatory response of a vascular microphysiological system created from human neonatal dermal fibroblasts (hNDFs) embedded within a dense collagen gel matrix and endothelialized with late-outgrowth endothelial progenitor cells (EPCs). We have evaluated our model using EPCs from derived from the peripheral blood of coronary artery disease patients (CAD EPCs). CAD EPCs express markers of healthy endothelium and have demonstrated healthy endothelial function and response to flow *in vitro* under 2D[64] and 3D[187] conditions. CAD EPCs have also functioned *in vivo* as an endothelial source for synthetic grafts in a rat femoral artery model[65]. Little information exists on the inflammatory response of CAD EPCs, and therefore it is important to evaluate their response to pro-inflammatory cytokines in order to validate their potential use in autologous transplantation procedures.

We have used acute doses of pro-inflammatory cytokine tumor necrosis factor – α (TNF-α) to induce endothelial dysfunction within TEBVs endothelialized with CAD

EPCs, and assessed changes in vasoactivity by measuring changes in endothelium-dependent vasodilation in response to acetylcholine. We have then compared the effect of three commonly prescribed statins toward mediating the TNF-α induced inflammatory response. Using TNF-α to activate endothelium instead of oxLDL allows us to directly measure the pleiotropic effects of statins toward mediating endothelial dysfunction in a cholesterol-independent model.

Lastly, we have compared the inflammatory response of CAD EPC TEBVs to TEBVs endothelialized with late outgrowth EPCs from the peripheral blood of young, healthy volunteers (HV EPCs). We have further attempted to validate the effects seen in 3D with two-dimensional studies assessing the effects of statins toward preventing TNF-α-induced endothelial senescence and activation. Overall, this study serves to evaluate the feasibility of our microphysiological system for use in healthy and inflammatory conditions by evaluating its response to drugs with well-characterized outcomes.

4.2 Methods

4.2.1 Cell Isolation and Culture

All isolations of endothelial progenitor cells from blood were performed in accordance with the protocol approved by the Duke University Institutional Review Board for the collection of peripheral blood from consenting patients undergoing left heart catheterization at Duke University Medical Center. Informed consent was obtained

from all donors prior to blood withdrawal. CAD EPCs from four donors with advanced CAD were isolated and grown as previously described[204]. EPCs from healthy volunteers were isolated from individuals under 35 at the Duke Center for Living. EPCs were maintained in EC medium comprised of Endothelial Basal Medium (EBM-2) with an EGM-2 Single Quots Kit (Lonza) supplemented with 10% heat-inactivated fetal bovine serum (HI-FBS, Gibco) and 1% Pen/Strep (Lonza). EPCs were passaged at 80% confluence using 0.025% trypsin/EDTA (Lonza) and neutralized with 1:1 ratio of EC medium. Cells in passages 6-8 were used for all experiments.

Human neonatal dermal fibroblasts were purchased from Clonetics and maintained in hNDF medium comprised of Dulbecco's Modified Eagle's Medium (DMEM) with 4.5 g/L glucose (Gibco) supplemented with 10% HI-FBS, 1% Pen/Strep, 1x Non-essential amino acids (NEAA, Gibco), 1x Sodium Pyruvate (Gibco), 1x Glutamax (Gibco) and 0.1% β-mercaptoethanol (Gibco). hNDFs were passaged at 80% confluence using 0.05% trypsin/EDTA (Lonza) and neutralized with a 1:1 ratio of hNDF media. Passages 6-9 were used for all experiments.

TEBVs under static and flow conditions were maintained in culture medium comprised of DMEM with 1.1 g/L glucose, L-glutamine, and 110 mg/L sodium pyruvate (Gibco) supplemented with 3.3% HI-FBS, 1x NEAA, 1% Pen-Strep, and 0.1% β-mercaptoethanol. After 1 week in culture, 2 mg/mL ε-aminocaproic acid was added to the TEBV medium to minimize TEBV constriction under long-term culture conditions.

4.2.2 Flow Cytometry

Proliferative colonies of isolated CAD EPCs and HV EPCs were characterized using flow cytometry. Cells were positive for endothelial cell markers CD31 and CD144, and negative for CD45, CD115, and CD14. Additionally, surface levels of VCAM-1 (CD106), ICAM-1 (CD54), and E-selectin (CD62E) were analyzed. Mouse IgG1 and untreated cells were used as controls. Antibodies (Biolegend) were conjugated with either FITC or phycoerythrin. Detailed antibody information can be found in Appendix F. EPCs were passaged using 0.025% trypsin/EDTA at 80% confluence. Approximately 500,000 EPCs were resuspended in 100 μL 1% bovine serum albumin buffered with Dulbecco's PBS with calcium and magnesium. Cells were incubated at room temperature for 30 minutes with 5 μL of preconjugated antibody before washing with 1% BSA solution. Cells were collected after centrifugation at 400x g for 7 minutes and fixed using 10% neutral buffered formalin before storage at 4°C until analysis. Flow cytometry analysis was performed by collecting 9,000 events per sample.

4.2.3 TEBV Fabrication, Endothelialization, and Perfusion Culture

TEBVs were fabricated from collagen gels and plastically compressed to increase the collagen fiber density[103,203], then endothelialized and placed in flow culture circuits as previously described[187]. Rat-tail collagen I (BD Biosciences) was diluted to 2.05 mg/mL using 0.6% acetic acid (Sigma). A serum-free 10x Dulbecco's Modified Eagle's Medium (DMEM) was added at a 1:10 ratio to the collagen (Sigma). The pH was raised to 8.5

using 5M sodium hydroxide (Sigma). A suspension of hNDFs was added at an initial cell density of $5x10^5$ cells/mL. Gel solutions were immediately transferred to a 3-cc syringe with a closed two-way luer-lock stopcock (Cole-Parmer) attached. An 810-μm diameter steel mandrel was inserted in the center to create the TEBV lumen and held in place with Parafilm (Kimberly Clark) at the top of the syringe. Solutions were allowed to gel for 30 minutes at room temperature. Immediately afterward, gel solutions were suspended on 10 KimWipes under a 0.8 μm membrane filter (Whatman). After removal of the water, TEBVs were immediately placed in TEBV media until mounting in a chamber.

TEBVs were mounted in custom-made vascular perfusion chambers that could accommodate 1-2 TEBVs on grips (0.760 mm outer diameter) (Fig. 1). TEBVs were sutured in place using 4-0 black silk sutures. Endothelialization was performed by injecting 500,000 EPCs through the lumen of each TEBV, and the chamber was sealed and rotated at 10 rotations per hour (rph) on a custom-made rotation platform for 30 minutes at 37 ºC to allow for cell adhesion. A peristaltic pump (Masterflex) with a minicartridge pump head with 8 rollers (Ismatec) was used to create pulseless flow through the TEBVs. Flow circuits accommodating 1 or 2 TEBVs were created using a reservoir and a combination of silicone and PharMed BPT tubing (Cole-Parmer). Circuits contained 25 mL of flow media as described above per TEBV. Media was changed every 2-3 days. TEBVs were maintained at a flow rate of 2 mL/min throughout all experiments.

4.2.4 Analysis of TEBV Vasoactivity

Endothelium-independent vasoconstriction in response to phenylephrine and endothelium-dependent vasodilation was assessed non-destructively to monitor changes in TEBV health and function as previously described[187]. TEBVs were placed under a stereoscope connected to a video camera (Amscope). Video recordings of the vessel outer diameter were analyzed using Image J. Endothelium-independent vasoconstriction response was evaluated by adding 1 μM phenylephrine (Sigma) to the flow circuit. After 5 minutes, 1 μM acetylcholine (Sigma) was added to the flow circuit to assess the endothelium-dependent vasodilation response[196]. A silicone syringe port (Ibidi) was added to the flow circuit and drugs were added to the system via a syringe connected to a sterile 27-gauge needle. Changes in outer diameter are expressed as percent change from the baseline outer diameter.

4.2.5 Activation of TEBVs with TNF-α

Endothelial dysfunction and recovery was evaluated via acute exposure to TNF-α[232]. Endothelialized TEBVs were allowed to mature for 7 days. A 500 μL media sample was collected and frozen at -20 ºC for NO analysis. TEBV vasoactivity was evaluated after 7 days using the phenylephrine-acetylcholine assay listed above. TNF-α was introduced to the flow circuit for 4.5 hours at a final concentration of 200 U/mL (~1 ng/mL) or 500 U/mL (~2.5 ng/mL). TEBV vasoactivity was evaluated after 7 days using the phenylephrine-acetylcholine assay. Media was changed directly afterward to TEBV

media with 2 mg/mL ε-aminocaproic acid. TEBV vasoactivity was assessed using the phenylephrine-acetylcholine assay three days and seven days later to evaluate endothelial recovery after removal of the TNF-α stimulus.

4.2.6 Treatment of TEBVs with Statins

Three statins were evaluated to assess their effect toward mediating the TEBV inflammatory response toward TNF-α. Lovastatin, Atorvastatin, and Rosuvastatin were purchased from Sigma-Aldrich and resuspended in DMSO to produce stock solutions of 0.01 M, 0.0165 M, and 0.02 M, respectively. The effect of statins toward mediating TEBV response toward TNF-α was evaluated by culturing endothelialized TEBVs made with hNDFs for 1 week. On Day 7, lovastatin, atorvastatin, or rosuvastatin was introduced into the flow circuit to produce a final concentration of 1 μM. The TNF-α response of control TEBVs not exposed to statins was evaluated. TEBVs were treated with statins for 3 days, and then exposed to 200 U/mL TNF-α for 4.5 hours. TEBV vasoactivity was assessed using the phenylephrine-acetylcholine assay at Day 7, Day 10, and Day 10 after treatment with TNF-α. Media samples were collected from the flow circuit prior to every vasoactivity study to assess nitric oxide production. The effect of rosuvastatin was evaluated under higher doses of TNF-α by repeating the previously outlined experiment and exposing TEBVs to 500 U/mL TNF-α for 4.5 hours.

4.2.7 Quantification of Nitric Oxide Produced by TEBVs

Prior to each vasoactivity study, 5 mL media samples were removed from the flow circuit and maintained at -20ºC. After thawing, proteins were removed from a 500 μL sample using 10,000 MWCO spin columns (Corning) microcentrifuged at 10,000 rpm for 5 minutes. Total nitrite and nitrate in each sample was assessed using a Greiss reagent assay kit (Cayman Chemical). Absorbance at 540 nm was measured using a μQuant microplate reader (Bio-Tek). Samples were normalized to pure media controls.

4.2.8 RNA Isolation and Reverse Transcriptase-Polymerase Chain Reaction Analysis

NCBI reference sequences for the mRNA of each gene were obtained from PubMed, and primer sequences (Appendix) were generated using the online design program Primer-Blast. Primer pairs that demonstrated uniform and single-product melt curves upon reaction with hNDF reference RNA were selected. Primer efficiencies were calculated using standard curves with reference RNA. Primer efficiencies between 90-115% were deemed acceptable.

Cells were extracted from the TEBV matrix by submerging TEBVs in 1 mg/mL collagenase solution in PBS at 37 ºC for 30 minutes. TEBVs were spun down at 300 x g for 5 minutes to pellet cells. EPCs and hNDFs were separated using 25 μL CD31 Dynabeads (Life Technologies). Total RNA from hNDFs was isolated using an Aurum Total RNA Mini Kit (BioRad). RNA purity and concentration was assessed using a NanoDrop Spectrophotometer. Reverse transcription of RNA into cDNA was performed

using 250 ng of hNDF RNA using the iScript cDNA Synthesis Kit (BioRad). RT-PCR was performed using the iQ SYBR Green Supermix (Bio-Rad) and the CFX Connect Real-Time PCR Detection System (Bio-Rad). Fold change from reference RNA was calculated as previously described [206].

4.2.9 Immunofluorescent Staining of TEBVs

TEBVs were fixed in 10% formalin for 30 minutes, rinsed three times with DPBS, then cut *en face*. Blocking was performed with 10% goat serum (Gibco) in DPBS for at least 8 hours at room temperature. Primary antibody staining was performed at 1:100 in 10% goat serum overnight. The following primary antibodies were used: mouse anti-VCAM-1, rabbit anti-E-selectin, and mouse anti-ICAM-1. Detailed antibody information can be found in the Appendix. After staining overnight with primary antibody, samples were rinsed 3 times with DPBS and stained for 1 hour at 37 °C with 1:500 goat anti-rabbit Alexa Fluor 594 or goat anti-mouse Alexa Fluor 488 (Life Technologies). Samples were rinsed 3 times and stained with 1 μL/mL Hoechst 33342 dye in DPBS for 5 minutes at room temperature, then rinsed 3 times with DPBS. Samples were mounted onto slides using FluorSave reagent (Calbiochem) and covered with a cover slip. Z-stack images of TEBVs were obtained on a Zeiss 510 inverted confocal microscope at 20X magnification. Images were analyzed using a Zeiss LSM image browser and Image J (NIH).

4.2.10 β-galactosidase assay for Cell Senescence in 2D

The effect of statins toward mediating the TNF-α-induced sencesence response of EPCs was evaluated using a β-galactosidase assay. CAD EPCs and HV EPCs were plated at a density of 5000 cells/cm^2 in a 24-well TCPS plate. The following day after plating, media was changed to either 1 μM atorvastatin or 1 μM rosuvastatin. Control cells were kept in TEBV media, and a baseline EPC control condition was used. Cells were maintained in test media for 24 hours, after which 200 U/mL was added to a subset of test samples for 4.5 hours. Afterward, cells were fixed and assayed for senescence. A senescence β-galactosidase staining kit (Cell Signaling Technology) was used according to the manufacturer's protocol to stain for senescent cells. The stain was visualized with microscopy at 20X magnification (Nikon TE2000U, Tokyo, Japan) and digital camera (DS-Qi1Mc, Nikon). Ten random images were taken per condition. The percentage of senescent cells was calculated as the total number of cells that contained the blue β-galactosidase stain divided by the total number of cells in the field of view[233]. Cells at P7 were used for all assays. Three CAD EPC donors and two HV EPC donors were used for these experiments.

4.2.11 NF-kB P65 Nuclear Translocation and SIRT1 Expression

The NF-kB subunit P65 translocates into the cell nucleus upon activation with TNF-α[234]. The effect of atorvastatin and rosuvastatin on TNF-α induced P65 nuclear translocation was evaluated in CAD EPCs and HV EPCs cultured in 2D. CAD EPCs and

HV EPCs were plated at a density of 5,000 cells/cm^2 in a 24-well TCPS plate. The following day after plating, media was changed to either 1 μM atorvastatin or 1 μM rosuvastatin. Control cells were kept in TEBV media, and a baseline EPC control condition was used. Cells were maintained in test media for 24 hours, after which 200 U/mL was added to a subset of test samples for 4.5 hours. Afterward, samples were fixed in 10% neutral buffered formalin for 10 minutes at room temperature, rinsed three times with DPBS, and stored at 4 °C in DPBS until staining.

Immunofluorescent staining was performed by first permeabilizing the cells with 0.1% Triton-X for 5 minutes. Cells were rinsed 3 times with DPBS, then blocked with 10% goat serum (Gibco) in DPBS for 1 hour. Mouse anti-NF-kB P65 and a rabbit anti-Sirt1 (Santa Cruz Biotechnologies) antibodies were used at a concentration of 1:100 in 10% goat serum. Samples were incubated in primary antibody solutions overnight at room temperature on a rocker, then washed three times with DPBS for 5 minutes to remove unbound primary antibody. Samples were incubated with goat anti-mouse Alexa Fluor 488 and Goat anti-rabbit Alexa Fluor 594 (Life Technologies) secondary antibodies at a concentration of 1:250 in 10% goat serum for 1 hour at room temperature. Samples were rinsed three times with DPBS for 5 minutes to remove unbound secondary antibody, then treated with Hoechst dye at 1:1000 in DPBS for 5 minutes to stain nuclei. Samples were rinsed for 5 minutes in DPBS and stored in DPBS at 4 °C.

Samples were visualized with fluorescence microscopy at 20X magnification (Nikon TE2000U, Tokyo, Japan) and digital camera (DS-Qi1Mc, Nikon). Five random images were taken per condition of the Hoechest stain, the P65 stain, and the Sirt1 stain. Images were analyzed with ImageJ. Background was subtracted from all images, and a binary mask was made of the Hoechest stain to denote nuclei. Individual nuclei were added as Regions of Interest (ROIs) to an ROI Manager. The mean gray value of the P65 stain and the Sirt1 stain within each ROI was measured. Average mean gray value within each nuclear region was reported for each image, with 30-60 nuclei analyzed per image.

4.2.12. U937 Monocyte Adhesion to 2D EPC Cultures

Monocyte adhesion was used as another metric to quantify the activation of EPCs cultured alone on tissue culture polystyrene plates. U937 monocytes were purchased from American Tissue Culture Collection (ATCC) and maintained in RPMI medium supplemented with 10% fetal bovine serum (FBS) and 1% Pen/Strep.

CAD EPCs and HV EPCs were plated on TCPS 48-well plates at a density of 20,000 cells/cm^2 in EPC media. The following day, media was changed to TEBV media supplemented with rosuvastatin up to a final concentration of 1 μM. Control cells were kept in TEBV media, and a baseline EPC control condition was used. Cells were maintained in test media for 24 hours, after which 0, 100, 200, or 500 U/mL of TNF-α was added to wells for 4.5 hours. Two wells were analyzed per condition.

U937 monocytes were resuspended in a 2 μM solution of Cell Tracker Green (CMFDA) and incubated at 37 °C for 10 minutes, then centrifuged at 400 x g for 5 minutes. Monocytes were resuspended in RPMI media and evenly divided into 1.6-mL microcentrifuge tubes to obtain a plating density of 10,000 cells/well. Tubes were microcentrifuged at 3,000 rpm for 5 minutes to pellet monocytes, and cells were resuspended in one of the following media concentrations: TEBV media supplemented with 0.01% DMSO or 1 μM rosuvastatin with 0, 100, 200, or 500 U/mL TNF-α. EPC media and TEBV media were used as controls. Monocytes were added to well plates and allowed to adhere for 30 minutes, after which plates were fixed in 10% neutral buffered formalin for 10 minutes at room temperature, and rinsed three times with DPBS to remove formalin. Cells were maintained at 4 °C until imaging. Samples were visualized with fluorescence microscopy at 20X magnification (Nikon TE2000U, Tokyo, Japan) and digital camera (DS-Qi1Mc, Nikon). Five random images were taken per condition. Adhered monocytes were counted using a custom MATLAB program, and the average of the two wells in each condition were averaged.

4.2.13 Statistical Analysis

Statistical analyses were performed using JMP 11 (SAS Institute). All data were analyzed by one-way or two-way analysis of variance (ANOVA) with post hoc Tukey's test to compare means. A one-way repeated measures ANOVA was performed for all time and dose-dependent assays. All data are represented as means ± SEM. *P* values <

0.05 were considered significant. Power calculations were performed to ensure sample sizes yielded a power greater than 0.8.

4.3 Results

4.3.1 Comparison of CAD EPCs to Healthy Volunteer EPCs

CAD EPCs demonstrated greater activation at baseline levels compared to healthy volunteer EPCs. Flow cytometry to assess surface expression of surface markers VCAM-1, ICAM-1, and E-selectin demonstrated greater surface expression of VCAM-1 and E-selectin in CAD EPCs compared to HV EPCs. Isolations from CAD EPCs produced cells capable of proliferation up to passage 10; however, while all HV EPC isolations successfully produced colonies, only 2 out of the 6 HV EPC isolations produced EPCs capable of proliferation through passage 9; the other 4 isolations became senescent by passage 4, precluding flow cytometry and performance of experiments with cells from these donors. These results are consistent with those we have previously observed for EPCs isolated from healthy volunteers[64].

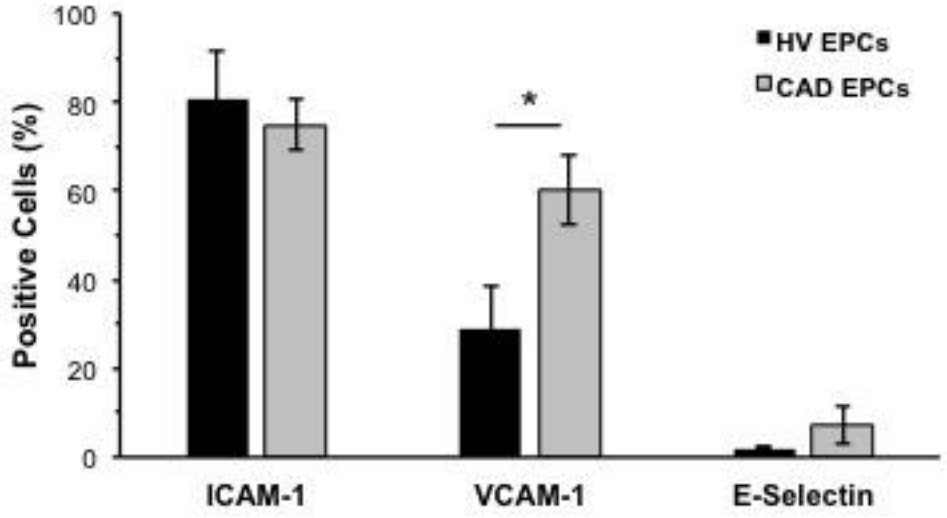

Figure 18: Baseline Adhesion Molecule Expression of EPCs

CAD EPCs and HV EPCs were evaluated for the adhesion molecules ICAM-1, VCAM-1, and E-selectin. 80.1 ± 10.6% of HV EPCs expressed ICAM-1 on their surface compared to 74.8 ± 5.8% of CAD EPCs. 29.1 ± 9.6% of HV EPCs expressed VCAM-1 on their surface, compared to 60.3 ± 7.8% of CAD EPCs. 2.1 ± 0.1% of HV EPCs expressed surface E-selectin, compared to 7.1 ± 4.2% of CAD EPCs. Data represented as mean ± SEM, N = 6 CAD donors, and N = 2 HV EPC donors. A one-way ANOVA with a Tukey's post-hoc test indicates significant difference in VCAM-1 expression (*P < 0.05)

4.3.2 Response of TEBVs to TNF-α

To evaluate an acute inflammatory response, TEBVs endothelialized with CAD EPCs were perfused for 1 week, then exposed to 200 U/mL TNF-α for 4.5 hours[154]. We examined the response to 1 μM phenylephrine and 1 μM acetylcholine before and up to 7 days after the transient exposure to TNF-α. After exposure to 200 U/mL TNF-α for 4.5 hours, TEBVs constricted after exposure to acetylcholine (Fig. 19a). The endothelium began to recover three days after TNF-α exposure, and 7 days post-exposure,

acetylcholine-induced vasodilation levels were the same as they were prior to exposure to TNF-α, indicating that the TEBV endothelium recovered from an acute inflammatory stimulus. The contractile response to phenylephrine was unaffected by TNF-α treatment (Fig. 19a).

Treatment with 200 U/mL TNF-α for 4.5 hours caused an increase in the rate of NO production compared to TEBVs under baseline conditions (Fig. 19b). TNF-α increases the amount of induced nitric oxide synthase expression within vascular smooth muscle cells[235]. Exposure to 200 U/mL TNF-α in the flow circuit resulted in increased expression of ICAM-1 mRNA in hNDFs within the vessel wall (Fig. 19c). In the absence of TNF-α, the protein expression of VCAM-1 (Fig. 20a), E-selectin (Fig. 20b), and ICAM-1 (Fig. 20c) is low or absent. *En face* images of the endothelium demonstrated increased expression of VCAM-1, E-selectin, and ICAM-1 after exposure to 200 U/mL TNF-α within the flow circuit for 4.5 hours (Fig. 20d-f), indicating endothelial activation[236].

Although exposure of CAD EPC TEBVs to 200 U/mL TNF-α for 4.5 hours did not produce a statistically significant change in phenylephrine-induced contraction, the same does not appear to be true for CAD EPC TEBVs exposed to 500 U/mL TNF-α for 4.5 hours. Preliminary experiments assessing the recovery of CAD EPC TEBVs matured for 7 days from an exposure of 500 U/mL TNF-α for 4.5 hours demonstrate an impairment of the phenylephrine induced constriction response. HV EPC TEBVs

exposed to a similar treatment did not demonstrate inhibition of this response. Both CAD EPC TEBVs and HV EPC TEBVs constricted in response to acetylcholine after exposure to 500 U/mL TNF-α for 4.5 hours; however, HV EPCs demonstrated full recovery in their response to acetylcholine one week after removal of TNF-α from the culture circuit, while CAD EPC TEBVs did not regain their level of vasodilation exhibited on Day 7. More replicates of these experiments will be performed to confirm these results.

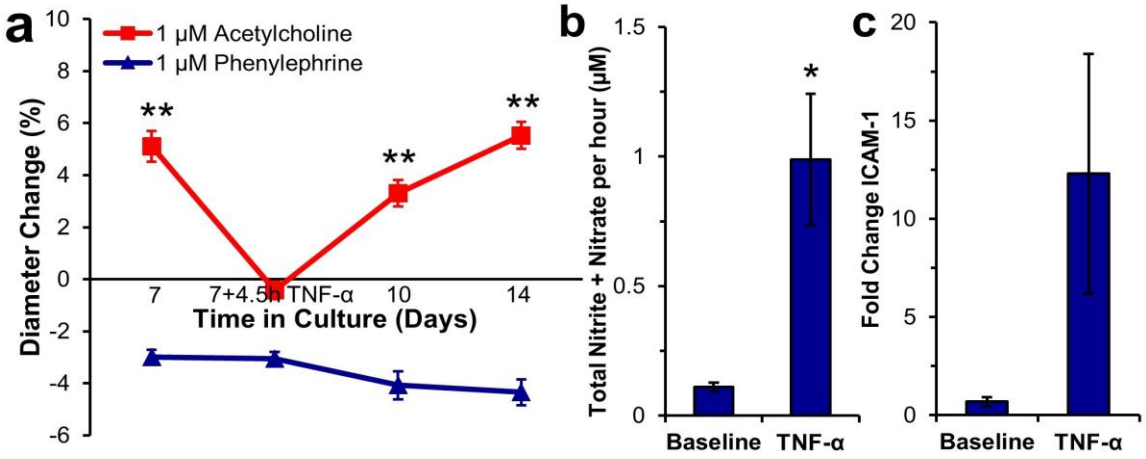

Figure 19: Vasoactive Response of CAD EPC TEBVs to 200 U/mL TNF-α

Endothelialized TEBVs elicit 5.1 ± 0.6% (mean ± SEM, N = 3 independent experiments. EPCs from 3 CAD donors were used and responses were pooled) dilation in response to 1 µM acetylcholine after 7 days of culture under laminar perfusion; however, after exposure to 200 U/mL TNF-α for 4.5 hours, TEBVs demonstrated an average vasoconstriction of -0.4 ± 0.3%. Three days after the removal of TNF-α, TEBVs demonstrated 3.3 ± 0.5% vasodilation in response to acetylcholine. Seven days after the removal of the TNF-α, TEBVs exhibited normal vasodilation in response to acetylcholine of 5.5 ± 0.5%, indicating that the endothelium is capable of recovering from an acute inflammatory stimulus. A one-way ANOVA indicates a significant effect of treatment day ($P < 0.0001$). A post-hoc Tukey's test indicates a statistically significant drop in dilation in response to acetylcholine with TNF-α treatment ($P < 0.005$ with respect to Day 7 + 4.5h TNF-α). (A). Treatment with 200 U/mL TNF-α for 4.5 hours increased the rate of nitric oxide within the TEBV circuit measured after perfusion for 48 hours (*$P < 0.05$) (B). Treatment with 200 U/mL TNF-α resulted in increased expression of ICAM-1 mRNA in hNDFs (C).**

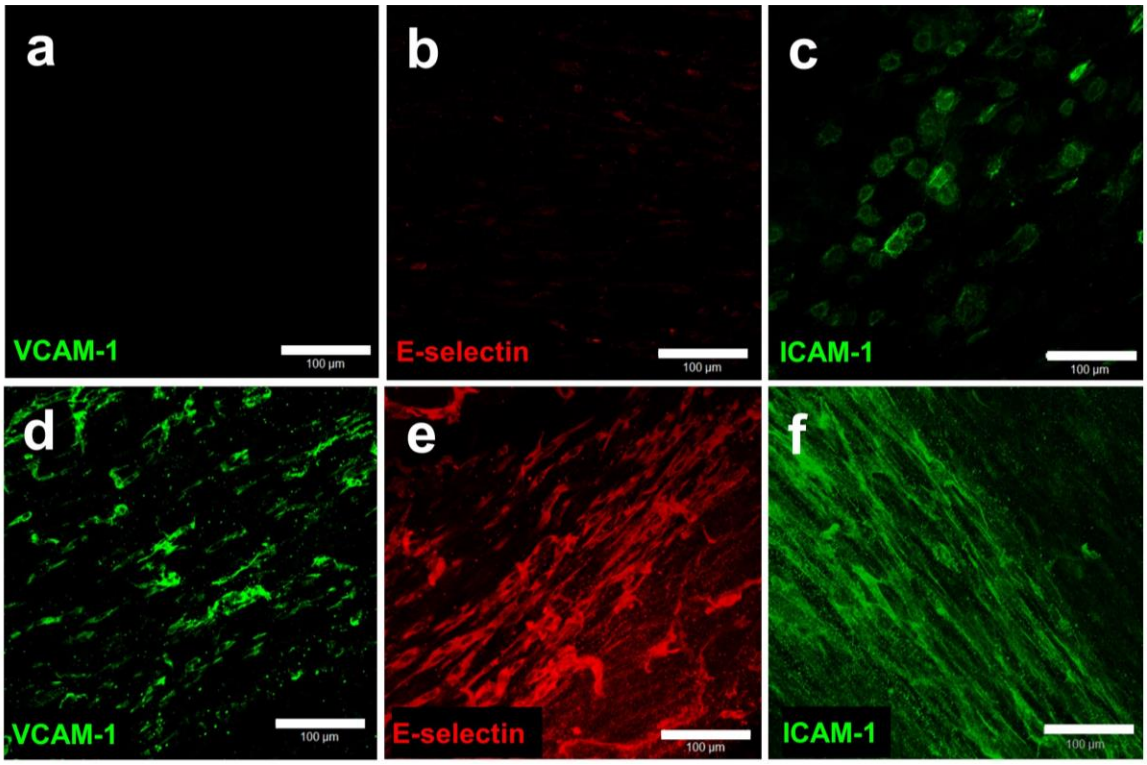

Figure 20: Adhesion Molecule Expression in TEBVs after 200 U/mL TNF-α

En face **images of TEBV endothelium demonstrate limited basal expression of cell adhesion molecules VCAM-1 (A), E-selectin (B), and ICAM-1 (C). Treatment with 200 U/mL TNF-α for 4.5 hours increases the expression of VCAM-1(D), E-selectin (E), and ICAM-1 (F).**

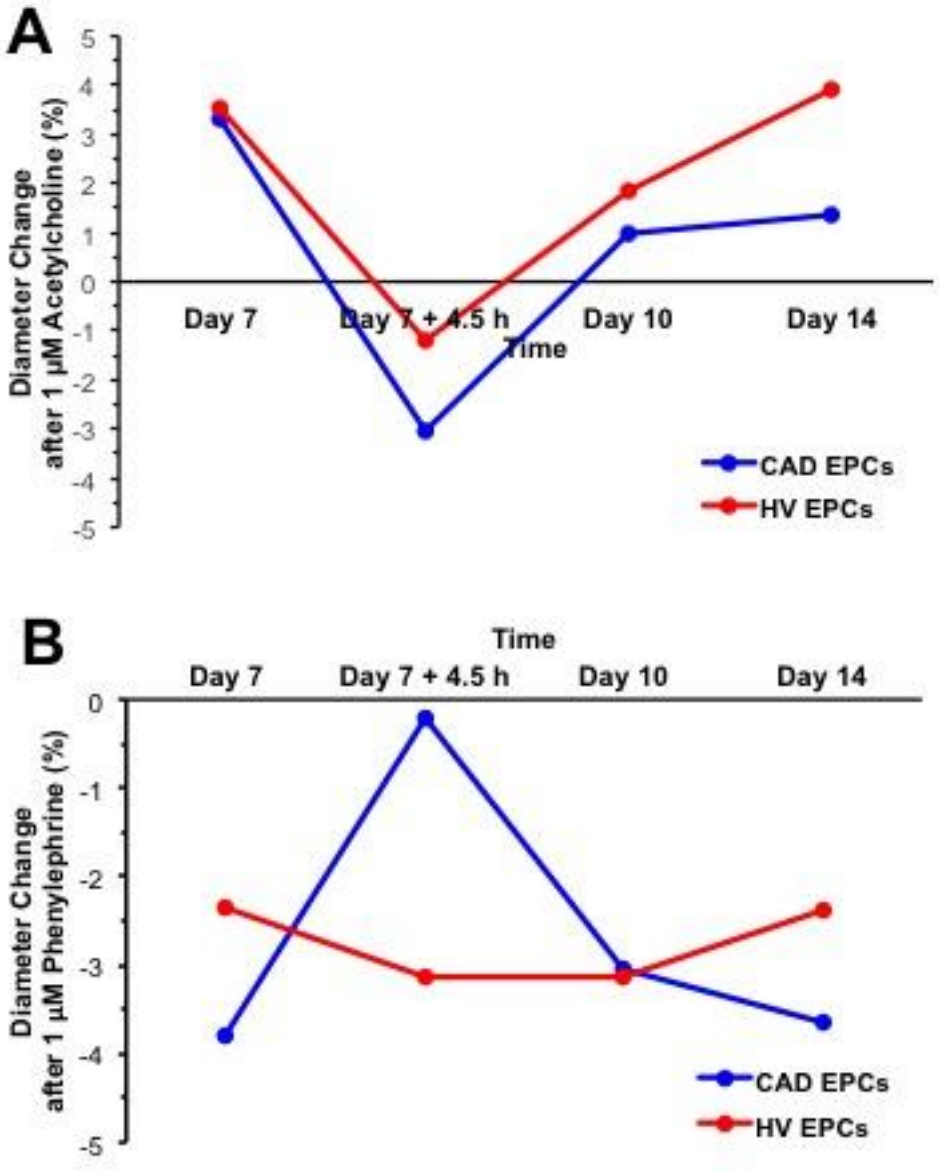

Figure 21: Recovery of TEBVs to Acute Exposure to 500 U/mL TNF-α

CAD EPC TEBVs and HV EPC TEBVs demonstrate constriction in response to 1 µM acetylcholine after exposure to 500 U/mL TNF-α for 4.5 hours, and some recovery after 7 days after removal of TNF-α from the culture circuit (A). Preliminary results suggest that acute exposure to 500 U/mL TNF-α inhibits the phenylephrine-induced vasoconstriction of CAD EPC TEBVs. This response is restored 7 days after removal of TNF-α from the culture circuit (B).

4.3.3 TEBV Response to Statins

Since statins exhibit pleotropic atheroprotective effects on endothelial cells[237], we examined whether statin treatment of TEBVs could block the TNF-α-induced vasoconstriction response to acetylcholine. Endothelialized TEBVs were matured for one week, and then exposed to 1 μM lovastatin, atorvastatin, or rosuvastatin in the flow circuit for 3 days, or maintained without treatment, after which they were exposed to 200 U/mL TNF-α for 4.5 hours. Exposure to 200 U/mL TNF-α or statins had no statistically significant effect on the endothelium-independent response to phenylephrine (Fig. 22a). While vessels not pre-treated with statins prior to exposure to TNF-α did not undergo vasodilation in response to acetylcholine, exposure to lovastatin for three days sustained vasodilation in response to acetylcholine after exposure to TNF-α on Day 10 (Fig. 22b). Vessels pre-treated with atorvastatin and rosuvastatin demonstrated an increase in acetylcholine-induced vasodilation at Day 10 after exposure to 200 U/mL TNF-α.

Nitric oxide measurements were performed from media samples taken from each flow circuit prior to vasodilation studies on Day 7 and Day 10 before and after incubation with TNF-α. Exposure of TEBVs to 200 U/mL TNF-α yielded an increase in the total nitrite and nitrate concentration within the TEBV circuit. TEBVs treated with 1 μM lovastatin and 1 μM rosuvastatin prior to the onset of TNF-α exposure did not demonstrate a statistically significant difference in their total nitrite and nitrate

concentration compared to controls not treated with statins. TEBVs pre-treated with 1 μM atorvastatin prior to TNF-α exposure demonstrated a surge of nitrite and nitrate production within the culture circuit.

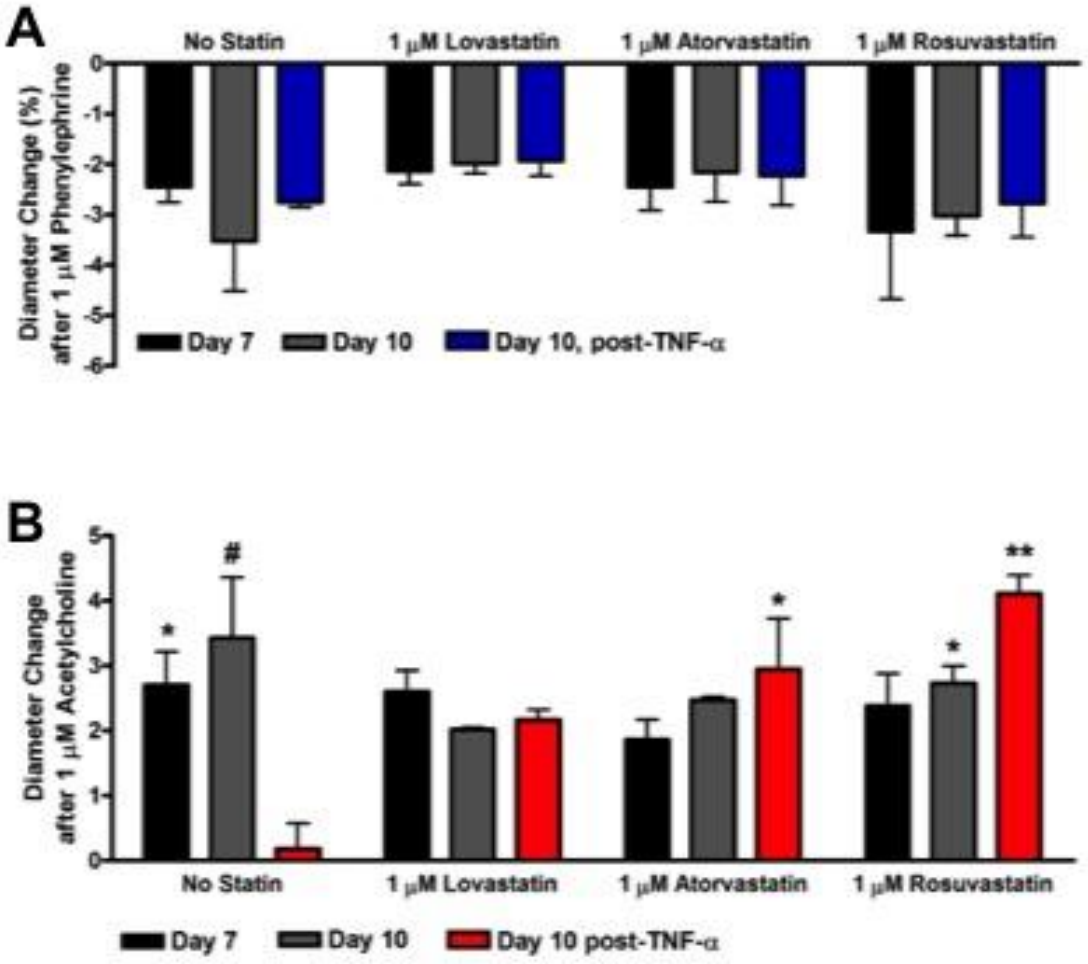

Figure 22: TEBV Vasoactivity Response to Statins and 200 U/mL TNF-α

Endothelialized CAD EPC TEBVs were cultured for 7 days and then exposed to 1 μM lovastatin, atorvastatin, or rosuvastatin for 3 days, or maintained without statin. On Day 10, TEBVs were exposed to 200 U/mL TNF-α for 4.5 hours, then exposed to 1 μM phenylephrine followed by 1 μM acetylcholine. Treatment with statins and TNF-α demonstrated no effect on the endothelium-independent vasoconstriction in response to phenylephrine (A). Treatment with statins substantially preserved the endothelium-dependent vasodilation response. A post-hoc Dunnett's test indicates a significant difference between the Day 7 vasodilation for both no statin and lovastatin conditions with respect to the No Statin Day 10 + TNF-α (* $P < 0.05$). No statin on Day 10 also demonstrated a significant difference with respect to the No Statin Day 10 + TNF-α ($P < 0.01$) (B).**

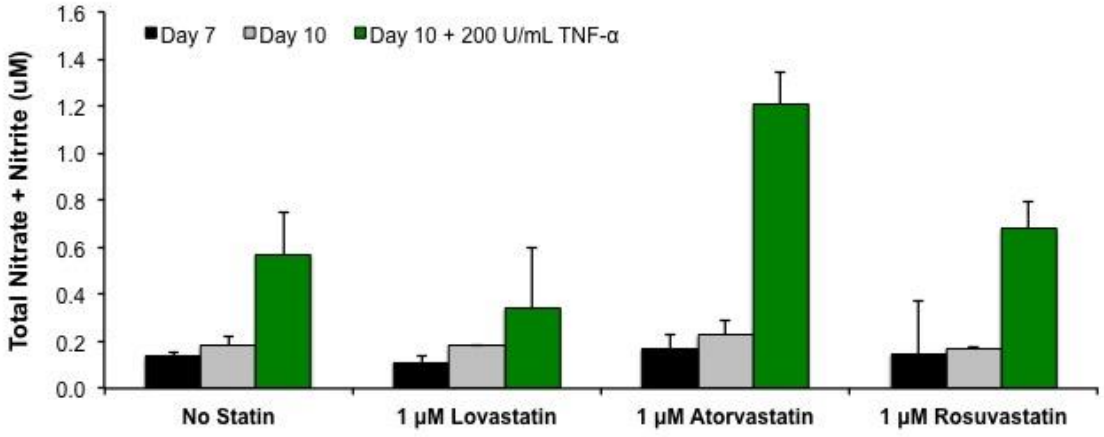

Figure 23: Nitric Oxide Production of Statin-Treated TEBVs exposed to 200 U/mL TNF-α.

The total nitrite and nitrate produced per hour was calculated for CAD EPC TEBVs treated with statins and 200 U/mL TNF-α. Data are represented as mean ± SEM. N =3 CAD donors.

The effect of 1 µM rosuvastatin on the vasoactivity after a larger dose of TNF-α was evaluated and compared between CAD EPC TEBVs and HV EPC TEBVs. A CAD EPC control TEBV not treated with statin exhibited the same behavior previously shown in Section 4.3.2 upon exposure to 500 U/mL TNF-α for 4.5 hours, in that the phenylephrine-induced contractile response was impaired. Preliminary results indicate that pre-treatment of CAD EPC and HV EPC TEBVs with 1 µM rosuvastatin for three days enhances the phenylephrine-induced contractile response. A CAD EPC control TEBV not exposed to TNF-α also constricted in response to acetylcholine as previously shown with 200 U/mL TNF-α, and CAD EPC and HV EPC TEBVs pre-treated with

rosuvastatin dilated in response to acetylcholine when exposed to 500 U/mL TNF-α. More replicates of these experiments will be performed to confirm preliminary responses. Media samples were collected at day 7 and day 10 before and after exposure to TNF-α. Nitric oxide measurements will be performed to evaluate the effects of statins and high doses of TNF-α on NO production.

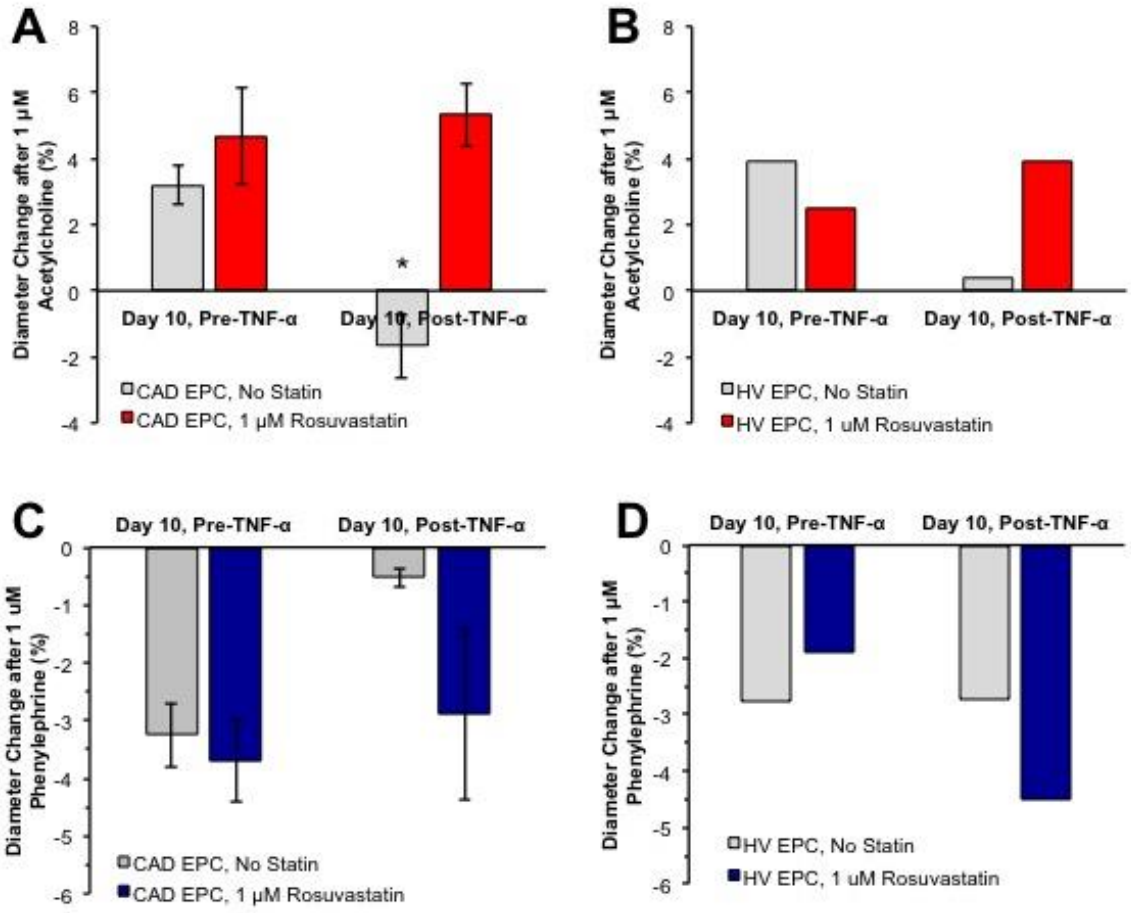

Figure 24: Effect of Rosuvastatin Treatment on TEBV Exposure to 500 U/mL TNF-α

CAD EPC and HV EPC TEBVs were treated with 1 µM rosuvastatin for 3 days prior to exposure to 500 U/mL TNF-α for 4.5 hours. Rosuvastatin prevented TNF-α-induced vasoconstriction in response to acetylcholine in both CAD EPCs (A) and HV EPCs (B). Preliminary results suggest that pre-treatment of CAD EPC TEBVs with 1 µM rosuvastatin prevents the inhibition of the contractile phenylephrine response after exposure to 500 U/mL TNF-α (C), compared to HV EPCs (D). N = 2-3 CAD and N = 1 HV EPC donor. A one-way repeated measures ANOVA indicates a significant effect of treatment in response to acetylcholine ($P < 0.05$). A post-hoc Tukey's test indicated a significant difference between CAD EPC TEBVs with no statin vs. 1 µM Rosuvastatin (*$P < 0.05$)

4.3.4 Effect of TNF-α and Statins on EPC Senescence in 2D

Two dimensional cell culture studies with CAD EPCs and HV EPCs were performed to validate the results achieved by the 3D studies within our microphysiological system model. In particular, the difference in response of CAD EPC TEBVs to high doses of TNF-α suggests that CAD EPCs may exhibit differential responses to TNF-α compared to EPCs from healthy volunteers. The effect of atorvastatin and rosuvastatin toward mediating senescence induced by TNF-α was measured using a β-galactosidase assay. Cells were plated on TCPS flasks at a sub-confluent density of 5,000 cells/cm^2 in order to prevent senescence due to overcrowding of the cells. Cells were incubated with 1 μM atorvastatin or rosuvastatin for 24 hours. TEBV media and EPC media were used as controls. The effect of 200 U/mL TNF-α for 4.5 hours in the presence of 1 μM atorvastatin, 1 μM rosuvastatin, or TEBV media controls was assessed. Cells positive for a dark blue β-galactosidase stain were considered senescent, and the percentage of senescent cells was reported.

Figure 25 illustrates the results of this study, in which three CAD donors and two healthy volunteer donors were evaluated. At baseline, CAD EPCs of the same passage had a greater percentage of senescent cells than HV EPCs. A dose of 200 U/mL TNF-α increased the percentage of β-galactosidase-positive CAD EPCs and HV EPCs by 1.6-fold and 1.5-fold, respectively. Incubation with atorvastatin and rosuvastatin reduced the TNF-α-induced senescence in both cell types. Analysis with more donors may be

necessary to note a statistically significant change in the percentage of senescent cells compared to cells without statins treated with 200 U/mL TNF-α.

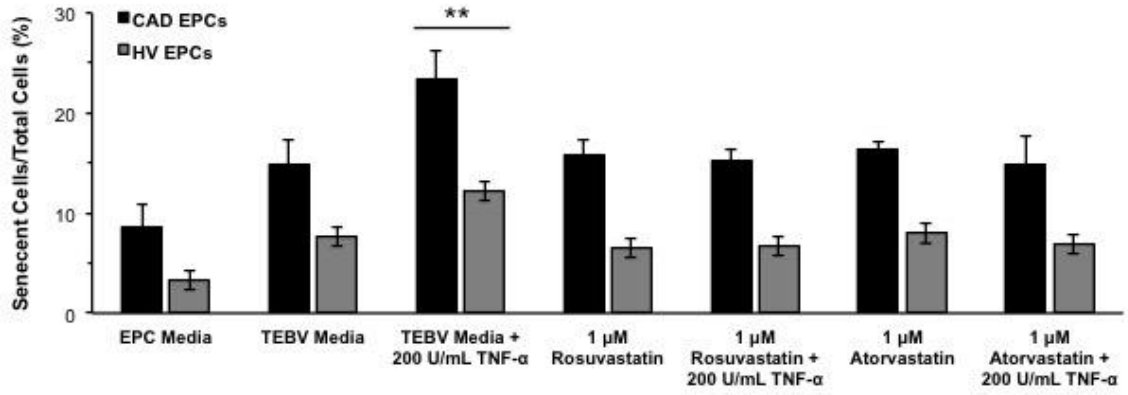

Figure 25: Effect of Statins toward Mediating TNF-α-Induced Senescence

A β-galactosidase assay for cellular senescence indicated that CAD EPCs exhibit greater levels of senescence compared to HV EPCs at baseline. Both CAD EPCs and HV EPCs exhibited similar trends in their responses to 200 U/mL TNF-α and statins. Data represented as mean ± SEM; n = 3 CAD donors and n = 2 HV donors. Two-way ANOVA indicated significant effects of treatment ($P < 0.005$) and donor ($P < 0.0001$). A post-hoc Tukey's test indicated a significant difference between treatment with 200 U/mL TNF-α and baseline senescence in EPC media for both CAD and HV EPCs ($P < 0.0005$)**

4.3.5 Effects of Statins and TNF-α on U937 Monocyte Adhesion to Endothelium in 2D

The potential for rosuvastatin to reduce endothelial activation was evaluated in both CAD EPCs and HV EPCs in 2D (Figure 26). EPCs were plated at slightly subconfluent densities in EPC media. The following day, cells were exposed to 1 μM rosuvastatin or a vehicle control of 0.01% DMSO for 24 hours prior to activation with 0, 100, 200, or 500 U/mL TNF-α for 4.5 hours. Afterward, U937 Monocytes labeled with Cell Tracker Green - CMFDA were plated in treatment medium over treated EPCs and allowed to adhere for 30 minutes. Unadhered cells were washed away with DPBS and cells were fixed in formalin prior to imaging on a fluorescent microscope.

CAD EPCs and HV EPCs pre-treated with 0.01% DMSO as a vehicle control demonstrated a sharp increase in monocyte adhesion over baseline values after exposure to 100 U/mL TNF-α. No statistically significant difference could be detected between doses of TNF-α in both CAD EPCs and HV EPCs. CAD EPCs demonstrated greater monocyte adhesion over baseline levels after exposure to TNF-α compared to HV EPCs under the same conditions. CAD EPCs also demonstrated greater standard deviations in monocyte adhesion fold change than HV EPCs between donors.

The effect of rosuvastatin toward preventing endothelial activation was evaluated in both CAD EPCs and HV EPCs. No statistically significant effect of rosuvastatin pre-treatment could be detected in CAD EPCs; however, in HV EPCs, exposure to 1 μM rosuvastatin for 24 hours prior to activation with 500 U/mL TNF-α

demonstrated lower levels of monocyte adhesion compared to HV EPCs treated with a vehicle control for 24 hours.

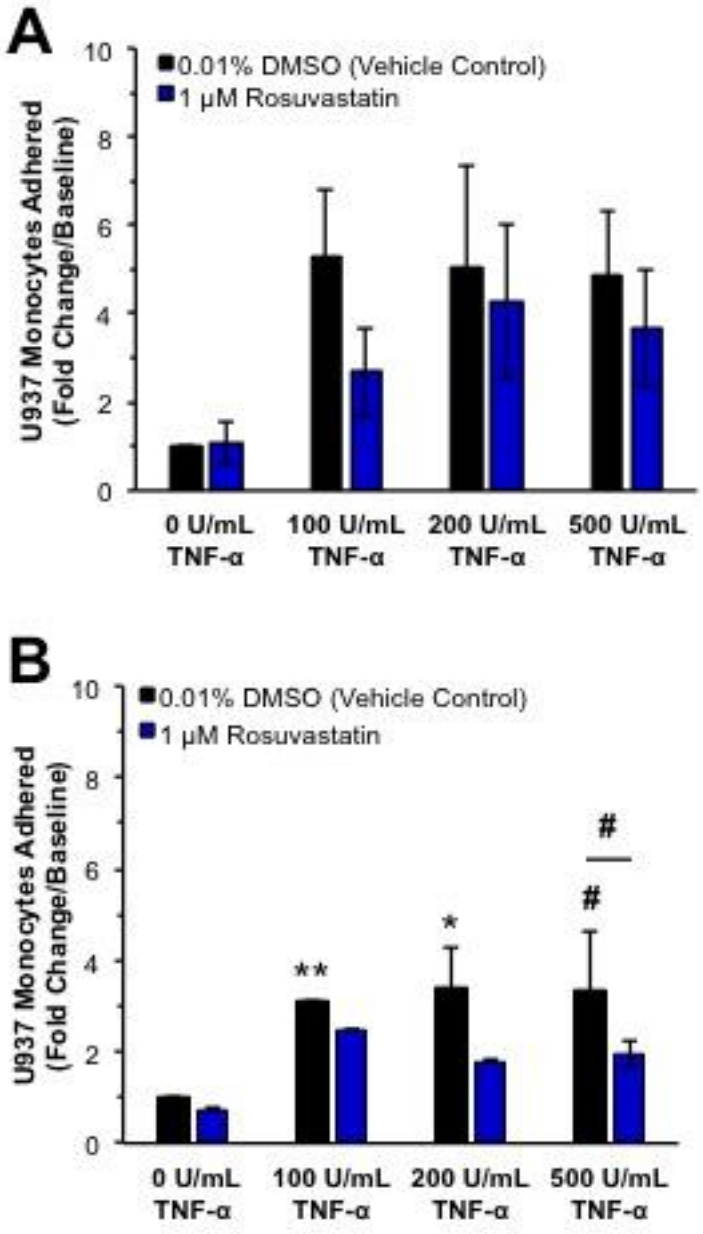

Figure 26: Effects of Rosuvastatin and TNF-α on U937 Monocyte Adhesion to EPCs

CAD EPCs (A) and HV EPCs (B) were evaluated. A two-way ANOVA indicated significant effects of treatment and dose ($P < 0.05$) in HV EPCs. Treatment with TNF-α increases monocyte adhesion in vehicle control samples (* $P < 0.1$, ** $P < 0.05$, # $P < 0.01$) compared to baseline values. Rosuvastatin reduces monocyte adhesion in HV EPCs at a dose of 500 U/mL TNF-α (# $P < 0.01$).

4.3.6 Effect of Statins and TNF-α on SIRT1 Expression and P65 Nuclear Translocation

Silent information regulator type-1 (SIRT1) is a member of the sirtuin family of nicotinamide adenine dinucleotide (NAD)-dependent class III histone deacetylases that represses p53-dependent apoptosis in response to DNA damage and oxidative stress[238]. We compared the expression of SIRT1 in CAD EPCs and HV EPCs exposed to 200 U/mL TNF-α for 4.5 hours after a 24-hour incubation with either 1 μM atorvastatin or rosuvastatin. EPC media and TEBV media were used as controls. We also assessed the extent to which the P65 subunit of the nuclear transcription factor NF-κB had translocated into cell nuclei by comparing the mean gray value of cell nuclei before and after activation with TNF-α. In preliminary experiments, CAD EPCs demonstrated lower levels of SIRT1 expression in the nucleus than HV EPCs (Figure 26). Exposure to TNF-α increased these levels in all conditions, including in the presence of statins. HV EPCs demonstrated higher levels of nuclear SIRT1, and demonstrated a similar trend to CAD EPCs in the presence of statins and TNF-α. More replicates of these experiments are required to establish a trend.

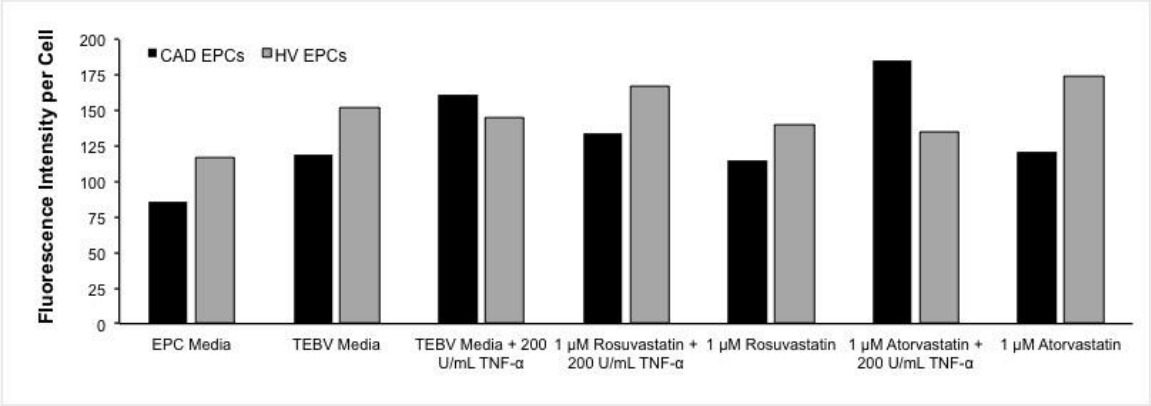

Figure 27: Effect of Statins and 200 U/mL TNF-α on EPC SIRT1 Expression

Exposure to pro-inflammatory mediators such as reactive oxygen species or TNF-α activates the transcription factor nuclear factor –κB (NF-κB) and promotes its translocation into the cell nucleus[239]. CAD EPCs and HV EPCs both demonstrated an increase in mean gray value of P65 stains within the nucleus after exposure to 200 U/mL TNF-α; however, HV EPCs exhibited a much higher fold increase from baseline than CAD EPCs (Figure 27). Statins appeared to have no impact on the P65 nuclear translocation of both CAD EPCs and HV EPCs. More replicates of these experiments are required to establish a trend.

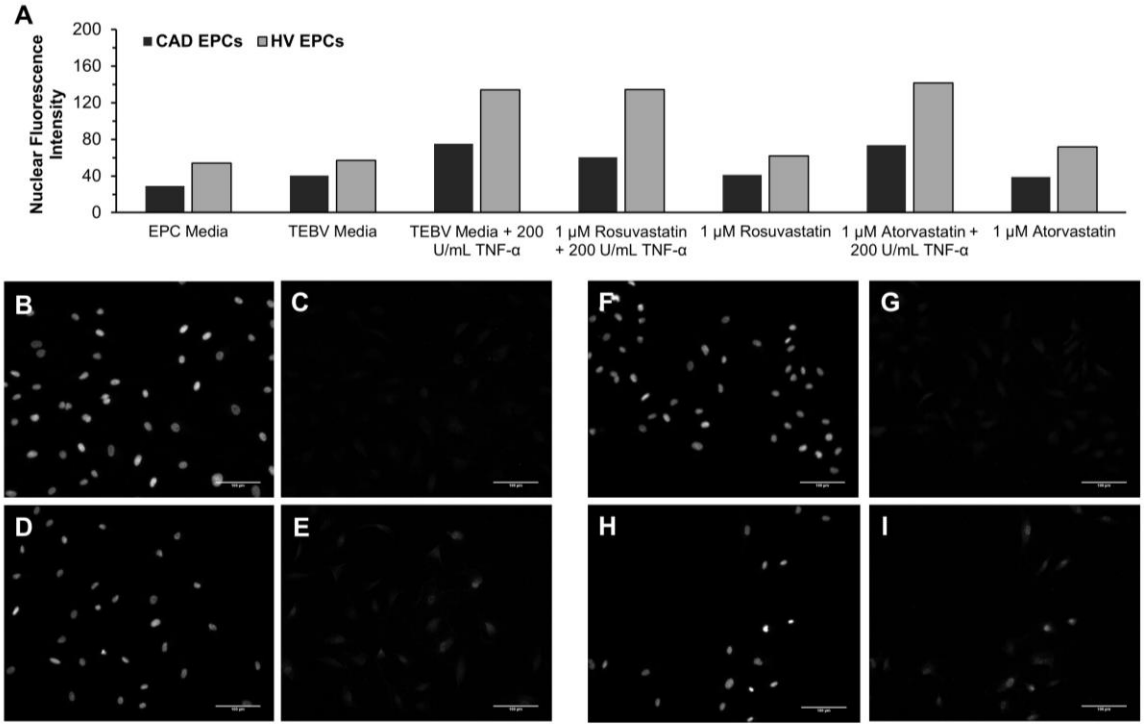

Figure 28: Effect of Statins and TNF-α on P65 Nuclear Translocation

The effect of statins toward preventing P65 nuclear translocation induced by TNF-α was calculated by determining the mean gray value of the nuclear region of cells stained with a P65 antibody. Nuclear fluorescence nearly doubles for both CAD EPCs and HV EPCs after exposure to 200 U/mL TNF-α for 4.5 hours. No change is detected in the mean gray value of EPCs exposed to 1 μM atorvastatin or 1 μM rosuvastatin for 24 hours prior to the onset of TNF-α exposure (A). Nuclei and P65 stains of CAD EPCs before (B and C, respectively), and after exposure to 200 U/mL TNF-α (D and E) and HV EPCs before (F and G) and after (H and I) demonstrate P65 nuclear translocation.

4.4 Discussion

An effective microphysiological system must be capable of measuring tissue responses under both healthy and diseased conditions. In this aim, acute endothelial activation was induced in response to the pro-inflammatory cytokine TNF-α to validate the inflammatory response of our TEBV system. TNF-α promotes expression of cell-surface adhesion molecules such as VCAM-1, ICAM-1, and E-selectin, which facilitate leukocyte adhesion to the vascular wall[221]. Furthermore, activated endothelium exhibit reduced expression of nitric oxide, leading to vasoconstriction in response to acetylcholine.

TEBVs initially elicited vasoconstriction in response to acetylcholine after exposure to 200 U/mL TNF-α, then recovered their vasodilation response to acetylcholine 7 days after removal of the stimulus in the flow circuit, suggesting endothelial activation and dysfunction without apoptotic injury[236]. Exposure of CAD EPC TEBVs to 500 U/mL TNF-α in the culture circuit for 4.5 hours led to vasoconstriction in response to acetylcholine that did not completely recover after 7 days. HV EPC TEBVs appear to recover from a dose of this dose of TNF-α, suggesting that HV EPCs may have a higher tolerance or greater resilience to injury than CAD EPCs.

Studies with rat aortas indicate slightly increased endothelium-independent vasoconstriction in response to phenylephrine upon exposure to TNF-α[240]. Endothelium-

independent vasoconstriction in response to phenylephrine demonstrated no change when CAD EPC TEBVs were treated with 200 U/mL TNF-α; however, the phenylephrine constriction response was impaired in CAD EPC TEBVs exposed to 500 U/mL TNF-α. The phenylephrine response of HV EPC TEBVs was not impacted by this dose of TNF-α, suggesting that high doses of TNF-α may impact the manner in which CAD EPCs communicate with the medial cell layer. The effect of the endothelium may be further explored by exposing TEBVs made without endothelium to 500 U/mL TNF-α. Understanding the impact of this higher dose of TNF-α on the medial cell layer is crucial to elucidate whether the impact on the phenylephrine response is due to injury of the hNDFs or through an endothelial-specific mechanism. The fact that HV EPC TEBVs do not experience this inhibition of endothelium-independent vasoconstriction implies that a combination of the two may be in effect.

We exposed CAD EPC TEBVs to 1 μM lovastatin, atorvastatin, or rosuvastatin for 3 days prior to exposure to 200 U/mL TNF-α, and pretreatment of TEBVs with statins enabled them to maintain endothelium-dependent vasodilation in response to acetylcholine after exposure to TNF-α, while untreated TEBVs experienced significantly reduced dilation. Statins have been shown to exhibit pleiotropic atheroprotective effects on endothelial cells by upregulating endothelial nitric oxide synthase (eNOS) expression under inflammatory conditions[241]. TEBVs experienced a burst of nitric oxide production after exposure to TNF-α. Future studies should be performed to elucidate whether this

due to an upregulation of iNOS. Exposure to lovastatin and rosuvastatin did not yield a statistically significant change in nitric oxide production after exposure to TNF-α; however, atorvastatin caused a surge in nitric oxide produced by the TEBVs after TNF-α. Future studies to compare eNOS and iNOS gene expression could demonstrate if statins had an effect over the source of the nitric oxide.

We evaluated the effect of rosuvastatin on endothelial activation in 2D by evaluating monocyte adhesion under static conditions. A statistically significant impact of rosuvastatin pre-treatment compared to cells treated with a vehicle control was not noted in CAD EPCs; however, HV EPCs demonstrated a statistically significant difference of TNF-α dose and an impact of rosuvastatin pre-treatment at 500 U/mL TNF-α. We noted greater variability between donors in CAD EPCs, leading to higher standard deviations between donors. The effect of pre-treating the U937 monocytes prior to adhesion to the EPC layer could be investigated; pre-treatment of monocytes with atorvastatin, cerivastatin, or simvastatin was found to result in a decrease in monocyte adhesion to endothelium, while the reverse was not effective[242].

TNF-α and other pro-inflammatory mediators induce endothelial cell apoptosis[243]. Sirt1 has been implicated in the development of atherosclerosis by directly affecting eNOS expression[244]. The effects of statins toward mediating this response have been explored in cultured cells *in vitro* and in clinical studies. Simvastatin was found to reduce apopotosis mediated by TNF-α through upregulation of SIRT1 in EPCs[243].

Atorvastatin and rosuvastatin administered to CAD patients elicited an inhibition of SIRT1 expression[245]. This phenomenon could be more effectively explored within our 3D model using Western blots for Sirt1, as well as with qRT-PCR.

Future directions for this work include further elucidating the role of Sirt1 in statin-induced TNF-α rescue, particularly the role of the levels of Sirt1 present in CAD EPCs compared to EPCs from healthy volunteers. Lastly, the role of Sirt1 in the TNF-α and statin studies was briefly assessed in 2D studies; however, this could be further explored by over-expressing Sirt1 within the endothelium and assessing its effect on vasoactivity under normal and inflammatory conditions. CAD EPCs expressed lower levels of Sirt1 than HV EPCs and demonstrated impaired P65 nuclear translocation.

Overall, the work in this aim served to validate the use of our model under inflammatory conditions, and as a potential model to assess differences between patient populations under inflammatory conditions.

4.5 Chapter-Specific Acknowledgements

Special thanks go to Ellen Weburg in the Truskey lab for her assistance with the β-galactosidase assay protocol, and to Allison Braithwaite for performing the β-galactosidase assays. The authors would like to thank S.J. Owen from the Duke Biomedical Engineering Machine Shop for his help constructing the custom rotation device, as well as the Duke Physics Machine Shop for their assistance manufacturing the

custom TEBV chambers. This work was supported by NIH grants UH2TR000505, 4UH3TR000505, and the NIH Common Fund for the Microphysiological Systems Initiative (to G.A.T.), and American Heart Association Pre-doctoral Fellowship 14PRE20500062 (to C.E.F.).

5. Dissertation Summary and Future Work

5.1 Dissertation Summary

Cardiovascular disease (CVD) is the leading cause of death in the United States, and development of new drugs and treatments for CVD is a pressing public health issue. However, pre-clinical animal studies are often a bottleneck in the distribution of new therapies to the public due to their high cost. Meanwhile, laboratory bench-top experiments are often conducted under isolated conditions that do not fully replicate the natural environment. Fast and accurate development and distribution of CVD therapies demands a bridge between laboratory bench-top research and animal studies. Overall, this research demonstrated the feasibility of creating a bench-top model of a functional human arteriole for drug testing under both healthy and inflammatory conditions.

In this work, we have developed and characterized an engineered blood vessel comprised of human cells and natural extracellular matrix materials. Late-outgrowth, peripheral blood-derived endothelial progenitor cells derived from coronary artery disease patients (CAD EPCs) were explored as a suitable endothelial source for TEBVs through 1) 2D direct two-dimensional co-culture with human aortic smooth muscle cells, 2) vasoactive behavior as an endothelial source within a tissue engineered blood vessel, and 3) evaluation of the inflammatory response of the endothelialized TEBV after exposure to TNF-α and statins. We created a tissue-engineered blood vessel comprised of a dense collagen gel embedded with human neonatal dermal fibroblasts or human

bone marrow-derived mesenchymal stem cells. We then evaluated the response of TEBVs endothelialized with CAD EPCs or EPCs from healthy volunteers to the pro-inflammatory cytokine tumor necrosis factor-α (TNF-α), and assessed the role of three commonly prescribed statins toward mediating changes in vasodilation induced by exposure to TNF-α.

Specific Aim 1 evaluated the feasibility of culturing late-outgrowth EPCs from the peripheral blood of CAD patients over cellular substrates. Understanding the adhesive properties of CAD EPCs was critical toward their potential use as an endothelial source for TEBVs, both for *in vitro* applications and for potential autologous transplantation applications. The adhesive behavior of CAD EPCs over a confluent, quiescent layer of human aortic smooth muscle cells (SMCs) was compared to that of human aortic endothelial cells (HAECs). CAD EPCs and HAECs could be cultured for one week in direct co-culture over a confluent layer of SMCs. Both cell types demonstrated network formation at low seeding densities and maintenance of a confluent layer for 7 days at high seeding densities, indicating that endothelium plated over another cell layer must be plated at high densities in order to maintain a confluent and quiescent monolayer, instead of forming branching networks as experienced in angiogenesis.

In addition to maintaining confluence over SMCs for 7 days, CAD EPCs demonstrated similar levels of adhesion compared to HAECs when exposed to short-

term supraphysiological levels of shear stress. CAD EPCs directly co-cultured over confluent, quiescent SMCs were also capable of aligning in the direction of flow and producing a burst of nitric oxide when exposed to physiological levels of steady, laminar shear stress for 48 hours. Lastly, blocking of integrins specific to connections with fibronectin in CAD EPCs yielded similar decreases in adhered cell quantities to a confluent SMC layer compared to HAECs. Overall, we demonstrated that CAD EPCs were able to adhere and function over a confluent SMC layer, indicating that they were suitable for use as a cell source for tissue engineering and autologous implantation applications.

Specific Aim 2 optimized the culture conditions for creating a tissue-engineered blood vessel capable of replicating a native response to vasoactive stimuli. Collagen gels were embedded with human neonatal dermal fibroblasts (hNDFs) or human bone marrow-derived mesenchymal stem cells (hMSCs) and allowed to gel in a mold comprised of a 3-cc syringe and a 0.87 mm-diameter stainless steel rod through the center. After gelation, collagen constructs were plastically compressed to yield collagen gels with a high fiber density. TEBV lumens were endothelialized with CAD EPCs and cultured for at least one week under steady, laminar fluid perfusion through the lumen and around the TEBV to create a physiological wall shear stress within the TEBV lumen. The mechanical strength of the TEBVs was assessed using burst pressure analysis. Endothelialized TEBVs made from hNDFs demonstrated burst pressures greater than

1770 mm Hg after one week of culture. Endothelialized hNDF TEBVs also reached a stable inner diameter after 3 weeks of culture and maintained this diameter for up to 5 weeks.

TEBVs were evaluated for their potential to secrete extracellular matrix proteins comparative to that within the native vascular wall. Endothelialized hNDF and hMSC TEBVs produced laminin, collagen IV, and fibronectin after one week in perfusion culture, and also expressed contractile proteins α-smooth muscle actin (α-SMA) and calponin within their vascular wall after one week. TEBVs made with hNDFs expressed greater amounts of ECM proteins and contractile proteins after one week compared to those made with hMSCs, although after 4 weeks of culture, hMSC TEBVs expressed similar levels of α-SMA and calponin within their vascular wall compared to hNDF TEBVs.

An intact layer of endothelium is an essential component of a TEBV suitable for microphysiological systems applications; most importantly, characterization of endothelial function is crucial for understanding the effects of inflammation or drugs within the vasculature. A clinically relevant assay was used to non-invasively assess endothelial function within the TEBVs over time. This assay was robust enough to detect changes in endothelial function induced by various conditions, making it ideal for assessing the endothelial health of the TEBVs under healthy and inflammatory conditions. We assessed endothelium-independent vasoconstriction of the TEBV

through exposure to the α-adrenergic receptor agonist phenylephrine, and assessed endothelium-dependent vasodilation of the TEBV through exposure to acetylcholine, which acts on both the muscarinic receptors of smooth muscle and elicits a burst of nitric oxide in healthy endothelium. TEBVs cultured for just one week demonstrated constriction in response to phenylephrine and dilation in response to acetylcholine. TEBVs made with hNDFs demonstrated greater vasoactivity than those made with hMSCs at one week, likely due to greater contractility of the medial cell source. Dose response curve assays indicated increasing constriction and dilation to increasing doses of phenylephrine and acetylcholine, respectively. TEBVs pre-incubated with the eNOS inhibitor L-NAME constricted in response to increasing doses of acetylcholine, similar to the response experienced by TEBVs without endothelium, confirming the endothelial-specific response of TEBVs to acetylcholine. TEBVs were also positive for von Willebrand factor (vWF) at 1 and 5 weeks, and also released similar levels of nitric oxide at 1 and 5 weeks. TEBVs also exhibited dose-dependent vasodilation in response to increasing doses of caffeine and theophylline, indicating their potential to assess changes in vascular tone produced by a variety of compounds.

Specific Aim 3 evaluated the effects of inducing endothelial dysfunction within a pro-inflammatory environment on the vasoactivity of the TEBV. Acute exposure to the pro-inflammatory cytokine TNF-α was used to induce endothelial activation within the TEBV. After 4.5 hours of exposure to 200 U/mL TNF-α, TEBVs demonstrated increased

expression of the adhesion molecules VCAM-1, ICAM-1, and E-selectin. Furthermore, changes in TEBV vasoactivity were detected after exposure to TNF-α, indicating a functional change in the behavior induced by endothelial dysfunction. TEBVs constricted in response to acetylcholine, indicating an impact on endothelial-specific vasoactivity. Endothelium-dependent vasoconstriction was completely restored 7 days after removal of the TNF-α from the culture circuit, indicating endothelial activation without apoptosis. Changes in the TEBV vasoconstriction response to phenylephrine at 200 U/mL TNF-α were not detected. TEBVs also showed a change in production of nitric oxide after exposure to TNF-α.

The effect of statins toward mediating the TEBV response to TNF-α was assessed through changes in vasoactivity. TEBVs were cultured for one week, then exposed to 1 μM lovastatin, atorvastatin, or rosuvastatin in the culture circuit for 3 days prior to activation with 200 U/mL TNF-α. All three statins prevented the endothelium-dependent vasoconstriction in response to acetylcholine after exposure to TNF-α that was demonstrated by controls treated with no statin. No statistically significant changes in phenylephrine-induced vasoconstriction were detected in TEBVs treated with statins compared to untreated controls. Statins produced changes in the nitric oxide production of the TEBVs.

The behavior of CAD EPCs in the TEBVs was compared to that of EPCs isolated from young, healthy volunteers (HV EPCs). At baseline, flow cytometry indicated that a

greater percentage of CAD EPCs expressed VCAM-1 than HV EPCs. Within the TEBV, no statistically significant differences in vasoactivity were detected in the CAD EPCs and HV EPCs after one week of culture; however, treatment with high doses of TNF-α illustrated a difference in their stress response. CAD EPC TEBVs treated with 500 U/mL TNF-α within the culture circuit for 4.5 hours exhibited an impaired phenylephrine response while also constricting in response to acetylcholine. CAD EPC TEBVs and HV EPC TEBVs treated with 1 μM rosuvastatin constricted in response to phenylephrine and dilated in response to acetylcholine after exposure to 500 U/mL TNF-α for 4.5 hours, similar to their behavior prior to exposure to TNF-α. HV EPC TEBVs not treated with statins demonstrated higher tolerance to 500 U/mL TNF-α. The phenylephrine response was not inhibited, but the acetylcholine response was affected as predicted, with constriction in response to acetylcholine.

Two-dimensional cell culture studies indicated that a greater population of the CAD EPCs was senescent compared to the HV EPCs. An assay for β-galactosidase demonstrated that exposure to 200 U/mL TNF-α for 4.5 hours increased the percentage of senescent cells present within the population for both CAD EPCs and HV EPCs. Pre-treatment with 1 μM rosuvastatin or 1 μM atorvastatin for 24 hours reduced the increase in senescence with TNF-α for both CAD EPCs and HV EPCs.

5.2 Strengths and Weaknesses of Work

The tissue-engineered human blood vessel in this study is rapidly producible, biologically active, and was confirmed to produce physiologically relevant functional responses under both healthy and inflammatory conditions. This model provides the unique opportunity to create and test drug therapies on human vascular cells in a 3D tissue while allowing the manipulation of pathologic parameters that would be labor and cost intensive in animal models. The work in this thesis was the first to demonstrate endothelium-specific vasoactivity within a tissue engineered blood vessel. It is now possible to assess changes in vascular tone non-destructively over time. This opens the door to studying a variety of cardiovascular conditions that have implications toward vascular tone, such as hypertension, drug-induced vascular injury, and developmental diseases impacting vascular tone such as Hutchinson-Gilford Progeria.

In Specific Aim 1, we assessed the adhesive behavior of CAD EPCs on a confluent, quiescent layer of smooth muscle cells, and we compared this behavior to that of human aortic endothelial cells (HAECs). This work expanded upon previous studies in our lab that optimized the isolation and characterization of late-outgrowth endothelial progenitor cells from cord blood and peripheral blood of healthy adults and adults with advanced CAD. Although the behavior of CAD EPCs had been evaluated *in vitro* under monoculture conditions[64] and *in vivo* in a rat vascular graft model[65], their behavior when plated over a confluent layer of medial wall cells had not been evaluated. We used a

model of direct co-culture of endothelium over a confluent, quiescent layer of smooth muscle cells that had been previously optimized in the Truskey lab to create direct co-cultures of CAD EPCs with SMCs[39,40]. This co-culture model gave us the opportunity to characterize the behavior of endothelium from diseased patients in an *in vitro* model with the potential to control and isolate specific variables affecting cell adhesion, such as wall shear stress and integrin availability.

The purpose of using HAECs as a control in Specific Aim 1 was to compare the adhesive behavior of CAD EPCs to that of a source of mature, healthy endothelium. In addition to HAECs, CAD EPCs could also have been compared to late outgrowth EPCs from healthy volunteers. Our group had previously demonstrated that CAD EPCs behaved similarly to HV EPCs under static and flow conditions over TCPS and Teflon-AF plates[64]. Our work in Specific Aim 3 suggests that CAD EPCs may exhibit a different stress response after exposure to TNF-α that somehow interacts with the medial layer underneath. Characterization of the SMC layer underneath the cells in the direct co-cultures, particularly whether or not the SMCs remained quiescent and contractile, could potentially have revealed some differences in the way the CAD EPCs interact with smooth muscle. Although our group had previously validated that CAD EPCs upregulated flow-specific genes eNOS and KLF2 under flow when cultured in monoculture over Teflon-AF plates, validating the gene expression of eNOS and KLF2 over SMCs in culture could have provided insight into the effect of a medial layer. Gene

expression studies could have been performed by splitting the two cell types using CD31-coated magnetic beads and assessing for activation markers such as VCAM-1, ICAM-1, and E-selectin in the endothelium, and upregulation of α-SMA, calponin, and myosin heavy chain-11 in the SMCs. Directly comparing these studies to HV EPCs would have provided a more in-depth characterization of the molecular differences between CAD EPCs and HV EPCs.

In Specific Aim 2, an arteriolar-scale TEBV was developed from natural matrix materials and human cells that could be fabricated in less than 3 hours and exhibited functional maturity after just one week and maintained functional maturity through five-week studies. This was a substantial improvement over culture times for previous techniques, which involves maturation of the scaffold prior to introduction to physiological fluid perfusion. Furthermore, we adapted a clinically relevant assay for endothelial function to assess endothelium-independent and endothelium-dependent vasoactivity non-destructively over time. Using this clinically relevant assay allowed us to compare the data from our *in vitro* studies to that of published human data – an important component of an effective microphysiological system with potential for screening of pharmaceutical drug candidates. Furthermore, we were able to evaluate the changes in vascular tone throughout maturation and after the introduction of drugs such as caffeine and theophylline that elicited changes in vascular tone.

TEBVs were constructed from dense collagen gels embedded with human neonatal dermal fibroblasts or human bone marrow-derived mesenchymal stem cells. Ideally, adult SMCs would be used as the cell source for the vessel wall; however, adult SMCs exhibit limited population doublings *in vitro* before undergoing senescence[219]. Instead, hNDFs were chosen as a proof of concept due to their attainability, contractile properties, and proliferative capacity. Despite these benefits, fibroblasts and myofibroblasts have been shown to promote a pro-inflammatory condition, which could potentially impact the behavior of the endothelium, particularly in studies evaluating the effects of inflammation on the vasculature. Other highly proliferative cell sources could have been used, including umbilical artery SMCs, or hMSCs. hMSCs have been used to create functional TEBVs[220], and may be differentiated to express characteristic SMC markers.

Our studies in Specific Aim 2 indicated that TEBVs made with hNDFs were more contractile, demonstrated greater vasoactivity, and expressed greater amounts of ECM proteins after one week compared to those made with hMSCs. However, hMSC TEBVs did express comparable levels of α-SMA and calponin at 4 weeks, suggesting that the hMSCs were differentiating toward SMCs in culture and needed more time to mature due to being a less contractile cell type initially. Since we were interested in creating a model that could be tested quickly, we ultimately chose hNDFs as the primary medial cell source due to their greater "maturity" after one week. We are currently evaluating

the response of our model with SMCs derived from induced pluripotent stem (iPS) cells, which would enable us to examine patient specific functional changes.

The TEBVs used in our study are matured under steady laminar flow using a peristaltic pump. Cyclic mechanical stress through pulsatile flow increases extracellular matrix production and mechanical strength of TEBVs[29,50]; however, laminar flow is sufficient to evaluate the effects of drug stimuli on the endothelium. Additionally, flow rate is the only metric controlled to evaluate the wall shear stress within the lumen of the TEBVs. Wall shear stress was calculated based on the initial inner diameter of the TEBVs; however, the TEBVs remodel in culture and we have shown that the inner diameter reduces between 0-2 weeks in culture. A feedback system that adjusts the flow rate based on the intraluminal pressure would be useful for maintaining a steady wall shear stress within the system. Pressures in our system were lower than those encountered in arterial systems and raising the pressure may facilitate differentiation.

Another limitation of our current TEBV culture system is the size and the throughput of samples. Currently, we can only culture 1 TEBV within a single chamber, with a total flow circuit volume of 25 mL per TEBV. We use a peristaltic pump that allows us to connect up to 8 separate flow circuits at once to a pump system; however, the labor intensity required to mount more than 4 TEBV circuits in one day precludes us from performing more studies at one time, and may contribute to a higher sample variability than desired. Optimizing a culture system that could culture more TEBVs

within one circuit could potentially lead to higher throughput studies with more replicates per experiment, and greater statistical precision.

Currently, we perform vasoactivity experiments by connecting the TEBVs to a bench top pump and placing them under a stereoscope attached to a video camera. The change in temperature from culturing the TEBVs at 37 °C in a humidified incubator to a 20-25 °C room temperature environment may have a notable impact on the vasoactivity of the TEBVs. Although we experienced vasoactivity levels similar to those recorded from *in vivo* human flow-mediated vasoactivity experiments[213], longer studies such as dose-response curves could be affected by the culture media and chamber cooling to room temperature. Designing an environmental chamber that could house the TEBV circuit during vasoactivity experiments could potentially improve the vasoactivity levels reported in future assays.

In Specific Aim 3, we evaluated the response of TEBVs made with CAD EPCs to the pro-inflammatory cytokine TNF-α for 4.5 hours to assess their response to an acute inflammatory stimulus, then compared the effects of three commonly prescribed statins toward mediating the changes in vasoactivity elicited by the inflammatory response. The assay developed in Specific Aim 2 allowed for non-destructive monitoring of vasoactivity, which allowed us to compare the effects of a functional and dysfunctional endothelium using clinically relevant metrics. We were able to validate the physiological relevance of our system using treatment with three commonly prescribed statins, and

we were able to study the pleiotropic effects of statins in a carefully controlled *in vitro* setting that isolated the vasculature from the effects of other organs, which is not possible in animal models that require systemic distribution of statins to measure the effect on the vasculature.

The work in Specific Aim 3 characterized the effects of an acute, short-term exposure to TNF-α within the TEBV model. The goal of this study was to elicit a change in vasoactivity; however, for a more accurate model of chronic inflammation, long-term culture of the TEBVs with lower doses of TNF-α should be evaluated. Pre-incubation of the TEBVs with statins simulated an environment where a patient already taking statins develops an acute infection; however, a more relevant case study would be administration of statins after evidence of low-grade chronic inflammation.

Two-dimensional studies of statin interactions with TNF-α were performed on TCPS under static conditions. The purpose of these studies was to validate the results from the TEBV assays, since 2D culture allows for the isolation of variables for mechanistic studies. Although the 2D studies performed did justify the results from the TEBV model, more accurate and physiologically relevant studies could have been performed using the direct co-culture model employed in Specific Aim 1 under both static and flow conditions. Particularly since statins impact production of flow-specific genes eNOS and KLF2, exposure to steady, laminar shear stress using a parallel plate flow chamber could have facilitated more physiologically accurate 2D studies.

Ideally, the effects of statins toward upregulating the flow-specific genes eNOS and KLF2 in the TEBVs would have been evaluated using qRT-PCR. However, performing qRT-PCR for endothelial-specific genes proved not to be trivial within our system. Prior to RNA isolation, we extracted the cells from the matrix with a collagenase digestion, and then separated the endothelium of the TEBVs from the medial cells with CD31-labeled magnetic beads. Due to the number of endothelial cells present within the final TEBVs after 1 week of culture, RNA isolations from the endothelium of one TEBV consistently gave RNA concentrations and quality that were too low for use in one-step or two-step qPCR systems. We are currently evaluating whether combining the endothelium from two TEBVs provides enough cells to yield high quality RNA at high enough concentrations for qPCR. Alternatively, using digital droplet PCR to analyze genes expressed by < 10% of the cells within the entire TEBV could be an option to evaluate the eNOS and KLF2 production within the TEBV.

5.3 Work Recommended to Complete Studies

Specific Aim 3 evaluated the effects of an acute dose of TNF-α toward creating a dysfunctional endothelium within the TEBVs, and assessed the effects of commonly prescribed statins toward reversing the activation response of the endothelium. Furthermore, the aim sought to evaluate the extent to which CAD EPCs expressed an activation response compared to HV EPCs; however, only two of the six donors yielded

HV EPCs that were proliferative enough to be cultured past passage 4. Since endothelial senescence has such a substantial impact upon the behavior of the vasculature, it was not suitable or even feasible to use the senescent donors within the TEBVs. Therefore, more donors of HV EPCs are necessary in order to complete all of the comparison studies within Specific Aim 3.

As mentioned in the previous section, optimization of qPCR within the TEBVs is critical toward being able to perform mechanistic studies of the effects of drugs and inflammatory stimuli within the TEBVs. Assessing changes in gene expression within the TEBVs, particularly changes in eNOS, KLF2, VCAM-1, ICAM-1, and E-selectin, would further validate the results demonstrated in the vasoactivity assays. Surface expression of adhesion molecules VCAM-1, ICAM-1, and E-selectin should be characterized using flow cytometry and fluorescence microscopy.

The 2D assays described in Specific Aim 3 were performed under static conditions with EPCs cultured in monoculture over TCPS plates. A more accurate correlation between the 2D studies and the TEBV studies could be made if the EPCs were exposed to flow in a parallel plate flow chamber. Gene expression of eNOS and KLF2 would be feasible and more physiologically relevant under flow than under static conditions.

5.4 Future Directions for TEBV Project

The work presented in Specific Aim 2 established the TEBV project within the Truskey lab. There are a variety of directions in which the project could evolve, and also several ways in which the TEBVs may be further improved, some of which are currently underway in the Truskey lab. The most important improvements and developments needed for the successful advancement of this project include development of a high-throughput fabrication technique and chamber system, optimizing the use of smooth muscle cells and endothelial cells from induced pluripotent stem cell sources, and improving the matrix composition of the TEBVs to promote elastin production. A variety of cardiovascular diseases and conditions may also be modeled, and the vascular constructs may also be combined with other systems to create microphysiological systems with multiple tissue-engineered organ constructs.

Throughout the optimization of the studies presented in Specific Aim 2, the TEBV system underwent a variety of changes, most notably in the volume of the system. We initially started using fibroblasts embedded within dense collage gel sheets that were rolled around a mandrel and tied on to the culture chamber perfusion posts. This model experienced substantial delamination of the TEBV layers and also had a high failure rate and poor reproducibility. Moving toward a syringe mold eliminated the problem of the delamination of layers and substantially improved the reproducibility and mechanical properties of the TEBV. We began using a 10-cc syringe mold with an

inner diameter of 0.87 mm. Although this was effective, the wall thickness was substantially larger than the physiological dimensions of an arteriole. Shrinking down to a 3-cc syringe improved the burst pressures and created wall thicknesses that were much closer to the physiological size of arterioles.

Initially when we began culturing the TEBVs, we used commercial and custom chambers that had a volume of 50 mL. Combined with the volume required for tubing and a reservoir, the TEBV culture circuits had volumes of 70 mL. These large volumes are not cost-effective or ideal for high-throughput studies because they use large volumes of media, which substantially dilutes the concentration of metabolites produced by the TEBVs, and also require greater volumes of drugs or other compounds to be added to the culture circuit to achieve relevant concentrations for drug studies. Our current chambers have a volume of 6 mL, giving us a total circuit volume of 25 mL, which is a notable improvement from where we started. Another drawback of the current system is that only one TEBV may be cultured within the circuit at one time, leading to low experimental output. Improvements to the system should include the capacity to culture multiple TEBVs within one circuit at a time, in order to be able to obtain more replicates within experiments.

Currently, elastin production within our TEBVs is highly limited and much lower than physiological levels; however, elastin production has generally been limited in TEBVs. Elastin modulates blood vessel mechanics at low strains and modulates

vessel elasticity and resilience[30], which is crucial toward enabling TEBVs to withstand native pressure fluctuations[31]. Elastin is critical toward actin stress fiber organization and signaling[32]. Arterial SMC proliferation is regulated by interactions between elastin receptors and soluble degradation products of elastin within the vascular wall[33], and SMC proliferation is uncontrolled in its absence[34].

Several attempts have been made to include elastin in vascular constructs; however, the most effective techniques will involve inducing production of elastin by the cells within the constructs, rather than adding elastin to the matrix, due to potential degradation of elastin in culture. TEBV scaffold topography and the presence of TGF-β1 regulate elastin gene expression and synthesis[246]. The quiescent, contractile phenotype of SMCs is promoted in a collagenous microenvironment, which can limit the synthesis of elastin precursors and assembly of elastin structures in the ECM[36]. Elastin is initially secreted into the ECM as soluble tropoelastin monomers, which are covalently bonded and cross-linked by lysyl oxidase and lysyl oxidase-like 1 to form elastin fibrils[32]. Tropoelastin gene expression is controlled by microRNA-29a (miR)29a, which binds to a sequence in the 3′ untranslated region of tropoelastin mRNA and inhibits tropoelastin synthesis[247,248]. We attempted to promote elastin production within our TEBVs by pre-treating fibroblasts with an inhibitor for microRNA-29a; continuation of this work may lead to increased elastin production within the TEBV matrix, and a more physiologically accurate construct.

5.5 Implications toward Cardiovascular Tissue Engineering

The establishment of microphysiological systems as platforms to test pharmaceutical drug candidates *in vitro* under healthy and diseased conditions is expected to grow substantially over the next decade. In this work, we created a rapidly producible tissue engineered blood vessel model capable of physiological responses to vasoactive agents such as phenylephrine, acetylcholine, caffeine, and theophylline. We also evaluated its function under healthy and inflammatory conditions, and assessed the potential to observe pleiotropic effects of statins on vessel vasoactivity and nitric oxide production. We evaluated primary endothelial progenitor cells from coronary artery disease patients and healthy volunteers, indicating differences in the function of the two patient populations under inflammatory conditions.

The TEBVs in this work were comprised of cells derived from primary human sources. The establishment of induced pluripotent stem cells (iPSCs) provides a lot of potential for using cells derived from the same source, eliminating any potential for donor mismatch within the culture system. Many avenues for exploration exist within this system, including the development of disease models using iPSCs from patient populations with known disease conditions. Overall, this work demonstrates the feasibility of using a three-dimensional construct to replicate physiological behavior of a functional vascular tissue unit.

Appendix A: Licensing Information for Previously Published Work

Permission to reuse portions of *Late outgrowth endothelial progenitors from patients with coronary artery disease: Endothelialization of confluent stromal cell layers*.

ELSEVIER LICENSE
TERMS AND CONDITIONS

Aug 19, 2016

This Agreement between Cristina E Fernandez ("You") and Elsevier ("Elsevier") consists of your license details and the terms and conditions provided by Elsevier and Copyright Clearance Center.

License Number 3932560436772

License date Aug 19, 2016

Licensed Content Publisher Elsevier

Licensed Content Publication Acta Biomaterialia

Licensed Content Title Late outgrowth endothelial progenitors from patients with coronary artery disease: Endothelialization of confluent stromal cell layers

Licensed Content Author Cristina E. Fernandez, Izundu C. Obionuoha, Charles S. Wallace, Lisa L. Satterwhite, George A. Truskey, William M. Reichert

Licensed Content Date February 2014

Licensed Content Volume Number 10

Licensed Content Issue Number 2

Licensed Content Pages 8

Start Page 893

End Page 900

Type of Use reuse in a thesis/dissertation

Portion full article

Format both print and electronic

Are you the author of this Elsevier article? Yes

Will you be translating? No

Order reference number

Title of your thesis/dissertation: Human Vascular Microphysiological Systems for Drug Screening

Expected completion date Dec 2016

Estimated size (number of pages) 225

Elsevier VAT number GB 494 6272 12

Requestor Location Cristina E Fernandez

701 Audubon Lake Drive, Apt. M

DURHAM, NC 27713

United States

Attn: Cristina E Fernandez

Total 0.00 USD

Terms and Conditions

INTRODUCTION

1. The publisher for this copyrighted material is Elsevier. By clicking "accept" in connection with completing this licensing transaction, you agree that the following terms and conditions apply to this transaction (along with the Billing and Payment terms and conditions established by Copyright Clearance Center, Inc. ("CCC"), at the time that you opened your Rightslink account and that are available at any time at http://myaccount.copyright.com).

GENERAL TERMS

2. Elsevier hereby grants you permission to reproduce the aforementioned material subject to the terms and conditions indicated.

3. Acknowledgement: If any part of the material to be used (for example, figures) has appeared in our publication with credit or acknowledgement to another source, permission must also be sought from that source. If such permission is not obtained then that material may not be included in your publication/copies. Suitable acknowledgement to the source must be made, either as a footnote or in a reference list at the end of your publication, as follows:

"Reprinted from Publication title, Vol /edition number, Author(s), Title of article / title of chapter, Pages No., Copyright (Year), with permission from Elsevier [OR APPLICABLE SOCIETY COPYRIGHT OWNER]." Also Lancet special credit - "Reprinted from The Lancet, Vol. number, Author(s), Title of article, Pages No., Copyright (Year), with permission from Elsevier."

4. Reproduction of this material is confined to the purpose and/or media for which permission is hereby given.

5. Altering/Modifying Material: Not Permitted. However figures and illustrations may be altered/adapted minimally to serve your work. Any other abbreviations, additions, deletions and/or any other alterations shall be made only with prior written authorization of Elsevier Ltd. (Please contact Elsevier at permissions@elsevier.com)

6. If the permission fee for the requested use of our material is waived in this instance, please be advised that your future requests for Elsevier materials may attract a fee.

7. Reservation of Rights: Publisher reserves all rights not specifically granted in the combination of (i) the license details provided by you and accepted in the course of this licensing transaction, (ii) these terms and conditions and (iii) CCC's Billing and Payment terms and conditions.

8. License Contingent Upon Payment: While you may exercise the rights licensed immediately upon issuance of the license at the end of the licensing process for the

transaction, provided that you have disclosed complete and accurate details of your proposed use, no license is finally effective unless and until full payment is received from you (either by publisher or by CCC) as provided in CCC's Billing and Payment terms and conditions. If full payment is not received on a timely basis, then any license preliminarily granted shall be deemed automatically revoked and shall be void as if never granted. Further, in the event that you breach any of these terms and conditions or any of CCC's Billing and Payment terms and conditions, the license is automatically revoked and shall be void as if never granted. Use of materials as described in a revoked license, as well as any use of the materials beyond the scope of an unrevoked license, may constitute copyright infringement and publisher reserves the right to take any and all action to protect its copyright in the materials.

9. Warranties: Publisher makes no representations or warranties with respect to the licensed material.

10. Indemnity: You hereby indemnify and agree to hold harmless publisher and CCC, and their respective officers, directors, employees and agents, from and against any and all claims arising out of your use of the licensed material other than as specifically authorized pursuant to this license.

11. No Transfer of License: This license is personal to you and may not be sublicensed, assigned, or transferred by you to any other person without publisher's written permission.

12. No Amendment Except in Writing: This license may not be amended except in a writing signed by both parties (or, in the case of publisher, by CCC on publisher's behalf).

13. Objection to Contrary Terms: Publisher hereby objects to any terms contained in any purchase order, acknowledgment, check endorsement or other writing prepared by you, which terms are inconsistent with these terms and conditions or CCC's Billing and Payment terms and conditions. These terms and conditions, together with CCC's Billing and Payment terms and conditions (which are incorporated herein), comprise the entire agreement between you and publisher (and CCC) concerning this licensing transaction. In the event of any conflict between your obligations established by these terms and conditions and those established by CCC's Billing and Payment terms and conditions, these terms and conditions shall control.

14. Revocation: Elsevier or Copyright Clearance Center may deny the permissions described in this License at their sole discretion, for any reason or no reason, with a full refund payable to you. Notice of such denial will be made using the contact information provided by you. Failure to receive such notice will not alter or invalidate the denial. In no event will Elsevier or Copyright Clearance Center be responsible or liable for any costs, expenses or damage incurred by you as a result of a denial of your permission request, other than a refund of the amount(s) paid by you to Elsevier and/or Copyright Clearance Center for denied permissions.

LIMITED LICENSE

The following terms and conditions apply only to specific license types:

15. Translation: This permission is granted for non-exclusive world English rights only unless your license was granted for translation rights. If you licensed translation rights you may only translate this content into the languages you requested. A professional translator must perform all translations and reproduce the content word for word preserving the integrity of the article.

16. Posting licensed content on any Website: The following terms and conditions apply as follows: Licensing material from an Elsevier journal: All content posted to the web site must maintain the copyright information line on the bottom of each image; A hyper-text must be included to the Homepage of the journal from which you are licensing at http://www.sciencedirect.com/science/journal/xxxxx or the Elsevier homepage for books at http://www.elsevier.com; Central Storage: This license does not include permission for a scanned version of the material to be stored in a central repository such as that provided by Heron/XanEdu.

Licensing material from an Elsevier book: A hyper-text link must be included to the Elsevier homepage at http://www.elsevier.com . All content posted to the web site must maintain the copyright information line on the bottom of each image.

Posting licensed content on Electronic reserve: In addition to the above the following clauses are applicable: The web site must be password-protected and made

available only to bona fide students registered on a relevant course. This permission is granted for 1 year only. You may obtain a new license for future website posting.

17. For journal authors: the following clauses are applicable in addition to the above:

Preprints: A preprint is an author's own write-up of research results and analysis, it has not been peer reviewed, nor has it had any other value added to it by a publisher (such as formatting, copyright, technical enhancement etc.). Authors can share their preprints anywhere at any time. Preprints should not be added to or enhanced in any way in order to appear more like, or to substitute for, the final versions of articles however authors can update their preprints on arXiv or RePEc with their Accepted

Author Manuscript (see below).

If accepted for publication, we encourage authors to link from the preprint to their formal publication via its DOI. Millions of researchers have access to the formal publications on ScienceDirect, and so links will help users to find, access, cite and use the best available version. Please note that Cell Press, The Lancet and some society-owned have different preprint policies. Information on these policies is available on the journal homepage.

Accepted Author Manuscripts: An accepted author manuscript is the manuscript of an article that has been accepted for publication and which typically includes author

incorporated changes suggested during submission, peer review and editor-author communications.

Authors can share their accepted author manuscript:

- immediately via their non-commercial person homepage or blog by updating a preprint in arXiv or RePEc with the accepted manuscript via their research institute or institutional repository for internal institutional uses or as part of an invitation-only research collaboration work-group directly by providing copies to their students or to research collaborators for their personal use for private scholarly sharing as part of an invitation-only work group on commercial sites with which Elsevier has an agreement

- after the embargo period via non-commercial hosting platforms such as their institutional repository via commercial sites with which Elsevier has an agreement

In all cases accepted manuscripts should:

- link to the formal publication via its DOI

- bear a CC-BY-NC-ND license - this is easy to do

- if aggregated with other manuscripts, for example in a repository or other site, be shared in alignment with our hosting policy not be added to or enhanced in any way to appear more like, or to substitute for, the published journal article.

Published journal article (JPA): A published journal article (PJA) is the definitive final record of published research that appears or will appear in the journal and

embodies all value-adding publishing activities including peer review co-ordination, copy-editing, formatting, (if relevant) pagination and online enrichment.

Policies for sharing publishing journal articles differ for subscription and gold open access articles:

Subscription Articles: If you are an author, please share a link to your article rather than the full-text. Millions of researchers have access to the formal publications on ScienceDirect, and so links will help your users to find, access, cite, and use the best available version.

Theses and dissertations which contain embedded PJAs as part of the formal submission can be posted publicly by the awarding institution with DOI links back to the formal publications on ScienceDirect.

If you are affiliated with a library that subscribes to ScienceDirect you have additional private sharing rights for others' research accessed under that agreement. This includes use for classroom teaching and internal training at the institution (including use in course packs and courseware programs), and inclusion of the article for grant funding purposes.

Gold Open Access Articles: May be shared according to the author-selected end-user license and should contain a CrossMark logo, the end user license, and a DOI link to the formal publication on ScienceDirect.

Please refer to Elsevier's posting policy for further information.

18. For book authors the following clauses are applicable in addition to the above:

Authors are permitted to place a brief summary of their work online only. You are not allowed to download and post the published electronic version of your chapter, nor may you scan the printed edition to create an electronic version. Posting to a repository: Authors are permitted to post a summary of their chapter only in their institution's repository.

19. Thesis/Dissertation: If your license is for use in a thesis/dissertation your thesis may be submitted to your institution in either print or electronic form. Should your thesis be published commercially, please reapply for permission. These requirements include permission for the Library and Archives of Canada to supply single copies, on demand, of the complete thesis and include permission for Proquest/UMI to supply single copies, on demand, of the complete thesis. Should your thesis be published commercially, please reapply for permission. Theses and dissertations which contain embedded PJAs as part of the formal submission can be posted publicly by the awarding institution with DOI links back to the formal publications on ScienceDirect.

Elsevier Open Access Terms and Conditions

You can publish open access with Elsevier in hundreds of open access journals or in nearly 2000 established subscription journals that support open access publishing.

Appendix B: Protocol for Constructing Collagen I Vascular Constructs

Version 8: Adapted by Cristina Fernandez, 7/29/13

References

1. C.E. Ghezzi, *et. al.* An airway smooth muscle cell niche under physiological pulsatile flow culture using a tubular dense collagen construct. *Biomaterials* 34 (2013) 1954-1966.[101]

2. J. B. Phillips and R. Brown. Micro-structured Materials and Mechanical Cues in 3D Collagen Gels. *3D Cell Culture: Methods and Protocols*, Methods in Molecular Bioogy vol. 695 (2011) Chapter 12, pp 183-196[249].

Materials

1. Rat tail collagen I (BD Biosciences Cat #: 354236)
2. Acetic acid, (0.6%), sterile
3. Dulbecco's Modified Eagle's Medium, Low Glucose, 10X (Sigma Cat #: D2429)
4. 5M NaOH, sterile
5. Neonatal human dermal fibroblasts (hNDFs), P6-11
6. Neonatal human dermal fibroblast media, warmed
7. 50 mL falcon tube
8. 3-mL sterile disposable syringe, BD Biosciences
9. Two-way stopcock with luer lock, autoclaved
10. Stainless steel mandrel, 0.032" (0.81mm) diameter

11. 10-12 Kimwipes, autoclaved
12. Nylon mesh, 0.8 μm pore size (Whatman)
13. Parafilm
14. Two stainless steel tweezers, autoclaved.

Preparation of Fibroblast-seeded 3-mL Collagen Constructs

Note: Calculations based on 3.81 mg/mL collagen I stock solution.

Collagen I, acetic acid, and NaOH concentrations must be re-calculated whenever a new collagen solution is ordered!!

Table 6: Sample TEBV Calculations

Reagent	**2-mL TEBVs**	**3-mL TEBVs**
Rat Tail Collagen I	861 uL	1.291 mL
0.6% Acetic Acid	739 uL	1.109 mL
10X DMEM	200 uL	300 uL
5M NaOH	25.2 uL	37.8 uL
Cell Suspension (5x10^6 cells/mL of total TEBV volume)	200 uL	300 uL

Instructions based on 3-mL TEBVs with 1,500,000 cells each.

1. Prepare the syringe mold by attaching the syringe to the luer lock of the stopcock and closing the stopcock.

2. Passage hNDFs according to normal protocol. Set aside 1,500,000 hNDFs in 300μL hNDF media for use in collagen gel and place in water bath. Work as quickly as possible.

3. Make 2.4 mL of a 2.05 mg/mL solution of rat-tail collagen I in 0.6% acetic acid by adding 760 uL acetic acid to 1.64 mL collagen I in a 50-mL falcon tube.

a. *Note: collagen I stock solution is highly viscous – squeeze out pipette several times.*

4. Add 300 μL 10X DMEM to collagen solution. Cap the falcon tube and gently swirl to mix solution, being careful not to create bubbles.

5. Raise pH to 8.5 by adding 25.9 μL (proportional to acetic acid) of 5M NaOH. Gently mix solution as before. Solution should change from yellow to bright pink.

a. *Note: This step is critical for gelation – collagen will not gel if solution is orange or red.*

6. Add hNDF suspension to collagen solution.

7. Pour the collagen I-hNDF solution into the syringe mold and place the mandrel in the center. Use the Parafilm to keep the mandrel in the center of the syringe.

8. Incubate the collagen gel solution in the cell culture hood at room temperature for 30 minutes.

9. Lay down 10 autoclaved kimwipes on top of each other, with the nylon mesh in the center. After the collagen solution has gelled, gently push the collagen tube out of the

open end of the syringe, keeping the gel on the mandrel. Use sterilized tweezers to hold the mandrel and gently lay the gel in the center of the nylon mesh.

10. Fold the Kimwipes around the gelled solution and pinch at the top. Suspend solution for 7-8 minutes.

11. Remove vessel from Kimwipes and place immediately in warm hNDF media.

Endothelializing TEBVs

1. Mount TEBV in perfusion chamber, held in place with sutures tied in double knots. Fill chamber with TEBV media.

2. Passage EPCs and prepare a solution of 500,000 EPCs in 0.5 mL EPC media.

3. Place 1-mL syringe on one outlet of the chamber. Fill another 1-mL syringe with EPCs in solution. Slowly push solution through, counteracting by pulling on the other syringe to act as a pressure balance. Ensure that media is going through the TEBV (EPC media is lighter pink than TEBV media, so it should be evident that it is perfusing through).

4. Push media back and forth 2-3 times. Remove syringes and cap inlet/outlet with connectors.

5. Mount chamber on rotation device and place in incubator. Allow rotating for 30 minutes.

6. Remove chamber from rotator and mount to perfusion system.

Appendix C: TEBV Media Compositions

Human Neonatal Dermal Fibroblast (hNDF) Media

1. DMEM Media, 4.5 g/L glucose, no L-glutamine or sodium pyruvate (Gibco, 11960)
2. Heat-inactivated fetal bovine serum (HI-FBS), 50 mL
3. Sodium pyruvate (Gibco 11360-070), 5 mL
4. MEM Non-essential amino acids (Gibco 11140-076), 5 mL
5. GlutaMAX (Gibco, 35050-061), 5 mL
6. Beta-mercaptoethanol, 500 uL
7. Pen/Strep, 5 mL

Human Bone Marrow-Derived Mesenchymal Stem Cells (hMSC) Media

1. MEM Alpha Base Media (Gibco, 12561-056)
2. HI-FBS, 100 mL
3. L-Glutamine, 10 mL
4. Pen/Strep, 5 mL

Endothelial Cell Media (for use with HAECs, CB-EPCs, CAD EPCs)

1. Endothelial Basal Media-2 (EBM-2, Lonza)
2. EGM-2 Single Quots (Lonza, add all except the FBS)
3. Heat-inactivated fetal bovine serum (HI-FBS), 50 mL

4. Pen/Strep, 5 mL

Tissue Engineered Blood Vessel (TEBV) Media - First Week

1. DMEM Media, 1 g/L glucose, with sodium pyruvate and L-glutamine (Gibco, 11885)
2. Heat-inactivated fetal bovine serum (HI-FBS), 18.5 mL
3. MEM Non-essential amino acids (Gibco 11140-076), 5 mL
4. Beta-mercaptoethanol, 500 uL
5. Pen/Strep, 5 mL

Tissue Engineered Blood Vessel (TEBV) Media - After 1 week

1. DMEM Media, 1 g/L glucose, with sodium pyruvate and L-glutamine (Gibco, 11885)
2. Heat-inactivated fetal bovine serum (HI-FBS), 18 mL
3. MEM Non-essential amino acids (Gibco 11140-076), 5 mL
4. Beta-mercaptoethanol, 500 uL
5. Pen/Strep, 5 mL
6. Add approximately 1,057 mg of 6-aminocaproic acid (Sigma) for a 2 mg/mL solution

Appendix D: TEBV Vasoactivity Assay

Materials:

Phenylephrine hydrochloride (Sigma, P6126) 100 mM stock solution in PBS

Acetylcholine chloride (Sigma, A6625) 10 mM stock solution in PBS

Protocol:

1. Start video recording of vessels perfused at 2 mL/min to acquire vessel baseline diameter.
2. **Endothelium-independent vasoconstriction:** Add phenylephrine at 1 μM to media reservoir. Swirl gently to ensure mixing.
3. Record response for 5 minutes.
4. **Endothelium-dependent vasodilation:** Add acetylcholine at 1 μM to media reservoir. Swirl gently to ensure mixing.
5. Record response for 5 minutes.
6. Measure diameter changes of TEBV with ImageJ.

Relevant Citations:

1. Lakin, RO, et. al. Techniques to harvest diseased human peripheral arteries and measure endothelial function in an ex vivo model. *J Vasc Surg* 2013; 58:470-477[250].
2. Crowley, CM, et. al. The mechanism of excitation-contraction coupling in phenylephrine-stimulated human saphenous vein. *Am J Physiol Heart Circ Physiol* 2002; 283:H1271-H1281[214].

3. Golledge, J, et. al. Development of an in vitro model to study the response of saphenous vein endothelium to pulsatile arterial flow and circumferential deformation. *Eur J Vasc Endovasc Surg* 1997; 13:605-612[251].

4. He, T, et. al. Transplantation of circulating endothelial progenitor cells restores endothelial function of denuded rabbit carotid arteries. *Stroke* 2004; 35:2378-2384[252].

Appendix E: Primers for qRT-PCR

Table 7: Primers for qRT-PCR

Target (Gene)	Primer Sequence
ICAM-1 (ICAM1)	Fwd: 5′-CAC CCT AGA GCC AAG GTG AC-3′
	Rev: 5′- GGG CCA TAC AGG ACA CGA AG-3′
α-SMA (ACTA2)	Fwd: 5′-GAC CTT TGG CTT GGC TTG TC-3′
	Rev: 5′-GTG CGG ACA GGA ATT GAA GC-3′
Calponin1 (CNN1)	Fwd: 5′-AGG TTA AGA ACA AGC TGG CCC-3′
	Rev: 5′-ATG AAG TTG TTG CCG ATG CG-3′
B2-microglobulin (B2M)	Fwd: 5′-GGC TAT CCA GCG TAC TCC AAA G-3′
	Rev: 5′-CAA CTT CAA TGT CGG ATG GAT G-3′

Appendix F: Antibodies for Flow Cytometry

Table 8: Antibodies for Flow Cytometry

Antigen	Conjugate	Source	Isotype	Vendor	Clone
CD31	FITC	Mouse	IgG1, κ	BioLegend	WM59
CD144	PE	Mouse	IgG2a, κ	BioLegend	BV9
CD14	FITC	Mouse	IgG1, κ	BioLegend	HCD14
CD45	FITC	Mouse	IgG1, κ	BioLegend	HI30
CD115	PE	Rat	IgG1, κ	BioLegend	9-4D2-1E4
CD54	PE	Mouse	IgG1, κ	BioLegend	HA58
CD106	PE	Mouse	IgG1, κ	BioLegend	STA
CD62E	PE	Mouse	IgG2a, κ	BioLegend	HCD62E
Mouse IgG1	FITC	Rat	IgG	BioLegend	RMG1-1

Appendix G: Antibodies for Immunofluorescence

Table 9: Primary Antibodies for Immunofluorescence

Antigen	Conjugate	Source	Clonality	Isotype	Vendor	Number
vWF	--	Rabbit	Polyclonal	IgG	Abcam	ab6994
α-SMA	--	Rabbit	Polyclonal	IgG	Abcam	ab5694
Calponin	--	Rabbit	Monoclonal	IgG	Abcam	ab46794
Fibronectin	--	Mouse	Monoclonal	IgG1	Abcam	ab26245
Collagen IV	--	Rabbit	Polyclonal	IgG	Abcam	ab6586
Laminin	--	Rabbit	Polyclonal	IgG	Abcam	ab91006
VCAM-1	--	Mouse	Monoclonal	IgG1	Santa Cruz	sc-13160
E-selectin	--	Rabbit	Polyclonal	IgG	Santa Cruz	sc-14011
ICAM-1	--	Mouse	Monoclonal	IgG1	Santa Cruz	sc-107
Rabbit IgG	--	Rabbit	--	IgG	Life Technologies	02-6102
Mouse IgG	Alexa Fluor 488	Goat	Polyclonal	IgG	Life Technologies	A-11001
Rabbit IgG	Alexa Fluor 594	Goat	Polyclonal	IgG	Life Technologies	A-11012

Appendix H: Protocol for Cell Separation and RNA Isolation from Endothelialized TEBVs

Version 3: April 19, 2016, C. Fernandez

Materials:

1. Collagenase (Sigma, C2674, available at CCF)
2. PBS with calcium and magnesium
3. CD31 Dynabeads (Invitrogen, 11155D)
4. Dynal MPC-S Magnet
5. 0.1% BSA solution in PBS, pH 7.4 (kept at 4C)
6. RNAse Zap
7. BioRad Aurum Total RNA Mini Kit
8. Molecular Biology grade Ethanol (available at CCF)
9. Molecular Biology grade water (available at CCF)

Protocol:

I. Releasing Cells from TEBV

1. Prepare 1 mL per TEBV of a 1 mg/mL collagenase (Sigma, C2674) solution in PBS.
2. Add collagenase solution to a 1.6-mL microcentrifuge tube. Submerge TEBV in solution and incubate at 37 ºC for 30 minutes.
3. Centrifuge dissolved TEBV at 300 x g for 5 minutes to pellet cells.
    a. If necessary, cells may be flash frozen in liquid nitrogen and stored at -80 ºC until RNA isolation. For best cell separation results, continue to part II.

II. Separating Endothelium from Medial Cells (hDNFs, hMSCs, iSMCs, SMCs, etc)

1. Make 50 mL of a 0.1% BSA solution in PBS
    a. Weigh 50 mg of BSA and add to 50 mL of PBS
    b. Sterile filter solution and store at 4 ºC until cell separation
2. Washing Dynabeads:
    a. Resuspend Dynabeads in the vial by vortexing for 1 minute.
    b. Add 1 mL of 0.1% BSA to a 1.6-mL centrifuge tube.
    c. Add 25 uL of Dynabeads to centrifuge tube and mix by pipetting.
    d. Put tube in magnet for 1 minute. Discard supernatant while tube is in magnet.
    e. Remove tube from magnet and resuspend beads with 1 mL of 0.1% BSA.
3. Cell Separation:
    a. Resuspend pelleted cells from TEBV with 1 mL washed Dynabead solution.
    b. Move cell-dynabead solution to 1.6-mL centrifuge tube.
    c. Incubate for 20 minutes at room temperature with gentle rotation.
    d. Place tube in Dynal magnet for 2 minutes.
    e. Collect supernatant that contains cells not specific for CD31 (medial cells) with a pipette while tube is still in the magnet. Place supernatant in a 1.6-mL tube to pellet cells for RNA isolation.
    f. Spin down cells from supernatant for 5 minutes at 300 x g to pellet cells. Aspirate supernatant and place cells on ice until RNA isolation.

g. Cells may be flash frozen in liquid nitrogen and stored at -80 ºC until RNA isolation, or protocol may proceed with Part III: RNA Isolation.

4. Removing Beads from ECs (if ECs are desired):

    a. Resuspend cells attached to beads (ECs) in 1 mL of 0.1% BSA. Place in magnet for 1 minute and aspirate supernatant while tube is still in the magnet. Repeat 3 more times to wash cells.

    b. Resuspend Dynabeads-ECs with 500 uL DPBS.

    c. Add Dynabead-EC solution for magnet for 2 minutes to remove beads. Collect supernatant while tube is still attached to magnet. Place supernatant in a 1.6-mL tube on ice for RNA isolation.

    d. Pellet cells by centrifuging for 5 min at 300 xg in a centrifuge tube. Aspirate supernatant.

    e. Cells may be flash frozen in liquid nitrogen and stored at -80 ºC until RNA isolation, or protocol may proceed with Part III: RNA Isolation.

III. RNA Isolation Protocol (with BioRad Aurum Total RNA Mini Kit) (Written by C. Cheng, adapted for TEBVs by C. Fernandez)

1. RNase Zap bench surface and wipe down all micropipettors, tip boxes, and the aspirator tip. RNase Zap your gloves.
2. Make a fresh 70% ethanol solution using molecular biology grade ethanol and water.

3. Get 1 capped 1.6-mL tube, 1 capless tube + filter ("RNA binding column") per sample.
4. Place 50 μL of elution solution *per sample* into one capped 1.6-mL tube and place into heat block set to 70 ºC.
5. Add 350 μL of lysis solution to the cell pellet.
6. Vortex tube for 1 minute to lyse cells.
7. Let sit for 5 minutes on ice.
8. Add 350 μL of 70% ethanol to tube and vortex 1 min.
9. Transfer solution into filter. Centrifuge for 30 sec at speed 10.
10. After centrifugation, hold filter while aspirating filtered liquid. Place filter back into tube.
11. Add 700 μL of low stringency wash solution to filter. Centrifuge 30 sec at speed 10; aspirate filtered liquid.
12. For each sample, mix 5 μL of reconstituted DNase I (in -20ºC freezer) with 75 μL DNase dilution solution in a 1.5-mL capped tube. Add 80 μL of mixture directly to the membrane of each filter. Incubate at room temperature for 15 min.
13. Centrifuge for 30 sec at speed 10. Aspirate liquid.
14. Add 700 μL of high stringency wash solution to filter; centrifuge for 30 sec at speed 10; aspirate liquid.

15. Add 700 μL of low stringency wash solution to filter; centrifuge for 1 min at speed 10; aspirate liquid.
16. Centrifuge for 2 min to remove residual wash solution.
17. Transfer filter to a new 1.6-mL capped tube and pipet 40 μL of warmed elution solution onto membrane in the filter. Let sit for 1 min to allow solution to saturate membrane.
18. Centrifuge uncapped for 3 minutes at speed 10 to elute the RNA from the filter.
19. Place filter in biohazard trash and cap the tube. Label tube with date and sample name. Place tube into box and store in -80 ºC freezer until qRT-PCR.

References

1. Arrowsmith, J. & Miller, P. Trial watch: phase II and phase III attrition rates 2011-2012. *Nature reviews. Drug discovery* **12**, 569 (2013).

2. Kola, I. & Landis, J. Can the pharmaceutical industry reduce attrition rates? *Nature reviews. Drug discovery* **3**, 711-715 (2004).

3. DiMasi, J.A., Hansen, R.W. & Grabowski, H.G. The price of innovation: new estimates of drug development costs. *Journal of health economics* **22**, 151-185 (2003).

4. Esch, M.B., King, T.L. & Shuler, M.L. The role of body-on-a-chip devices in drug and toxicity studies. *Annual review of biomedical engineering* **13**, 55-72 (2011).

5. Shanks, N., Greek, R. & Greek, J. Are animal models predictive for humans? *Philosophy, ethics, and humanities in medicine : PEHM* **4**, 2 (2009).

6. Seok, J., *et al.* Genomic responses in mouse models poorly mimic human inflammatory diseases. *Proceedings of the National Academy of Sciences of the United States of America* **110**, 3507-3512 (2013).

7. Wikswo, J.P. The relevance and potential roles of microphysiological systems in biology and medicine. *Exp Biol Med (Maywood)* **239**, 1061-1072 (2014).

8. Baker, B.M. & Chen, C.S. Deconstructing the third dimension: how 3D culture microenvironments alter cellular cues. *Journal of cell science* **125**, 3015-3024 (2012).

9. Go, A.S., *et al.* Heart disease and stroke statistics--2014 update: a report from the American Heart Association. *Circulation* **129**, e28-e292 (2014).

10. Taylor, L.M., Jr., Edwards, J.M. & Porter, J.M. Present status of reversed vein bypass grafting: five-year results of a modern series. *Journal of vascular surgery* **11**, 193-205; discussion 205-196 (1990).

11. Baguneid, M.S., *et al.* Tissue engineering of blood vessels. *The British journal of surgery* **93**, 282-290 (2006).

12. Wagenseil, J.E. & Mecham, R.P. Vascular extracellular matrix and arterial mechanics. *Physiological reviews* **89**, 957-989 (2009).

13. Martinez-Lemus, L.A. The dynamic structure of arterioles. *Basic & clinical pharmacology & toxicology* **110**, 5-11 (2012).

14. Sumpio, B.E., Riley, J.T. & Dardik, A. Cells in focus: endothelial cell. *Int J Biochem Cell B* **34**, 1508-1512 (2002).

15. LeBleu, V.S., MacDonald, B. & Kalluri, R. Structure and function of basement membranes. *Exp Biol Med* **232**, 1121-1127 (2007).

16. Yurchenco, P.D. Basement membranes: cell scaffoldings and signaling platforms. *Cold Spring Harbor perspectives in biology* **3**(2011).

17. Bosman, F.T. & Stamenkovic, I. Functional structure and composition of the extracellular matrix. *J Pathol* **200**, 423-428 (2003).

18. Bergmeier, W. & Hynes, R.O. Extracellular Matrix Proteins in Hemostasis and Thrombosis. *Cold Spring Harb Perspect Biol* (2011).

19. Davis, G.E. & Senger, D.R. Endothelial extracellular matrix: biosynthesis, remodeling, and functions during vascular morphogenesis and neovessel stabilization. *Circulation research* **97**, 1093-1107 (2005).

20. Hynes, R.O., *et al.* The diverse roles of integrins and their ligands in angiogenesis. *Cold Spring Harb Symp Quant Biol* **67**, 143-153 (2002).

21. Hirschi, K.K. & D'Amore, P.A. Pericytes in the microvasculature. *Cardiovasc Res* **32**, 687-698 (1996).

22. Beamish, J.A., He, P., Kottke-Marchant, K. & Marchant, R.E. Molecular regulation of contractile smooth muscle cell phenotype: implications for vascular tissue engineering. *Tissue engineering. Part B, Reviews* **16**, 467-491 (2010).

23. Stegemann, J.P., Hong, H. & Nerem, R.M. Mechanical, biochemical, and extracellular matrix effects on vascular smooth muscle cell phenotype. *J Appl Physiol* **98**, 2321-2327 (2005).

24. Moiseeva, E.P. Adhesion receptors of vascular smooth muscle cells and their functions. *Cardiovasc Res* **52**, 372-386 (2001).

25. Bulick, A.S., *et al.* Impact of endothelial cells and mechanical conditioning on smooth muscle cell extracellular matrix production and differentiation. *Tissue Eng Part A* **15**, 815-825 (2009).

26. Ricard-Blum, S. The collagen family. *Cold Spring Harb Perspect Biol* **3**, a004978 (2011).

27. Williamson, M.R., Shuttleworth, A., Canfield, A.E., Black, R.A. & Kielty, C.M. The role of endothelial cell attachment to elastic fibre molecules in the enhancement of monolayer formation and retention, and the inhibition of smooth muscle cell recruitment. *Biomaterials* **28**, 5307-5318 (2007).

28. Robert, L. Cell-elastin interaction and signaling. *Pathol Biol (Paris)* **53**, 399-404 (2005).

29. Isenberg, B.C. & Tranquillo, R.T. Long-term cyclic distention enhances the mechanical properties of collagen-based media-equivalents. *Annals of Biomedical Engineering* **31**, 937-949 (2003).

30. Long, J.L. & Tranquillo, R.T. Elastic fiber production in cardiovascular tissue-equivalents. *Matrix biology : journal of the International Society for Matrix Biology* **22**, 339-350 (2003).

31. Debelle, L. & Alix, A.J. The structures of elastins and their function. *Biochimie* **81**, 981-994 (1999).

32. Patel, A., Fine, B., Sandig, M. & Mequanint, K. Elastin biosynthesis: The missing link in tissue-engineered blood vessels. *Cardiovascular Research* **71**, 40-49 (2006).

33. Mochizuki, S., Brassart, B. & Hinek, A. Signaling pathways transduced through the elastin receptor facilitate proliferation of arterial smooth muscle cells. *J Biol Chem* **277**, 44854-44863 (2002).

34. Li, D.Y., *et al.* Elastin is an essential determinant of arterial morphogenesis. *Nature* **393**, 276-280 (1998).

35. Hong, H., McCullough, C.M. & Stegemann, J.P. The role of ERK signaling in protein hydrogel remodeling by vascular smooth muscle cells. *Biomaterials* **28**, 3824-3833 (2007).

36. Bashur, C.A., Venkataraman, L. & Ramamurthi, A. Tissue engineering and regenerative strategies to replicate biocomplexity of vascular elastic matrix assembly. *Tissue Eng Part B Rev* **18**, 203-217 (2012).

37. Simon-Assmann, P., Orend, G., Mammadova-Bach, E., Spenle, C. & Lefebvre, O. Role of laminins in physiological and pathological angiogenesis. *Int J Dev Biol* **55**, 455-465 (2011).

38. Durbeej, M. Laminins. *Cell Tissue Res* **339**, 259-268 (2010).

39. Wallace, C.S., Champion, J.C. & Truskey, G.A. Adhesion and function of human endothelial cells co-cultured on smooth muscle cells. *Annals of Biomedical Engineering* **35**, 375-386 (2007).

40. Lavender, M.D., Pang, Z., Wallace, C.S., Niklason, L.E. & Truskey, G.A. A system for the direct co-culture of endothelium on smooth muscle cells. *Biomaterials* **26**, 4642-4653 (2005).

41. Brown, M.A., Wallace, C.S., Angelos, M. & Truskey, G.A. Characterization of umbilical cord blood-derived late outgrowth endothelial progenitor cells exposed to laminar shear stress. *Tissue Eng Part A* **15**, 3575-3587 (2009).

42. Wang, Y.H., *et al.* Vascular smooth muscle cells promote endothelial cell adhesion via microtubule dynamics and activation of paxillin and the extracellular signal-regulated kinase (ERK) pathway in a co-culture system. *European journal of cell biology* **88**, 701-709 (2009).

43. Qi, Y.X., *et al.* PDGF-BB and TGF-{beta}1 on cross-talk between endothelial and smooth muscle cells in vascular remodeling induced by low shear stress. *Proceedings of the National Academy of Sciences of the United States of America* **108**, 1908-1913 (2011).

44. Redmond, E.M., *et al.* Endothelial cells inhibit flow-induced smooth muscle cell migration: role of plasminogen activator inhibitor-1. *Circulation* **103**, 597-603 (2001).

45. Looft-Wilson, R.C., Billaud, M., Johnstone, S.R., Straub, A.C. & Isakson, B.E. Interaction between nitric oxide signaling and gap junctions: effects on vascular function. *Biochimica et biophysica acta* **1818**, 1895-1902 (2012).

46. Meens, M.J., Pfenniger, A., Kwak, B.R. & Delmar, M. Regulation of cardiovascular connexins by mechanical forces and junctions. *Cardiovascular research* **99**, 304-314 (2013).

47. Blackburn, J.P., *et al.* Upregulation of connexin43 gap junctions during early stages of human coronary atherosclerosis. *Arteriosclerosis, thrombosis, and vascular biology* **15**, 1219-1228 (1995).

48. Matsushita, T., Rama, A., Charolidi, N., Dupont, E. & Severs, N.J. Relationship of connexin43 expression to phenotypic modulation in cultured human aortic smooth muscle cells. *European journal of cell biology* **86**, 617-628 (2007).

49. Kwak, B.R., Mulhaupt, F., Veillard, N., Gros, D.B. & Mach, F. Altered pattern of vascular connexin expression in atherosclerotic plaques. *Arteriosclerosis, thrombosis, and vascular biology* **22**, 225-230 (2002).

50. Syedain, Z.H., Meier, L.A., Bjork, J.W., Lee, A. & Tranquillo, R.T. Implantable arterial grafts from human fibroblasts and fibrin using a multi-graft pulsed flow-stretch bioreactor with noninvasive strength monitoring. *Biomaterials* **32**, 714-722 (2011).

51. Caplan, A.I. Adult mesenchymal stem cells for tissue engineering versus regenerative medicine. *Journal of cellular physiology* **213**, 341-347 (2007).

52. Tiwari, A., Salacinski, H.J., Hamilton, G. & Seifalian, A.M. Tissue engineering of vascular bypass grafts: role of endothelial cell extraction. *Eur J Vasc Endovasc Surg* **21**, 193-201 (2001).

53. Bajpai, V.K. & Andreadis, S.T. Stem cell sources for vascular tissue engineering and regeneration. *Tissue Eng Part B Rev* **18**, 405-425 (2012).

54. Li, Z., Hu, S., Ghosh, Z., Han, Z. & Wu, J.C. Functional characterization and expression profiling of human induced pluripotent stem cell- and embryonic stem cell-derived endothelial cells. *Stem Cells Dev* **20**, 1701-1710 (2011).

55. Margariti, A., *et al.* Direct reprogramming of fibroblasts into endothelial cells capable of angiogenesis and reendothelialization in tissue-engineered vessels. *Proc Natl Acad Sci U S A* **109**, 13793-13798 (2012).

56. Zhao, Y.L., *et al.* The development of a tissue-engineered artery using decellularized scaffold and autologous ovine mesenchymal stem cells. *Biomaterials* **31**, 296-307 (2010).

57. Asahara, T., *et al.* Isolation of putative progenitor endothelial cells for angiogenesis. *Science* **275**, 964-967 (1997).

58. Beranek, J.T. Vascular endothelial cell is a stem cell for neointimal formation after injury. *J Thorac Cardiovasc Surg* **121**, 820-821 (2001).

59. Tongers, J., Roncalli, J.G. & Losordo, D.W. Role of endothelial progenitor cells during ischemia-induced vasculogenesis and collateral formation. *Microvasc Res* **79**, 200-206 (2010).

60. Yoder, M.C., *et al.* Redefining endothelial progenitor cells via clonal analysis and hematopoietic stem/progenitor cell principals. *Blood* **109**, 1801-1809 (2007).

61. Kalka, C., *et al.* Transplantation of ex vivo expanded endothelial progenitor cells for therapeutic neovascularization. *Proc Natl Acad Sci U S A* **97**, 3422-3427 (2000).

62. He, H., Shirota, T., Yasui, H. & Matsuda, T. Canine endothelial progenitor cell-lined hybrid vascular graft with nonthrombogenic potential. *J Thorac Cardiovasc Surg* **126**, 455-464 (2003).

63. Ahmann, K.A., Johnson, S.L., Hebbel, R.P. & Tranquillo, R.T. Shear stress responses of adult blood outgrowth endothelial cells seeded on bioartificial tissue. *Tissue Eng Part A* **17**, 2511-2521 (2011).

64. Stroncek, J.D., *et al.* Comparison of endothelial cell phenotypic markers of late-outgrowth endothelial progenitor cells isolated from patients with coronary artery disease and healthy volunteers. *Tissue Eng Part A* **15**, 3473-3486 (2009).

65. Stroncek, J.D., Ren, L.C., Klitzman, B. & Reichert, W.M. Patient-derived endothelial progenitor cells improve vascular graft patency in a rodent model. *Acta Biomater* **8**, 201-208 (2012).

66. Vartanian, K.B., *et al.* Distinct extracellular matrix microenvironments of progenitor and carotid endothelial cells. *J Biomed Mater Res A* **91**, 528-539 (2009).

67. Ji, H., *et al.* Transdifferentiation of human endothelial progenitors into smooth muscle cells. *Biomaterials* **85**, 180-194 (2016).

68. Lippmann, E.S., Al-Ahmad A, Azarin, S.M., Palecek, S.P. & EV., S. A retinoic acid-enhanced, multicellular human blood-brain barrier model derived from stem cell sources. *Sci Rep* **4**, 4160 (2014).

69. Patsch, C., *et al.* Generation of vascular endothelial and smooth muscle cells from human pluripotent stem cells. *Nature cell biology* **17**, 994-1003 (2015).

70. Zhang, Z.X., *et al.* In vitro study of endothelial cells lining vascular grafts grown within the recipient's peritoneal cavity. *Tissue engineering. Part A* **14**, 1109-1120 (2008).

71. L'Heureux, N., *et al.* Human tissue-engineered blood vessels for adult arterial revascularization. *Nature medicine* **12**, 361-365 (2006).

72. Dahl, S.L., *et al.* Readily available tissue-engineered vascular grafts. *Science translational medicine* **3**, 68ra69 (2011).

73. Teebken, O.E., Bader, A., Steinhoff, G. & Haverich, A. Tissue engineering of vascular grafts: human cell seeding of decellularised porcine matrix. *European journal of vascular and endovascular surgery : the official journal of the European Society for Vascular Surgery* **19**, 381-386 (2000).

74. Isenberg, B.C., Williams, C. & Tranquillo, R.T. Endothelialization and flow conditioning of fibrin-based media-equivalents. *Ann Biomed Eng* **34**, 971-985 (2006).

75. L'heureux, N., Paquet, S., Labbe, R., Germain, L. & Auger, F.A. A completely biological tissue-engineered human blood vessel. *Faseb Journal* **12**, 47-56 (1998).

76. Weinberg, C.B. & Bell, E. A blood vessel model constructed from collagen and cultured vascular cells. *Science* **231**, 397-400 (1986).

77. Shinoka, T., *et al.* Creation of viable pulmonary artery autografts through tissue engineering. *J Thorac Cardiovasc Surg* **115**, 536-545; discussion 545-536 (1998).

78. Roh, J.D., *et al.* Small-diameter biodegradable scaffolds for functional vascular tissue engineering in the mouse model. *Biomaterials* **29**, 1454-1463 (2008).

79. Hibino, N., *et al.* Late-term results of tissue-engineered vascular grafts in humans. *J Thorac Cardiov Sur* **139**, 431-U233 (2010).

80. Udelsman, B.V., Maxfield, M.W. & Breuer, C.K. Tissue engineering of blood vessels in cardiovascular disease: moving towards clinical translation. *Heart* **99**, 454-460 (2013).

81. Hjortnaes, J., *et al.* Intravital Molecular Imaging of Small-Diameter Tissue-Engineered Vascular Grafts in Mice: A Feasibility Study. *Tissue Eng Pt C-Meth* **16**, 597-607 (2010).

82. Harrington, J.K., *et al.* Determining the fate of seeded cells in venous tissue-engineered vascular grafts using serial MRI. *Faseb J* **25**, 4150-4161 (2011).

83. Roh, J.D., *et al.* Tissue-engineered vascular grafts transform into mature blood vessels via an inflammation-mediated process of vascular remodeling. *Proc Natl Acad Sci U S A* **107**, 4669-4674 (2010).

84. Hashi, C.K., *et al.* Antithrombogenic property of bone marrow mesenchymal stem cells in nanofibrous vascular grafts. *Proc Natl Acad Sci U S A* **104**, 11915-11920 (2007).

85. Roh, J.D., *et al.* Tissue-engineered vascular grafts transform into mature blood vessels via an inflammation-mediated process of vascular remodeling. *P Natl Acad Sci USA* **107**, 4669-4674 (2010).

86. Yu, J., *et al.* The effect of stromal cell-derived factor-1alpha/heparin coating of biodegradable vascular grafts on the recruitment of both endothelial and smooth muscle progenitor cells for accelerated regeneration. *Biomaterials* **33**, 8062-8074 (2012).

87. Melchiorri, A.J., Hibino, N. & Fisher, J.P. Strategies and Techniques to Enhance the In Situ Endothelialization of Small-Diameter Biodegradable Polymeric Vascular Grafts. *Tissue Eng Part B Rev* (2013).

88. Avci-Adali, M., Ziemer, G. & Wendel, H.P. Induction of EPC homing on biofunctionalized vascular grafts for rapid in vivo self-endothelialization--a review of current strategies. *Biotechnol Adv* **28**, 119-129 (2010).

89. Olausson, M., *et al.* Transplantation of an allogeneic vein bioengineered with autologous stem cells: a proof-of-concept study. *Lancet* **380**, 230-237 (2012).

90. Quint, C., Arief, M., Muto, A., Dardik, A. & Niklason, L.E. Allogeneic human tissue-engineered blood vessel. *J Vasc Surg* (2011).

91. Quint, C., *et al.* Decellularized tissue-engineered blood vessel as an arterial conduit. *Proc Natl Acad Sci U S A* **108**, 9214-9219 (2011).

92. Bader, A., *et al.* Engineering of human vascular aortic tissue based on a xenogeneic starter matrix. *Transplantation* **70**, 7-14 (2000).

93. Cho, S.W., *et al.* Small-diameter blood vessels engineered with bone marrow-derived cells. *Ann Surg* **241**, 506-515 (2005).

94. Niklason, L.E., *et al.* Functional arteries grown in vitro. *Science* **284**, 489-493 (1999).

95. Rashid, S.T., Fuller, B., Hamilton, G. & Seifalian, A.M. Tissue engineering of a hybrid bypass graft for coronary and lower limb bypass surgery. *Faseb J* **22**, 2084-2089 (2008).

96. Dahan, N., *et al.* Porcine Small Diameter Arterial Extracellular Matrix Supports Endothelium Formation and Media Remodeling Forming a Promising Vascular Engineered Biograft. *Tissue Eng Part A* (2011).

97. Leyh, R.G., *et al.* Tissue engineering of viable pulmonary arteries for surgical correction of congenital heart defects. *Ann Thorac Surg* **81**, 1466-1470; discussion 1470-1461 (2006).

98. Heine, J., *et al.* Preclinical assessment of a tissue-engineered vasomotive human small-calibered vessel based on a decellularized xenogenic matrix: histological and functional characterization. *Tissue Eng Part A* **17**, 1253-1261 (2011).

99. Neff, L.P., *et al.* Vascular smooth muscle enhances functionality of tissue-engineered blood vessels in vivo. *J Vasc Surg* **53**, 426-434 (2011).

100. Yao, L., Liu, J. & Andreadis, S.T. Composite fibrin scaffolds increase mechanical strength and preserve contractility of tissue engineered blood vessels. *Pharm Res* **25**, 1212-1221 (2008).

101. Ghezzi, C.E., *et al.* An airway smooth muscle cell niche under physiological pulsatile flow culture using a tubular dense collagen construct. *Biomaterials* **34**, 1954-1966 (2013).

102. Ghezzi, C.E., Muja, N., Marelli, B. & Nazhat, S.N. Real time responses of fibroblasts to plastically compressed fibrillar collagen hydrogels. *Biomaterials* **32**, 4761-4772 (2011).

103. Ghezzi, C.E., Marelli, B., Muja, N. & Nazhat, S.N. Immediate production of a tubular dense collagen construct with bioinspired mechanical properties. *Acta Biomaterialia* **8**, 1813-1825 (2012).

104. Cleary, M.A., *et al.* Vascular tissue engineering: the next generation. *Trends Mol Med* **18**, 394-404 (2012).

105. Dudash, L.A., Kligman, F., Sarett, S.M., Kottke-Marchant, K. & Marchant, R.E. Endothelial cell attachment and shear response on biomimetic polymer-coated vascular grafts. *J Biomed Mater Res A* **100**, 2204-2210 (2012).

106. Walluscheck, K.P., Steinhoff, G., Kelm, S. & Haverich, A. Improved endothelial cell attachment on ePTFE vascular grafts pretreated with synthetic RGD-containing peptides. *Eur J Vasc Endovasc Surg* **12**, 321-330 (1996).

107. Williams, S.K., Rose, D.G. & Jarrell, B.E. Microvascular endothelial cell sodding of ePTFE vascular grafts: improved patency and stability of the cellular lining. *J Biomed Mater Res* **28**, 203-212 (1994).

108. Meinhart, J.G., *et al.* Enhanced endothelial cell retention on shear-stressed synthetic vascular grafts precoated with RGD-cross-linked fibrin. *Tissue Eng* **11**, 887-895 (2005).

109. Deutsch, M., *et al.* Long-term experience in autologous in vitro endothelialization of infrainguinal ePTFE grafts. *J Vasc Surg* **49**, 352-362; discussion 362 (2009).

110. Hoerstrup, S.P., *et al.* Tissue engineering of small caliber vascular grafts. *Eur J Cardiothorac Surg* **20**, 164-169 (2001).

111. Kaushal, S., *et al.* Functional small-diameter neovessels created using endothelial progenitor cells expanded ex vivo. *Nat Med* **7**, 1035-1040 (2001).

112. Borschel, G.H., *et al.* Tissue engineering of recellularized small-diameter vascular grafts. *Tissue Eng* **11**, 778-786 (2005).

113. L'Heureux, N., *et al.* Human tissue-engineered blood vessels for adult arterial revascularization. *Nat Med* **12**, 361-365 (2006).

114. Isenberg, B.C., Williams, C. & Tranquillo, R.T. Endothelialization and flow conditioning of fibrin-based media-equivalents. *Ann Biomed Eng* **34**, 971-985 (2006).

115. Wu, H.C., *et al.* Coculture of endothelial and smooth muscle cells on a collagen membrane in the development of a small-diameter vascular graft. *Biomaterials* **28**, 1385-1392 (2007).

116. Kerdjoudj, H., *et al.* Re-endothelialization of human umbilical arteries treated with polyelectrolyte multilayers: A tool for damaged vessel replacement. *Adv Funct Mater* **17**, 2667-2673 (2007).

117. Aper, T., Schmidt, A., Duchrow, M. & Bruch, H.P. Autologous blood vessels engineered from peripheral blood sample. *Eur J Vasc Endovasc Surg* **33**, 33-39 (2007).

118. Narita, Y., *et al.* Decellularized ureter for tissue-engineered small-caliber vascular graft. *J Artif Organs* **11**, 91-99 (2008).

119. Jimenez-Vergara, A.C., *et al.* Approach for fabricating tissue engineered vascular grafts with stable endothelialization. *Ann Biomed Eng* **38**, 2885-2895 (2010).

120. Ross, R. Atherosclerosis--an inflammatory disease. *N Engl J Med* **340**, 115-126 (1999).

121. Hansson, G.K. & Hermansson, A. The immune system in atherosclerosis. *Nature immunology* **12**, 204-212 (2011).

122. Gimbrone, M.A., Jr., Topper, J.N., Nagel, T., Anderson, K.R. & Garcia-Cardena, G. Endothelial dysfunction, hemodynamic forces, and atherogenesis. *Annals of the New York Academy of Sciences* **902**, 230-239; discussion 239-240 (2000).

123. Coutinho, T., Rooke, T.W. & Kullo, I.J. Arterial dysfunction and functional performance in patients with peripheral artery disease: a review. *Vascular medicine* **16**, 203-211 (2011).

124. Ley, K., Laudanna, C., Cybulsky, M.I. & Nourshargh, S. Getting to the site of inflammation: the leukocyte adhesion cascade updated. *Nature reviews. Immunology* **7**, 678-689 (2007).

125. Owens, G.K., Kumar, M.S. & Wamhoff, B.R. Molecular regulation of vascular smooth muscle cell differentiation in development and disease. *Physiological reviews* **84**, 767-801 (2004).

126. Tse, K., Tse, H., Sidney, J., Sette, A. & Ley, K. T cells in atherosclerosis. *International immunology* **25**, 615-622 (2013).

127. Zhang, L., *et al.* Expression of tumor necrosis factor receptor-1 in arterial wall cells promotes atherosclerosis. *Arteriosclerosis, thrombosis, and vascular biology* **27**, 1087-1094 (2007).

128. Sasaguri, T., *et al.* A role for interleukin 4 in production of matrix metalloproteinase 1 by human aortic smooth muscle cells. *Atherosclerosis* **138**, 247-253 (1998).

129. Higuchi, S., *et al.* Effects of histamine and interleukin-4 synthesized in arterial intima on phagocytosis by monocytes/macrophages in relation to atherosclerosis. *FEBS letters* **505**, 217-222 (2001).

130. van Bussel, B.C., *et al.* Endothelial dysfunction and low-grade inflammation are associated with greater arterial stiffness over a 6-year period. *Hypertension* **58**, 588-595 (2011).

131. Fisher, G., Hunter, G.R. & Glasser, S.P. Associations between arterial elasticity and markers of inflammation in healthy older women. *The journals of gerontology. Series A, Biological sciences and medical sciences* **68**, 382-388 (2013).

132. Zieman, S.J., Melenovsky, V. & Kass, D.A. Mechanisms, pathophysiology, and therapy of arterial stiffness. *Arteriosclerosis, thrombosis, and vascular biology* **25**, 932-943 (2005).

133. Wang, M., *et al.* Chronic matrix metalloproteinase inhibition retards age-associated arterial proinflammation and increase in blood pressure. *Hypertension* **60**, 459-466 (2012).

134. Wang, M., Jiang, L., Monticone, R.E. & Lakatta, E.G. Proinflammation: the key to arterial aging. *Trends in endocrinology and metabolism: TEM* **25**, 72-79 (2014).

135. Thyberg, J., Blomgren, K., Roy, J., Tran, P.K. & Hedin, U. Phenotypic modulation of smooth muscle cells after arterial injury is associated with changes in the distribution of laminin and fibronectin. *The journal of histochemistry and cytochemistry : official journal of the Histochemistry Society* **45**, 837-846 (1997).

136. Yue, T.L., *et al.* Interleukin-8. A mitogen and chemoattractant for vascular smooth muscle cells. *Circulation research* **75**, 1-7 (1994).

137. Chandrasekar, B., *et al.* The pro-atherogenic cytokine interleukin-18 induces CXCL16 expression in rat aortic smooth muscle cells via MyD88, interleukin-1 receptor-associated kinase, tumor necrosis factor receptor-associated factor 6, c-Src, phosphatidylinositol 3-kinase, Akt, c-Jun N-terminal kinase, and activator protein-1 signaling. *The Journal of biological chemistry* **280**, 26263-26277 (2005).

138. Young, J.L., Libby, P. & Schonbeck, U. Cytokines in the pathogenesis of atherosclerosis. *Thrombosis and haemostasis* **88**, 554-567 (2002).

139. Huynh, J., *et al.* Age-related intimal stiffening enhances endothelial permeability and leukocyte transmigration. *Science translational medicine* **3**, 112ra122 (2011).

140. Tousoulis, D., Kampoli, A.M., Tentolouris, C., Papageorgiou, N. & Stefanadis, C. The role of nitric oxide on endothelial function. *Curr Vasc Pharmacol* 4-18 (2012).

141. Lind, L., Berglund, L., Larsson, A. & Sundstrom, J. Endothelial function in resistance and conduit arteries and 5-year risk of cardiovascular disease. *Circulation* **123**, 1545-1551 (2011).

142. Iglarz, M. & Clozel, M. At the heart of tissue: endothelin system and end organ damage. *Clin Sci* **119**, 453-463 (2010).

143. Hadi, H.A. & Suwaidi, J.A. Endothelial dysfunction in diabetes mellitus. *Vasc Health Risk Manag* **3**, 853-876 (2007).

144. Landmesser, U., Hornig, B. & Drexler, H. Endothelial dysfunction in hypercholesterolemia: mechanisms, pathophysiological importance, and therapeutic interventions. *Semin Thromb Hemost* **26**, 529-537 (2000).

145. Powell, J.T. Vascular damage from smoking: disease mechanisms at the arterial wall. *Vascular medicine* **3**, 21-28 (1998).

146. Zhang, J., Defelice, A.F., Hanig, J.P. & Colatsky, T. Biomarkers of endothelial cell activation serve as potential surrogate markers for drug-induced vascular injury. *Toxicol Pathol* **38**, 856-871 (2010).

147. Stegemann, J.P. & Nerem, R.M. Altered response of vascular smooth muscle cells to exogenous biochemical stimulation in two- and three-dimensional culture. *Exp Cell Res* **283**, 146-155 (2003).

148. Li, S., *et al.* Genomic analysis of smooth muscle cells in 3-dimensional collagen matrix. *Faseb J* **17**, 97-99 (2003).

149. Grassl, E.D., Oegema, T.R. & Tranquillo, R.T. A fibrin-based arterial media equivalent. *Journal of biomedical materials research. Part A* **66**, 550-561 (2003).

150. Imberti, B., Seliktar, D., Nerem, R.M. & Remuzzi, A. The response of endothelial cells to fluid shear stress using a co-culture model of the arterial wall. *Endothelium* **9**, 11-23 (2002).

151. Vunjak-Novakovic, G., Bhatia, S., Chen, C. & Hirschi, K. HeLiVa platform: integrated heart-liver-vascular systems for drug testing in human health and disease. *Stem cell research & therapy* **4 Suppl 1**, S8 (2013).

152. Cicha, I., *et al.* Shear stress preconditioning modulates endothelial susceptibility to circulating TNF-alpha and monocytic cell recruitment in a simplified model of arterial bifurcations. *Atherosclerosis* **207**, 93-102 (2009).

153. Rainger, G.E. & Nash, G.B. Cellular pathology of atherosclerosis: smooth muscle cells prime cocultured endothelial cells for enhanced leukocyte adhesion. *Circulation research* **88**, 615-622 (2001).

154. Wallace, C.S. & Truskey, G.A. Direct-contact co-culture between smooth muscle and endothelial cells inhibits TNF-alpha-mediated endothelial cell activation. *Am J Physiol Heart Circ Physiol* **299**, H338-346 (2010).

155. Kim, Y., *et al.* Probing nanoparticle translocation across the permeable endothelium in experimental atherosclerosis. *Proceedings of the National Academy of Sciences of the United States of America* **111**, 1078-1083 (2014).

156. Wang, Y.I., *et al.* Triglyceride-rich lipoprotein modulates endothelial vascular cell adhesion molecule (VCAM)-1 expression via differential regulation of endoplasmic reticulum stress. *PloS one* **8**, e78322 (2013).

157. Robert, J., *et al.* A three-dimensional engineered artery model for in vitro atherosclerosis research. *PloS one* **8**, e79821 (2013).

158. Fernandez, C.E., *et al.* Late-outgrowth endothelial progenitors from patients with coronary artery disease: endothelialization of confluent stromal cell layers. *Acta Biomater* **10**, 893-900 (2014).

159. Kakisis, J.D., Liapis, C.D., Breuer, C. & Sumpio, B.E. Artificial blood vessel: The Holy Grail of peripheral vascular surgery. *Journal of Vascular Surgery* **41**, 349-354 (2005).

160. Heyligers, J.M., Arts, C.H., Verhagen, H.J., de Groot, P.G. & Moll, F.L. Improving small-diameter vascular grafts: from the application of an endothelial cell lining to the construction of a tissue-engineered blood vessel. *Ann Vasc Surg* **19**, 448-456 (2005).

161. Asakage, M., *et al.* Early-outgrowth of endothelial progenitor cells can function as antigen-presenting cells. *Cancer Immunol Immunother* **55**, 708-716 (2006).

162. Ingram, D.A., *et al.* Identification of a novel hierarchy of endothelial progenitor cells using human peripheral and umbilical cord blood. *Blood* **104**, 2752-2760 (2004).

163. Hur, J., *et al.* Characterization of two types of endothelial progenitor cells and their different contributions to neovasculogenesis. *Arterioscler Thromb Vasc Biol* **24**, 288-293 (2004).

164. Stroncek, J.D., Ren, L.C., Klitzman, B. & Reichert, W.M. Patient-derived endothelial progenitor cells improve vascular graft patency in a rodent model. *Acta Biomaterialia* **8**, 201-208 (2012).

165. Cao, L., Wu, A. & Truskey, G.A. Biomechanical effects of flow and coculture on human aortic and cord blood-derived endothelial cells. *J Biomech* **44**, 2150-2157 (2011).

166. Peters, E.B., Christoforou, N., Leong, K.W. & Truskey, G.A. Comparison of mixed and lamellar coculture spatial arrangements for tissue engineering capillary networks in vitro. *Tissue Eng Part A* **19**, 697-706 (2013).

167. Hirschi, K.K., Ingram, D.A. & Yoder, M.C. Assessing identity, phenotype, and fate of endothelial progenitor cells. *Arterioscler Thromb Vasc Biol* **28**, 1584-1595 (2008).

168. Brown, M.A., *et al.* The use of mild trypsinization conditions in the detachment of endothelial cells to promote subsequent endothelialization on synthetic surfaces. *Biomaterials* **28**, 3928-3935 (2007).

169. Allen, J.D., *et al.* Plasma nitrite response and arterial reactivity differentiate vascular health and performance. *Nitric Oxide* **20**, 231-237 (2009).

170. Kang, S.D., *et al.* Isolation of Functional Human Endothelial Cells from Small Volumes of Umbilical Cord Blood. *Ann Biomed Eng* (2013).

171. Brown, M.A., Wallace, C.S., Angelos, M. & Truskey, G.A. Characterization of Umbilical Cord Blood Derived Late Outgrowth Endothelial Progenitor Cells Exposed to Laminar Shear Stress. *Tissue Eng Part A* **15**, 3575-3587 (2009).

172. Guven, H., Shepherd, R.M., Bach, R.G., Capoccia, B.J. & Link, D.C. The number of endothelial progenitor cell colonies in the blood is increased in patients with angiographically significant coronary artery disease. *J Am Coll Cardiol* **48**, 1579-1587 (2006).

173. Wallace, C.S., Champion, J.C. & Truskey, G.A. Adhesion and function of human endothelial cells co-cultured on smooth muscle cells. *Ann Biomed Eng* **35**, 375-386 (2007).

174. Sabatino, M., *et al.* The establishment of a bank of stored clinical bone marrow stromal cell products. *Journal of translational medicine* **10**, 23 (2012).

175. Wu, X., *et al.* Tissue-engineered microvessels on three-dimensional biodegradable scaffolds using human endothelial progenitor cells. *Am J Physiol Heart Circ Physiol* **287**, H480-487 (2004).

176. Melero-Martin, J.M., *et al.* In vivo vasculogenic potential of human blood-derived endothelial progenitor cells. *Blood* **109**, 4761-4768 (2007).

177. Melero-Martin, J.M., *et al.* Engineering robust and functional vascular networks in vivo with human adult and cord blood-derived progenitor cells. *Circ Res* **103**, 194-202 (2008).

178. Brown, D.J., *et al.* Endothelial cell activation of the smooth muscle cell phosphoinositide 3-kinase/Akt pathway promotes differentiation. *J Vasc Surg* **41**, 509-516 (2005).

179. Xia, Y., Bhattacharyya, A., Roszell, E.E., Sandig, M. & Mequanint, K. The role of endothelial cell-bound Jagged1 in Notch3-induced human coronary artery smooth muscle cell differentiation. *Biomaterials* **33**, 2462-2472 (2012).

180. Rzucidlo, E.M., Martin, K.A. & Powell, R.J. Regulation of vascular smooth muscle cell differentiation. *J Vasc Surg* **45 Suppl A**, A25-32 (2007).

181. Anamelechi, C.C., Truskey, G.A. & Reichert, W.M. Mylar and Teflon-AF as cell culture substrates for studying endothelial cell adhesion. *Biomaterials* **26**, 6887-6896 (2005).

182. Wallace, C.S., Strike, S.A. & Truskey, G.A. Smooth muscle cell rigidity and extracellular matrix organization influence endothelial cell spreading and adhesion formation in coculture. *Am J Physiol Heart Circ Physiol* **293**, H1978-1986 (2007).

183. Yang, C., *et al.* Enhancement of neovascularization with cord blood CD133+ cell-derived endothelial progenitor cell transplantation. *Thromb Haemost* **91**, 1202-1212 (2004).

184. Murohara, T., *et al.* Transplanted cord blood-derived endothelial precursor cells augment postnatal neovascularization. *J Clin Invest* **105**, 1527-1536 (2000).

185. Ladhoff, J., Fleischer, B., Hara, Y., Volk, H.D. & Seifert, M. Immune privilege of endothelial cells differentiated from endothelial progenitor cells. *Cardiovasc Res* **88**, 121-129 (2010).

186. Suarez, Y., Shepherd, B.R., Rao, D.A. & Pober, J.S. Alloimmunity to human endothelial cells derived from cord blood progenitors. *J Immunol* **179**, 7488-7496 (2007).

187. Fernandez, C.E., *et al.* Human Vascular Microphysiological System for in vitro Drug Screening. *Scientific reports* **6**, 21579 (2016).

188. Truskey, G.A. & Fernandez, C.E. Tissue-engineered blood vessels as promising tools for testing drug toxicity. *Expert opinion on drug metabolism & toxicology* **11**, 1021-1024 (2015).

189. Vassilakopoulou, M., *et al.* Paclitaxel chemotherapy and vascular toxicity as assessed by flow-mediated and nitrate-mediated vasodilatation. *Vascular pharmacology* **53**, 115-121 (2010).

190. Gilbert, S.E., Tew, G.A., Bourke, L., Winter, E.M. & Rosario, D.J. Assessment of endothelial dysfunction by flow-mediated dilatation in men on long-term androgen deprivation therapy for prostate cancer. *Experimental physiology* **98**, 1401-1410 (2013).

191. Fernandez, C.E., Achneck, H.E., Reichert, W.M. & Truskey, G.A. Biological and engineering design considerations for vascular tissue engineered blood vessels (TEBVs). *Curr Opin Chem Eng* **3**, 83-90 (2014).

192. Seifu, D.G., Purnama, A., Mequanint, K. & Mantovani, D. Small-diameter vascular tissue engineering. *Nat. Rev. Cardiol.* **10**, 410-421 (2013).

193. Boccafoschi, F., Rajan, N., Habermehl, J. & Mantovani, D. Preparation and characterization of a scaffold for vascular tissue engineering by direct-assembling of collagen and cells in a cylindrical geometry. *Macromol Biosci* **7**, 719-726 (2007).

194. Tousoulis, D., Kampoli, A.M., Tentolouris, C., Papageorgiou, N. & Stefanadis, C. The role of nitric oxide on endothelial function. *Curr Vasc Pharmacol* **10**, 4-18 (2012).

195. Flammer, A.J., *et al.* The assessment of endothelial function: from research into clinical practice. *Circulation* **126**, 753-767 (2012).

196. Halcox, J.P., *et al.* Prognostic value of coronary vascular endothelial dysfunction. *Circulation* **106**, 653-658 (2002).

197. Schachinger, V., Britten, M.B. & Zeiher, A.M. Prognostic impact of coronary vasodilator dysfunction on adverse long-term outcome of coronary heart disease. *Circulation* **101**, 1899-1906 (2000).

198. Ludmer, P.L., *et al.* Paradoxical vasoconstriction induced by acetylcholine in atherosclerotic coronary arteries. *N Engl J Med* **315**, 1046-1051 (1986).

199. Laflamme, K., *et al.* Tissue-engineered human vascular media with a functional endothelin system. *Circulation* **111**, 459-464 (2005).

200. Schutte, S.C., Chen, Z., Brockbank, K.G. & Nerem, R.M. Tissue engineering of a collagen-based vascular media: Demonstration of functionality. *Organogenesis* **6**, 204-211 (2010).

201. Campbell, J.H., Efendy, J.L. & Campbell, G.R. Novel vascular graft grown within recipient's own peritoneal cavity. *Circulation research* **85**, 1173-1178 (1999).

202. Jung, Y., *et al.* Scaffold-free, Human Mesenchymal Stem Cell-Based Tissue Engineered Blood Vessels. *Scientific reports* **5**, 15116 (2015).

203. Micol, L.A., *et al.* High-density collagen gel tubes as a matrix for primary human bladder smooth muscle cells. *Biomaterials* **32**, 1543-1548 (2011).

204. Stroncek, J.D., *et al.* Comparison of endothelial cell phenotypic markers of late outgrowth EPCs isolated from coronary artery disease patients and healthy volunteers. *Tissue Eng* **35**, 3473-3486 (2009).

205. Wang, Y.X., Poon, C.I. & Pang, C.C. Vascular pharmacodynamics of NG-nitro-L-arginine methyl ester in vitro and in vivo. *The Journal of pharmacology and experimental therapeutics* **267**, 1091-1099 (1993).

206. Pfaffl, M.W. A new mathematical model for relative quantification in real-time RT-PCR. *Nucleic acids research* **29**, e45 (2001).

207. Reneman, R.S. & Hoeks, A.P. Wall shear stress as measured in vivo: consequences for the design of the arterial system. *Medical & biological engineering & computing* **46**, 499-507 (2008).

208. Konig, G., *et al.* Mechanical properties of completely autologous human tissue engineered blood vessels compared to human saphenous vein and mammary artery. *Biomaterials* **30**, 1542-1550 (2009).

209. Cseh, B., *et al.* Autocrine fibronectin directs matrix assembly and crosstalk between cell-matrix and cell-cell adhesion in vascular endothelial cells. *Journal of cell science* **123**, 3989-3999 (2010).

210. Mikaelian, I., *et al.* Nonclinical Safety Biomarkers of Drug-induced Vascular Injury: Current Status and Blueprint for the Future. *Toxicologic pathology* **42**, 635-657 (2014).

211. Echeverri, D., Montes, F.R., Cabrera, M., Galan, A. & Prieto, A. Caffeine's Vascular Mechanisms of Action. *International journal of vascular medicine* **2010**, 834060 (2010).

212. L'Heureux, N., McAllister, T.N. & de la Fuente, L.M. Tissue-engineered blood vessel for adult arterial revascularization. *The New England journal of medicine* **357**, 1451-1453 (2007).

213. Tilling, L., Hunt, J., Donald, A., Clapp, B. & Chowienczyk, P. Arterial injury and endothelial repair: rapid recovery of function after mechanical injury in healthy volunteers. *Cardiology research and practice* **2014**, 367537 (2014).

214. Crowley, C.M., *et al.* The mechanism of excitation-contraction coupling in phenylephrine-stimulated human saphenous vein. *American journal of physiology. Heart and circulatory physiology* **283**, H1271-1281 (2002).

215. Bruning, T.A., Hendriks, M.G., Chang, P.C., Kuypers, E.A. & van Zwieten, P.A. In vivo characterization of vasodilating muscarinic-receptor subtypes in humans. *Circulation research* **74**, 912-919 (1994).

216. Grossmann, M., Braune, J., Ebert, U. & Kirch, W. Dilatory effects of phosphodiesterase inhibitors on human hand veins in vivo. *European journal of clinical pharmacology* **54**, 35-39 (1998).

217. Bendjama, K., *et al.* Translation Strategy for the Qualification of Drug-induced Vascular Injury Biomarkers. *Toxicologic pathology* **42**, 658-671 (2014).

218. Soultati, A., *et al.* Endothelial vascular toxicity from chemotherapeutic agents: preclinical evidence and clinical implications. *Cancer Treat Rev* **38**, 473-483 (2012).

219. Bonin, L.R., *et al.* Generation and characterization of human smooth muscle cell lines derived from atherosclerotic plaque. *Arteriosclerosis, thrombosis, and vascular biology* **19**, 575-587 (1999).

220. Liu, J.Y., *et al.* Functional tissue-engineered blood vessels from bone marrow progenitor cells. *Cardiovascular research* **75**, 618-628 (2007).

221. Libby, P. Inflammation in atherosclerosis. *Nature* **420**, 868-874 (2002).

222. Mann, D., Reynolds, K., Smith, D. & Muntner, P. Trends in statin use and low-density lipoprotein cholesterol levels among US adults: impact of the 2001 National Cholesterol Education Program guidelines. *The Annals of pharmacotherapy* **42**, 1208-1215 (2008).

223. Calabro, P. & Yeh, E.T. The pleiotropic effects of statins. *Current opinion in cardiology* **20**, 541-546 (2005).

224. Koh, K.K. Effects of statins on vascular wall: vasomotor function, inflammation, and plaque stability. *Cardiovascular research* **47**, 648-657 (2000).

225. Eccles, K.A., *et al.* Simvastatin alters human endothelial cell adhesion molecule expression and inhibits leukocyte adhesion under flow. *Atherosclerosis* **200**, 69-79 (2008).

226. Indolfi, C., *et al.* Effects of hydroxymethylglutaryl coenzyme A reductase inhibitor simvastatin on smooth muscle cell proliferation in vitro and neointimal formation in vivo after vascular injury. *Journal of the American College of Cardiology* **35**, 214-221 (2000).

227. Vasa, M., *et al.* Increase in circulating endothelial progenitor cells by statin therapy in patients with stable coronary artery disease. *Circulation* **103**, 2885-2890 (2001).

228. SenBanerjee, S., *et al.* KLF2 Is a novel transcriptional regulator of endothelial proinflammatory activation. *The Journal of experimental medicine* **199**, 1305-1315 (2004).

229. Parmar, K.M., *et al.* Integration of flow-dependent endothelial phenotypes by Kruppel-like factor 2. *The Journal of clinical investigation* **116**, 49-58 (2006).

230. Parmar, K.M., *et al.* Statins exert endothelial atheroprotective effects via the KLF2 transcription factor. *The Journal of biological chemistry* **280**, 26714-26719 (2005).

231. Sen-Banerjee, S., *et al.* Kruppel-like factor 2 as a novel mediator of statin effects in endothelial cells. *Circulation* **112**, 720-726 (2005).

232. Picchi, A., *et al.* Tumor necrosis factor-alpha induces endothelial dysfunction in the prediabetic metabolic syndrome. *Circulation research* **99**, 69-77 (2006).

233. Cheung, T.M., *et al.* Endothelial Cell Senescence Increases Traction Forces due to Age-Associated Changes in the Glycocalyx and SIRT1. *Cellular and molecular bioengineering* **8**, 63-75 (2015).

234. Ding, G.J., *et al.* Characterization and quantitation of NF-kappaB nuclear translocation induced by interleukin-1 and tumor necrosis factor-alpha. Development and use of a high capacity fluorescence cytometric system. *The Journal of biological chemistry* **273**, 28897-28905 (1998).

235. Browner, N.C., Sellak, H. & Lincoln, T.M. Downregulation of cGMP-dependent protein kinase expression by inflammatory cytokines in vascular smooth muscle cells. *American journal of physiology. Cell physiology* **287**, C88-96 (2004).

236. Zhang, J., Defelice, A.F., Hanig, J.P. & Colatsky, T. Biomarkers of endothelial cell activation serve as potential surrogate markers for drug-induced vascular injury. *Toxicologic pathology* **38**, 856-871 (2010).

237. Blum, A. & Shamburek, R. The pleiotropic effects of statins on endothelial function, vascular inflammation, immunomodulation and thrombogenesis. *Atherosclerosis* **203**, 325-330 (2009).

238. Yi, J. & Luo, J. SIRT1 and p53, effect on cancer, senescence and beyond. *Biochimica et biophysica acta* **1804**, 1684-1689 (2010).

239. True, A.L., Rahman, A. & Malik, A.B. Activation of NF-kappaB induced by H(2)O(2) and TNF-alpha and its effects on ICAM-1 expression in endothelial cells. *American journal of physiology. Lung cellular and molecular physiology* **279**, L302-311 (2000).

240. Giardina, J.B., Green, G.M., Cockrell, K.L., Granger, J.P. & Khalil, R.A. TNF-alpha enhances contraction and inhibits endothelial NO-cGMP relaxation in systemic vessels of pregnant rats. *American journal of physiology. Regulatory, integrative and comparative physiology* **283**, R130-143 (2002).

241. Laufs, U., La Fata, V., Plutzky, J. & Liao, J.K. Upregulation of endothelial nitric oxide synthase by HMG CoA reductase inhibitors. *Circulation* **97**, 1129-1135 (1998).

242. Teupser, D., Bruegel, M., Stein, O., Stein, Y. & Thiery, J. HMG-CoA reductase inhibitors reduce adhesion of human monocytes to endothelial cells. *Biochemical and biophysical research communications* **289**, 838-844 (2001).

243. Du, G., *et al.* Simvastatin attenuates TNFalphainduced apoptosis in endothelial progenitor cells via the upregulation of SIRT1. *International journal of molecular medicine* **34**, 177-182 (2014).

244. Ota, H., *et al.* Induction of endothelial nitric oxide synthase, SIRT1, and catalase by statins inhibits endothelial senescence through the Akt pathway. *Arteriosclerosis, thrombosis, and vascular biology* **30**, 2205-2211 (2010).

245. Kilic, U., Gok, O., Elibol-Can, B., Uysal, O. & Bacaksiz, A. Efficacy of statins on sirtuin 1 and endothelial nitric oxide synthase expression: the role of sirtuin 1 gene variants in human coronary atherosclerosis. *Clinical and experimental pharmacology & physiology* **42**, 321-330 (2015).

246. Lin, S., Sandig, M. & Mequanint, K. Three-dimensional topography of synthetic scaffolds induces elastin synthesis by human coronary artery smooth muscle cells. *Tissue Eng Part A* **17**, 1561-1571 (2011).

247. Bashir, M.M., *et al.* Characterization of the complete human elastin gene. Delineation of unusual features in the 5'-flanking region. *The Journal of biological chemistry* **264**, 8887-8891 (1989).

248. Dong, X.R. & Majesky, M.W. Restoring elastin with microRNA-29. *Arteriosclerosis, thrombosis, and vascular biology* **32**, 548-551 (2012).

249. Phillips, J.B. & Brown, R. Micro-structured materials and mechanical cues in 3D collagen gels. *Methods in molecular biology* **695**, 183-196 (2011).

250. Lakin, R.O., Zhu, W., Feiten, L. & Kashyap, V.S. Techniques to harvest diseased human peripheral arteries and measure endothelial function in an ex vivo model. *Journal of vascular surgery* **58**, 470-477 (2013).

251. Golledge, J., Tumer, R.J., Harley, S.L., Springall, D.R. & Powell, J.T. Development of an in vitro model to study the response of saphenous vein endothelium to pulsatile arterial flow and circumferential deformation. *European journal of vascular and endovascular surgery : the official journal of the European Society for Vascular Surgery* **13**, 605-612 (1997).

252. He, T., *et al.* Transplantation of circulating endothelial progenitor cells restores endothelial function of denuded rabbit carotid arteries. *Stroke; a journal of cerebral circulation* **35**, 2378-2384 (2004).

Biography

Cristina Elena Fernandez was born on November 20, 1986 in Caracas, Venezuela to Antonio Fernandez and Maria Elena Pozo de Fernandez. She was raised in Melbourne, Florida. She received her Bachelor of Science degree from the University of Florida in 2008 in Materials Science & Engineering with a concentration in Biomaterials. She earned a Master of Science degree from the University of Florida in 2010 in Materials Science & Engineering advised by Dr. Christopher Batich, where she studied the effects of a bioactive coating for endovascular coils toward improving cerebral aneurysm treatment.

While at Duke University, she received a National Institutes of Health T-32 training grant fellowship through the Center for Biomolecular and Tissue Engineering, and a pre-doctoral fellowship from the American Heart Association. She also completed an industrial internship in the regenerative medicine laboratory at United Therapeutics in Research Triangle Park, NC. While at Duke, she helped found the Biomedical Engineering PhD Student Association (BEPSA) and served as a member of its executive board for two years. She also tutored eighth grade students at Durham Nativity School for two years, and served for two years as a mentor in SENSOR academy, training and mentoring eighth grade students on engineering and science techniques.

Research Papers:

1. Fernandez CE, Braithwaite AB, Henderson KB, Povsic TJ, Truskey GA. Effects of TNF-α and Statins within a Human Vascular Microphysiological Model of Endothelial Dysfunction. *In draft.*
2. Fernandez CE, Yen RW, Perez SM, Bedell HW, Povsic TJ, Reichert WM, Truskey GA. Human Vascular Microphysiological System for in vitro Drug Screening. *Scientific Reports* 6:21579 (2016).
3. Truskey GA, Fernandez CE. Tissue Engineered Blood Vessels as Promising Tools for Drug Toxicity Testing. Expert Opinion on Drug Metabolism and Toxicology 11 (7) 1-4 (2015).
4. Fernandez CE, Obi-onuoha IC, Wallace CS, Satterwhite LL, Truskey GA, Reichert WM. Late Outgrowth Endothelial Progenitors from Patients with Coronary Artery Disease: Endothelialization of Confluent Stromal Cell Layers**.** *Acta Biomaterialia* 10 (2), 893-900 (2014).
5. Fernandez CE, Achneck HE, Reichert WM, Truskey GA. Biological and Engineering Design Considerations for Vascular Tissue Engineered Blood Vessels (TEBVs). *Current Opinion in Chemical Engineering* 3:83-90 (2014).
6. Truskey GA, Achneck HE, Bursac N, Chan HF, Cheng, CS, Fernandez C, Hong S, Jung Y, Koves T, Kraus WE, Leong K, Madden L, Reichert WM, Zhao X. Design

Considerations for an Integrated Microphysiological Muscle Tissue for Drug and Tissue Toxicity Testing. *Stem Cell Research and Therapy* 4 (Suppl 1), S10 (2013).

7. Hoh BL, Hosaka K, Downes DP, Nowicki KW, Fernandez CE, Batich CD, Scott EW. Monocyte Chemotactic Protein-1 Promotes Inflammatory Vascular Repair of Murine Carotid Aneurysms via a Macrophage Inflammatory Protein-1α and Macrophage Inflammatory Protein-2-Dependent Pathway. *Circulation* 124 (20), 2243-2252 (2011).